FORMATION AND REMOVAL OF OZONATION BY-PRODUCTS IN DRINKING WATER BIOFILTERS

by

Stephen Daniel John Booth

A thesis
presented to the University of Waterloo
in the fulfilment of the
thesis requirement for the degree of
Doctor of Philosophy
in
Civil Engineering

Waterloo, Ontario, Canada, 1998

The University of Waterloo requires the signatures of all persons using or photocopying this thesis. Please sign below, and give address and date.

ABSTRACT

The removal of organic ozonation by-products in biologically active filters was studied in this research. In particular, the effect of the presence of specific ozonation by-products on the removal rate of a given ozonation by-product in biofilters, was studied. The ozonation by-products examined were acetate, formate, pyruvate, oxalate, formaldehyde, and methylglyoxal.

A conceptual metabolic model was developed in this research, which assembled and simplified a number of relevant metabolic pathways. This conceptual model was used to demonstrate that the metabolism of acetate, pyruvate, and methylglyoxal were closely linked, and that the metabolism of formate, formaldehyde, and oxalate were similarly linked.

In batch experiments it was found that these ozonation by-products were readily biodegraded, as expected. In most instances biodegradation rates were independent of the other added ozonation by-products. An exception was the transient accumulation of measurable amounts of extracellular pyruvate during methylglyoxal utilization.

Further experiments were carried out in bench-scale biofilters, operated under conditions typical of drinking water filtration practice. Neither internal nor external mass transfer rates were found to limit the removal of the ozonation by-products studied in these biofilters.

Pyruvate was observed at intermediate filter depths in biofilters for which methylglyoxal was the sole feed compound. At steady-state the formed pyruvate was not observed in the filter effluents. However, both methylglyoxal and pyruvate were observed in the filter effluents upon increasing the influent methylglyoxal concentration by a factor of four. The time required to re-establish complete removals was found to be dependent on the hydraulic loading rate of the filter. Also, the removal of methylglyoxal was not found to be impaired following backwashing nor a 48 hour filter shut-down.

In a biofilter fed both pyruvate and methylglyoxal, pyruvate was found to have a lower removal rate than when it was the sole feed compound. This was postulated to have been caused by the formation of pyruvate during methylglyoxal biodegradation, as observed in previous experiments.

In a two-level factorial experiment it was found that neither the presence of two amino acids (serine and glycine) nor temperature (14 and 25°C) affected formaldehyde utilization rates. Serine and glycine were shown to be readily biodegradable in biofilters in this experiment, as expected.

A zero-order kinetic model, which took into account the biomass profile with filter depth, adequately described the concentrations of these components in the biofilters. Unexpectedly, kinetic parameter estimates calculated using the biofilter data were lower than the corresponding estimates based on the batch data.

ACKNOWLEDGEMENTS

I thank my family, Krissy, Nigel, and Tilley. Without Krissy's love, support, and advice I would not have been able to complete the research described in this thesis.

I thank my supervisor, Dr. Peter M. Huck, for all of his advice over the past five years. I would also like to express my gratitude to Peter for providing me with a number of exciting opportunities including speaking at international conferences, and participating in his research projects.

I am grateful for the patient and supportive participation of Dr. Barbara J. Butler and Dr. Robin M. Slawson in this research.

I would also like to acknowledge the technical assistance of Dr. Sigrid Peldszus, Mr. Bill Anderson, and Dr. Susan Andrews, within the Industrial NSERC Chair in Water Treatment. I would especially like to thank Sigrid for teaching me her IC method, for the measurement of carboxylic acids. I am also thankful for the friendship and administrative assistance of Lisa Collins and Leah Richards.

I am indebted to Andrea Chute, Lillian Liao, Val Goodfellow, and Monica van de Lande for their analytical expertise and analysis of my NPOC samples. Further, I thank Andrea and Sigrid for performing my amino acid analyses. I would also like to thank Bruce Stickney and Mark Sobon for their help in resolving various technical issues which arose during the assembly of the bench-scale filter system used in this research.

I appreciate the friendship and support of all the Water Resources graduate students that I have known over the past five years, especially Graham Gagnon and Daniel Urfer. In particular I thank Daniel for his helpful advice concerning the design and operation of my bench-scale filters. I would also like to thank my officemate, Bob McKillop, for his advice and for his thoughts on the game of golf.

Finally, I would like to express my gratitude to Peter Ollos. I thank Peter for being my tennis partner, drinking buddy, career advisor, and mostly for helping me to maintain my sanity over the past five years.

TABLE OF CONTENTS

LIST OF TABLES

LIST OF FIGURES

LIST OF ABBREVIATIONS

ANOVA	analysis of variance
AOC	assimilable organic carbon
BDOC	biodegradable organic carbon
BOD	biochemical oxygen demand
BOM	biodegradable organic matter
CFU	colony forming unit
CGR	coliform growth response
DBP	disinfection by-product
DO	dissolved oxygen
DOC	dissolved organic carbon
DPD	N,N-diethyl-p-phenylenediamine
EBCT	empty bed contact time
EMP	Embden-Meyerhof-Parnas
GAC	granular activated carbon
GC-ECD	gas chromatography with electron capture detection
HPC	heterotrophic plate count
HPLC	high pressure liquid chromatography
HLR	hydraulic loading rate
IC	ion chromatography
NOM	natural organic matter
NPOC	non-purgeable organic carbon
NSERC	National Science and Engineering Council
OPA	orthophthaldialdehyde
PEP	phosphoenolpyruvate
PFBHA	*o*-2,3,4,5,6-pentafluorobenzyl-hydroxylamine hydrochloride
RPM	revolutions per minute
SMP	soluble microbial product
TCA	tricarboxylic acid
TOC	total organic carbon
US EPA	United States Environmental Protection Agency

LIST OF SYMBOLS

A	specific surface area of filter bed, $M_{bed}^{-1}L^2$
D	molecular diffusivity, L^2T^{-1}
D_a	effective axial dispersion coefficient, L^2T^{-1}
D_f	molecular diffusivity within biofilm, L^2T^{-1}
D_p	diameter of the filter media, L
H_1	rapidly biodegradable fraction of BDOC, $M_{organic\ carbon}L^{-3}$
H_2	slowly biodegradable fraction of BDOC, $M_{organic\ carbon}L^{-3}$
k_0	zero-order rate coefficient, $M_{BOM}L^{-2}T^{-1}M_{biomass}^{-1}M_{media}$
$k_{biomass}$	exponential coefficient for biomass, L^{-1}
k_d	first-order mortality rate constant, T^{-1}
k_L	external mass transfer coefficient, LT^{-1}
L	external diffusion layer thickness, L
L_c	characteristic length, L
L_f	biofilm thickness, L
N_{Re}	Reynold's number
P_i	inorganic phosphate
r	general bioreaction term, $M_{BOM}L^{-3}T^{-1}$
R_{obs}	observed reaction rate, $M_{BOM}L^{-3}T^{-1}$
S_b	bulk substrate (BOM) concentration, $M_{BOM}L^{-3}$
S_{b_o}	filter influent bulk BOM concentration, $M_{BOM}L^{-3}$
S_f	BOM concentration within biofilm, $M_{BOM}L^{-3}$
S_{min}	minimum BOM concentration which can support a steady-state biofilm, $M_{BOM}L^{-3}$
S_s	BOM concentration at biofilm-water interface, $M_{BOM}L^{-3}$
Sc	Schmidt number
SP	maximum content of protected adsorption sites for biological attachment, $M_{organic\ carbon}L^{-3}$
X	biomass, $M_{biomass}M_{media}^{-1}$
X_0	biomass at the top of the filter, $M_{biomass}M_{media}^{-1}$

x	radial distance, L
$Y_{x/s}$	yield coefficient, $M_{biomass}M_{BOM}^{-1}$
z	depth within the filter (axial distance), L
ε	porosity of the filter bed
μ	dynamic viscosity of water, $M_{water}L^{-1}T^{-1}$
ρ	density of water, $M_{water}L^{-3}$
ρ_b	bulk density of filter bed, $M_{bed}L^{-3}$
Ω	overall effectiveness factor
ϕ	observed external mass transfer modulus
Φ	observed internal mass transfer modulus

CHAPTER 1: INTRODUCTION AND OBJECTIVES

INTRODUCTION

The use of granular activated carbon (GAC) filters, for the production of biologically stable water, has been recognized in Western Europe for at least two decades (Sontheimer *et al.*, 1978; 1979a,b). In these applications, GAC filters were located downstream of a filtration process designed for particle removal. Many additional studies have shown that biologically active GAC filters used in sequence with other granular media filters for particle removal, produce biologically-stable, low turbidity water. In a thorough review of the European practice of biological drinking water treatment Huck (1988) identified significantly different approaches. In Germany and the Netherlands biological treatment was historically achieved in slow sand filters, through bank filtration, or ground passage, whereas in France biological treatment has been performed in second stage biologically active GAC filters. Newer German and Dutch plants utilize first and second stage biological filtration.

North American regulations such as the Disinfectants/Disinfection By-Products Rule, the Surface Water Treatment Rule, and the Total Coliform Rule are forcing utilities to consider the use of ozone in combination with filtration (US EPA, 1990). If ozonation occurs upstream of a filtration step, then the filters would likely be biologically active. The ozone converts some

of the natural organic matter (NOM) in the water to a more biodegradable form, generally termed biodegradable organic matter (BOM). A substantial portion of BOM consists of a group of low molecular weight, biodegradable compounds known as ozonation by-products. If this BOM is removed in a biological filter, the total amount of NOM in the filtered water will be lower than in the filter influent. This has the benefit of reducing the formation of chlorinated disinfection by-products (DBPs) in a downstream disinfection step. Ozone can be used for other objectives such as disinfection, because it is effective for the inactivation of *Cryptosporidium*, *Giardia*, and viruses. For *Cryptosporidium*, chlorine has essentially no effect at the concentrations and contact times that can be achieved in drinking water disinfection. However, even when applied for the purpose of disinfection, ozonation will result in an increase in the BOM of the water. Again, it is possible to remove this BOM in an existing downstream biofilter.

If ozonation is not followed by biological filtration several problems may result. Although the exact relationship between the amount of BOM and microbial growth has yet to be determined, it is generally expected that more BOM will lead to an increase in the number of both suspended and biofilm microbes, in distribution system pipes (*e.g.* Ollos *et al.*, 1997). The proliferation of microbes in the distribution system is undesirable for many reasons, including the production of unpleasant taste and odours, a reduction in the capacity of the distribution system to maintain a disinfectant residual, and the proliferation of opportunistic pathogens (Rittmann and Snoeyink, 1984). Finally, if chlorination is performed prior to distributing the water, regrowth may be mitigated to some extent, however, the formation of DBPs may be encouraged. Some organic ozonation by-products have been shown to efficiently react with chlorine to form trihalomethanes, and other regulated contaminants (Reckhow and Singer, 1985).

Thus, the use of biologically active filtration is expected to increase in North America in the future. This process needs to be better understood in

order to develop design criteria and equations, and also operating parameters. Most of the research on biological filtration has used surrogate parameters to represent BOM, such as easily assimilable organic carbon (AOC) and biodegradable dissolved organic carbon (BDOC). Methods for measuring these parameters are discussed in Chapter 2. The present research investigates the formation and removal of specific ozonation by-products in biologically active filters.

As will be shown in Chapter 4, the compounds of interest in this research are microbial metabolites, and/or readily metabolized growth substrates. Metabolic processes may result in an impact on filter performance, with respect to the compounds in question, due to phenomena such as a preference for one compound over another, or the production of one compound via the metabolism of another. It is therefore hypothesized that the rate of utilization of a given compound may be dependent on the presence of other compounds. The utilization rates of these compounds need to be determined when they are alone and when they are in a mixture with other selected compounds. A comparison of these rates would allow this hypothesis to be tested. Furthermore, for scenarios where differences in utilization rates are found, it would be of value to the water treatment industry to perform experiments in a system representative of actual drinking water filters, to help determine how these differences in utilization rates impact filter performance.

RESEARCH OBJECTIVES

The overall objective of this research was to develop and implement a framework for determining if the removal rate of selected easily biodegradable ozonation by-products in biologically active filters, was dependent on the other compounds also present in the influent. Specific research objectives follow:

1. To develop a conceptual model which identifies and summarizes the major microbial metabolic pathways relevant to selected ozonation by-products. The ozonation by-products of interest were acetate, formate, pyruvate, oxalate, formaldehyde, and methylglyoxal.

2. To use this model to select specific groups of ozonation by-products for investigation in batch bioreactors. The objective of these experiments was to determine if the measured biodegradation rate of a given ozonation by-product, was dependent on the other ozonation by-products, also added to the bioreactor. A further objective was to monitor for detectable, extracellular transformation products.

3. To verify the batch results in a bench-scale system, which was representative of actual biologically active drinking water filters. This system allowed the effect of selected operational variables on the removal of ozonation by-products to be tested.

REFERENCES

Huck, P. M. (1988). Use of Biological Processes in Drinking Water Treatment - Review of European Technology. Report Submitted to the Biotechnology Research Institute, Montréal, Québec, Canada.

Ollos, P.J., R.M. Slawson, and P.M Huck (1997). Modeling of biofilm accumulation in drinking water distribution systems. CD-ROM Proc. AWWA WQTC, Denver, Colorado, USA.

Reckhow, D.A. and P.C. Singer (1985). Mechanisms of organic halide formation during fulvic acid chlorination and implications with respect to preozonation, in Water Chlorination: Chemistry, Environmental Impact and Health Effects, Vol. 5 pp. 1229-1257, R.L. Jolley (Ed.). Lewis Publishers, Chelsea, Michigan, USA.

Rittmann, B.E. and V.L. Snoeyink (1984). Achieving biologically stable drinking water. *Jour. AWWA*, Vol. 76 (10) pp. 106-114.

Sontheimer, H., E. Heilker, M.R. Jekel, H. Nolte, and F. Vollmer (1978). The Mülheim process. *Jour. AWWA*, Vol. 70 (7) pp. 393-396.

Sontheimer, H. (1979a). Applying oxidation and adsorption techniques: a summary of progress. *Jour. AWWA*, Vol. 71 (11) pp. 612-617.

Sontheimer, H. (1979b). Design criteria and process schemes for GAC filters. *Jour. AWWA*, Vol. 71 (11) pp. 618-622.

US EPA (1990). Guidance Manual for Compliance with the Filtration and Disinfection Requirements for Public Water Systems using Surface Water Sources, Prepared by Malcom Pirnie Inc. and HDR Engineering Inc.

CHAPTER 2: BACKGROUND

In this chapter background information relevant to this research is reviewed. A discussion of BOM and its measurement in treated drinking waters is followed by an introduction to the chemical components which comprise BOM, especially in ozonated waters. The formation of by-products due to ozonation is then discussed along with their removal in biologically active filters. A brief introduction to the concept of microbial product formation within biofilters follows. The chapter concludes with a short review of current approaches for modeling the removal of BOM in biologically active filters.

BIODEGRADABLE ORGANIC MATTER

The organic pool in a water typically consists of humic substances, combined amino acids, proteins, carbohydrates, and other compounds. A fraction of the total is usually biodegradable, although this amount will be water specific and is also dependent on the measurement method. It has been well documented in the literature that ozone increases the biodegradability of the NOM of waters (*e.g.* van der Kooij *et al.*, 1989). This is accomplished in several ways including cleaving larger molecules into smaller, more bio-available ones, by modifying the chemical structure of the NOM, and by producing compounds known to be easily degraded, such as acetate (Huck, 1994).

Because there is much less BOM present in most drinking waters than in industrial or municipal wastewaters, methods for BOM determination in drinking water are much less standardized. Most methods which are currently in use were developed within the last 10 to 15 years, compared to the biochemical oxygen demand (BOD) test which was originally devised about 100 years ago (Bailey and Ollis, 1986).

BOM Measurement Methods

Several different types of measurements have been used to estimate drinking water BOM and bacterial growth potential, however, Huck (1990) has suggested that the type of test used should be dictated by the intended use of the results. Two common uses are assessing the extent to which a water can support bacterial growth, and assessing the potential for DBP formation. In the former case a biomass-based method should be used and in the latter case the dissolved organic carbon (DOC) should be measured.

The coliform growth response test (CGR) measures the potential of waters to support coliform growth (Rice *et al.*, 1991). In this test an inoculum of one or more coliform organisms is added to the sample after filter sterilizing to remove the indigenous microbes. The samples are incubated for five days at 20°C. This test is particularly appropriate for North American utilities because it targets the group of organisms specified in US EPA drinking water regulations. Other methods are also in common use by the drinking water research community.

A biomass based method introduced by van der Kooij *et al.* (1982), and subsequently modified by van der Kooij and Hijnen (1984) incorporates two bacterial strains, *Pseudomonas fluorescens* strain P17 and *Spirillum* strain NOX. The number of colony forming units (CFUs) of these two strains is monitored over time, until a maximum number is achieved. Correlations between the maximum number of CFUs and the concentration of substrates added to a tap water allow the easily assimilable organic carbon (AOC)

concentration of a water to be calculated. The portion of AOC which is measured by P17 includes amino acids, carboxylic acids, hydroxycarboxylic acids, alcohols and carbohydrates, but excludes polysaccharides (van der Kooij *et al.*, 1982). The P17 strain cannot metabolize certain potentially important ozonation by-products, such as oxalate, formate, and glycolate, whereas NOX is capable of utilizing these compounds (van der Kooij and Hijnen, 1984).

A DOC-based method has been proposed by Servais *et al.* (1989). This method involves filter sterilizing the sample, then inoculating it with a sample of filter effluent. The DOC is measured initially and after four weeks. The difference between these two values is taken as the biodegradable dissolved organic carbon (BDOC) content of the water. Modifications to this method have been proposed by Joret *et al.* (1988) and Allgeier *et al.* (1996). Also, a different method proposed by Ribas *et al.* (1991) and further developed by Kaplan and Newbold (1995), involves the use of biofilm reactors. In this technique the water to be tested is passed through two glass columns containing non-porous siran beads. A biofilm develops on the beads which removes a portion of the DOC of the water. The combined residence time of the columns is about two hours. The BDOC is taken as the difference between the influent and effluent DOC values. Because these different assays report the result as BDOC, differences among methods should be considered prior to comparing results among studies. Also, the difference between the two DOC measurements (*i.e.* the BDOC) can be very small relative to a large background. In many instances this is given very little attention when BDOC results are reported.

Often a research group or utility will adopt one method for measuring the biodegradability of waters and ignore the others. This may be done for practical reasons such as cost, which may prohibit measuring a given parameter with more than one method. Unfortunately, this has precluded the establishment of a database from which meaningful comparisons among

methods can be made. The first North American attempt to make comparisons among methods was provided by Kaplan *et al.* (1994). They examined potential relationships among DOC, the Servais *et al.* (1989) BDOC method, AOC, and CGR. These authors found statistically significant correlations among DOC, BDOC, and AOC, although the correlation coefficients were in the range of 0.56 to 0.58. Correlations were not significant between CGR and AOC, nor between CGR and BDOC. This is an indication of the complexity of the relationships which may exist among these parameters and the need for the development of a more extensive database from which correlations can be sought.

OZONATION BY-PRODUCTS

Methods have been developed which measure the concentrations of specific BOM components. Generally the AOC and BDOC, regardless of the measurement method, will significantly increase upon ozonation, and decrease following a biofilm process, such as biofiltration. Since ozonation produces relatively high values of AOC and BDOC, the determination of specific compounds following this stage, has been most fruitful. The advantage of measuring specific components, following a given treatment stage, is that the results can be compared among investigations at different utilities. Specific examples of component concentrations, following ozonation, are discussed below.

There is a large number of compounds produced by the reaction of ozone with NOM in drinking water treatment, such as organic peroxides, hydrogen peroxide, various free radicals, aldehydes, and organic acids (Weinberg *et al.*, 1992). Specifically, the low molecular weight aldehydes have been acknowledged as ubiquitous ozonation by-products (*e.g.* Weinberg *et al.*, 1993), several low molecular weight keto-acids may be produced in relatively high concentrations (Xie and Reckhow, 1992), and a number of carboxylic acids were measured in a full-scale plant (Gagnon *et al.*, 1997a).

These are the three major groups of biodegradable organic ozonation by-products.

These aldehydes and organic acids are of interest for several reasons. The keto-acids, pyruvate and glyoxylate, readily promote the growth of the bacterial *Spirillum* strain NOX (Van der Kooij and Hijnen, 1984). Therefore, high levels of these organic acids, will likely result in high AOC values. Pyruvate has also been shown to be an efficient trihalomethane precursor (Reckhow and Singer, 1985). Aldehydes may also contribute to bacterial growth potential, however, they also raise potential health concerns. The aldehydes glyoxal and methylglyoxal have been shown to exert carcinogenic tumor promoting activity (Takahishi *et al.*, 1989), and Matsuda *et al.* (1992) showed that glyoxal exerted a major portion of the mutagenicity in an ozonated water. Furthermore, formaldehyde is a suspected human carcinogen (Sax, 1981).

Given the literature evidence that some ozonation by-products may promote bacterial regrowth in distribution systems (*e.g.* Gagnon *et al.*, 1996), or react with chlorine to form unwanted DBPs, and the health concerns of some aldehydes, the removal of these compounds in treatment plants is important. None of the ozonation by-products is currently regulated in North America, however, potential regulatory limits of some aldehydes have been proposed (Bull and Kopfler, 1991). Indeed, as regulations become more focused on preventing bacterial regrowth it is possible that specific ozonation by-products be named in regulations.

The compounds selected for investigation in this research include representative compounds from each of the major groups of ozone by-products: the aldehydes, methylglyoxal and formaldehyde; the keto-acid pyruvate; and the carboxylic acids acetate, oxalate, and formate. The six compounds selected do not exhaust the list of ozonation by-products, for example other compounds such as ketomalonate and glyoxal are also known to

be formed during the ozonation of drinking water. The compounds chosen for this research were selected because they are known to be common drinking water ozonation by-products (*e.g.* Weinberg *et al.*, 1993; Gagnon *et al.*, 1997a; and Niquette *et al.*, 1998), and analytical methods for their detection were available within the laboratories of the Industrial NSERC Chair for Drinking Water Treatment.

As discussed in Chapter 4, many of these ozonation by-products play an important role in bacterial metabolism. A quantitative understanding of the removal of ozonation by-products in biofilters requires that the important metabolic bioreactions be considered. This is further discussed in Chapter 4.

Formation of Ozonation By-Products

Several studies have examined the formation of ozonation by-products in full and pilot-scale studies. Data from selected studies which reported on the formation of three ozonation by-products of interest in the present research, are summarized in Table 2.1.

Krasner *et al.* (1993) investigated the formation and removal of aldehydes in a large pilot-scale facility. The two source waters used in this study were Colorado River water, and State Project water. Ozonation produced formaldehyde concentrations in the range of 14 to 22 μg/L, glyoxal concentrations of 9 to 12 μg/L, and 8 to 11 μg/L of methylglyoxal. The ozone to total organic carbon (TOC) ratio ranged from 0.4 to 0.5 mg/mg. Coffey *et al.* (1995) reported on keto-acid and AOC results for a study at the same facility which also analyzed other aspects of biofiltration, such as particle removal. State Project water was the raw water for this investigation. Post-ozone concentrations ranged from 24 to 42 μg/L for pyruvate, 33 to 48 μg/L for glyoxylate, and 30 to 45 μg/L for ketomalonate.

Table 2.1: Selected Ozone By-Product Formation Data

Study	Temp. (°C)	O_3:TOC (mg/mg)	Post-Ozone Concentration (μg/L) formaldehyde	methylglyoxal	pyruvate
1	19	0.77	23	4.8	36
2	10	0.70	25	5	-[5]
3	23	0.50	16	6	32
4[a]	13 to 27	0.38	20	6.5	-[5]
4[b]	2	0.28	1.6	2.5	6
4[c]	5	0.64	26.9	2.9	14

1. Gagnon *et al.* (1997a)
2. Niquette *et al.* (1998)
3. Coffey *et al.* (1995)
4. Data for pilot plants in a. Brantford, b. Ottawa, and c. Windsor (Anderson *et al.*, 1994).
5. Pyruvate was not analyzed in this study.

The author of this thesis contributed to a detailed analysis of the formation and removal of several carboxylic acids in a full-scale water treatment plant treating Grand River water (Gagnon *et al.*, 1997a). The four acids formed in the highest concentration were: formate, acetate, glycolate and pyruvate which averaged 226 μg/L, 132 μg/L, 46 μg/L, and 36 μg/L. respectively. The average ozone to TOC ratio in that study was about 0.7 mg/mg.

Niquette *et al.* (1998) reported on the formation of aldehydes and oxalate, in a pilot-scale investigation for which the raw water was sourced from the Mille-Iles River. That study employed an ozone to TOC ratio of about 0.7. Formaldehyde concentrations in the range of 10 to about 32 μg/L, and oxalate concentrations of 150 to almost 400 μg/L, were observed.

Some generalizations concerning the amounts of by-products formed on ozonation are emerging. Najm and Krasner (1995) suggested a linear relationship for keto-acid formation with TOC. This work was conducted in bench-scale ozone contactors, which used a test water that was spiked with various levels of TOC. Figure 2.1 shows an example regression line from that study, along with additional data added by the author of this thesis. The additional data were from the following locations: New Haven, CT (Xie and

Reckhow, 1992), La Verne, CA (Coffey *et al.*, 1995), Kitchener, ON (Gagnon *et al.*, 1997a), and Windsor, ON (Anderson *et al.*, 1994).

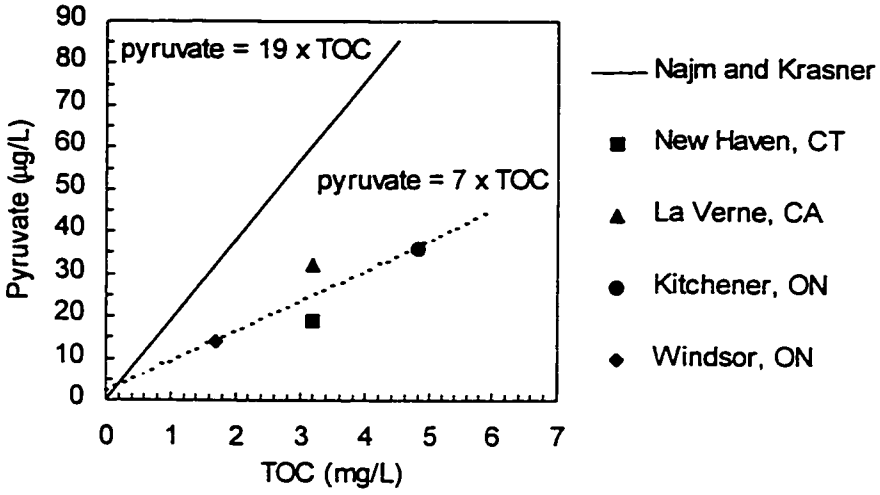

Figure 2.1: Pyruvate formation as a function of TOC.
(Reprinted from *Proceedings of the 1995 AWWA Water Quality Technology Conference*, by permission. Copyright © 1996, American Water Works Association.)

Figure 2.1 indicates that TOC was limiting for the formation of pyruvate in the Najm and Krasner synthetic water. A linear relationship between pyruvate and TOC was also found for the pyruvate formed in four different waters, with different types of NOM. These data were obtained at an average ozone to TOC ratio of approximately 0.6 mg/mg, while Najm and Krasner used a ratio of 2 mg/mg. It was therefore expected that the Najm and Krasner slope be about three times greater, as was calculated. Thus, this linear relationship may be more generally applicable, to different waters.

BIOLOGICAL FILTRATION

The author of this thesis contributed to a recent critical review of the literature on biological filtration for BOM and particle removal (Urfer *et al.*, 1997). This article reviewed the impact of filter media, contact time, backwashing, and temperature, in addition to other parameters and engineering variables on the removal of BOM. The major points from this review are summarized in this section.

Krasner *et al.* (1993) showed that formaldehyde was typically readily removed in biologically active filters, while glyoxal and methylglyoxal usually appeared to be less biodegradable. Other data from this facility also indicate that glyoxal is more recalcitrant than formaldehyde. For example, steady-state removal of glyoxal took longer to be re-established than for formaldehyde, after shock-chlorination (Coffey *et al.*, 1995). These results were found to be media dependent, with GAC filters recovering better performance, with respect to both compounds, in less time than anthracite/sand filters.

Data obtained at a demonstration plant have been discussed by Coffey *et al.* (1995). Two full scale anthracite/sand filters were run in parallel with a pilot scale GAC/sand filter containing virgin GAC. The empty bed contact time (EBCT) of the filters in this study ranged from 2.9 to 4.8 minutes. The study was roughly divided into two phases. Phase 1 which lasted about 90 days had an average water temperature between 20-25°C and was separated from phase 2 by a 24-hour shock chlorination. Water temperatures during phase 2 were around 20°C initially and dropped to about 10°C towards the end of the study. They reported that the percentage removal of formaldehyde and glyoxal were somewhat better with GAC/sand, especially during phase 2. However, since the influent concentration of glyoxal ranged from only 7 to 11 μg/L, small differences in the effluent concentration can result in large differences in the calculated percent removal. For example, for an influent glyoxal concentration of 10 μg/L and an effluent concentration of 5 μg/L, the calculated percent removal is 50%. However, if the effluent concentration dropped to 3 μg/L, the percent removal would be 70%. Thus in this example, a very small change in the effluent concentration can result in an apparently large difference in the calculated percent removal. Also, there was some evidence that the GAC may not have been exhausted with respect to NOM removal, and therefore, a portion of the removals may have been due to adsorption (Urfer *et al.*, 1997).

Gagnon *et al.* (1997a) provided formation and removal data for several carboxylic acids. Unexpectedly, incomplete removals were observed for formate, acetate, glycolate, and pyruvate, even though the filters were operated at EBCTs exceeding 24 minutes.

Another pilot investigation conducted by Prévost and co-workers compared first stage and second stage biological filtration (Niquette *et al.*, 1998 and Prévost *et al.*, 1995). Deep bed anthracite/sand and GAC/sand filters were operated in parallel during this investigation at EBCTs of about 13 minutes. Seeded GAC obtained from a full scale plant was used, and was assumed to be exhausted with respect to adsorption of NOM. The post-sedimentation ozone dosage was adjusted to maintain 0.4 mg/L in the effluent of the first ozonation column and this residual was maintained throughout the second column (Prévost *et al.*, 1995). Formaldehyde removals at 10°C were equal to about 50% in the anthracite/sand filter whereas GAC/sand filters removed over 80% of this easily biodegradable aldehyde. Glyoxal was totally removed by the GAC/sand filters whereas the anthracite/sand filter showed no glyoxal removal. Seasonal variations in oxalate removal were also observed in this study. Comparable removals of about 90% were observed for both GAC/sand and anthracite/sand filters in the winter, however, removals dropped to about 70% and 40%, respectively, in the spring. A possible explanation for the drop in performance is that influent oxalate concentration doubled between the winter and the spring.

Based on the results above, the authors concluded that the performance of GAC was superior to anthracite for aldehyde removal. However, formaldehyde removals of about 50% at an EBCT of 13 min and a water temperature of 10°C are surprisingly low. It seems possible that the ozone residual maintained at 0.4 mg/L throughout the second ozonation chamber led to the presence of ozone residuals in the filter influents. This would have a negative effect on the biological performance of the anthracite/sand filter (Weinberg *et al.*, 1993), whereas GAC would rapidly destroy the ozone,

permitting biofilm development. Considering this possibility, the superior performance of GAC may be primarily due to the presence of an ozone residual in the filter influent, and to a lesser extent to differences in the ability of these two media to support a biomass capable of removing aldehydes.

Wang *et al.* (1995) investigated the effect of chlorine residuals in the influent and backwash water of anthracite/sand filters in a pilot-scale study where the raw water was taken from the Ohio River. In the filter in which a chlorine residual was maintained in the filter influent, essentially no removal was observed for the aldehydes, and other parameters such as, BDOC, AOC-NOX and DBP formation potentials. When no chlorine was present in the influent, removals were much better, with good removals for formaldehyde (74%), and poorer removals for glyoxal (28%). Comparisons were also made with different GACs and sand filters. In filters which were not pre-chlorinated, AOC-NOX removals were not statistically different between these media and anthracite/sand filters. Aldehyde results were not reported for the GAC or sand filters.

These two studies emphasize the importance of eliminating oxidant residuals in the influent of anthracite/sand filters. When oxidants are minimized anthracite/sand filters often achieve a performance similar to GAC/sand filters.

SOLUBLE MICROBIAL PRODUCT FORMATION

Although the work described in this thesis focuses on ozonation by-products, a brief description of the relevant work on soluble microbial product (SMP) formation is also introduced here. An objective of this research is to investigate the possibility of microbial production of the ozonation by-product compounds in biologically active filters. Thus, the formation of SMPs is a related subject which deals with the formation of organic carbon by microbes.

SMP formation has been investigated by Rittmann and Namkung (1986) in waste water treatment biofilms. Some specific components were

identified such as humic substances, polysaccharides, proteins, and nucleic acids, although these same compounds may not be found in drinking water filters. They divided SMPs into two categories, utilization-associated products, and biomass-associated products. The production of the former category is controlled by the specific utilization rate of the original substrate, while the latter is controlled by the cell density in the biofilm. In lab-scale biofilm reactors they found that the majority of the organic carbon in the effluent was SMP, and very little of the original substrate. Also, the SMP may be biodegradable but at a much slower rate than the original substrate (Woolschlager and Rittmann, 1994).

Carlson *et al.* (1996) investigated the formation of SMPs in drinking water biofilters. Using pilot-scale filter data and modeling equations they were able to estimate SMP concentrations. They found that the SMP concentration in the filter effluent was a negligible fraction of the DOC. These authors acknowledged that SMP production would be more important at higher levels of influent BOM, biomass, and contact times, such as those observed in biological waste water treatment.

Therefore, the formation of SMP, as described here may not be significant under drinking water biofiltration conditions. This may be especially true when SMP formation is expressed as a fraction of the DOC of the water. However, the formation of individual SMP compounds within biologically active filters remains of interest if these compounds are DBP precursors, or have the potential to increase regrowth in distribution systems.

MODELING THE REMOVAL OF BOM

It is useful to discuss and interpret experimental data in terms of the processes which have been examined in engineering models. In addition to briefly introducing the major processes which are considered in current modeling approaches, some major disadvantages of the current approaches are also discussed. Table 2.2 summarizes the most widely known models for

drinking water applications. This table is not exhaustive, and a more thorough review of the different approaches is beyond the scope of this section. Gagnon *et al.* (1997b) have reviewed several models applicable to BOM utilization and microbial growth in distribution systems. Many of the processes considered in the distribution system models are the same as in biofiltration models.

Table 2.2: Summary of Selected Models

Ref.	Processes Considered	Number of Parameters measured + assumed = total	Output
1	mass transport, diffusion and reaction in biofilm, definition of S_{min}	5 + 3 = 8	substrate flux to biofilm, biofilm thickness, bulk substrate conc.
2	uptake of BDOC fractions, adsorption of bacteria, bacterial mortality, protozoan grazing	10 + 2 =12	attached and suspended biomass, BDOC fractions
3	mass transport, surface bioreaction, definition of DOC fractions, biomass as function of filter depth	7 + 3 = 10	bulk concentration of DOC fractions
4	application of Ref. 1 model, AOC as substrate, dimensionless EBCT definition	5 + 4 = 9	substrate flux to biofilm, bulk substrate conc.

1. Rittmann and McCarty (1980).
2. Billen *et al.* (1992).
3. Wang and Summers (1995).
4. Zhang and Huck (1996).

Rittmann and McCarty (1980) have introduced a steady-state model considering microbial kinetics and mass transport (*i.e.* Fick's second law). They assumed that all required nutrients are in excess except for the rate limiting substrate, S. An important contribution of their work was the identification of S_{min}, which was defined, by these authors, as the steady-state bulk substrate concentration below which a steady-state biofilm cannot exist. Consequently for substrate concentrations below S_{min} the biofilm thickness is

zero. At substrate concentrations above S_{min}, the biofilm thickness is determined by the growth rate, which is dependent on the substrate flux, and losses due to shear stress. Because the bulk substrate concentration decreases with depth in a filter, the substrate flux to the biofilm, and hence the biofilm thickness, are also expected to similarly decrease.

Rittmann and McCarty (1980) have included the major processes which are expected to be important in biofilm processes. These are: the flux of the substrate through an external diffusion layer to the biofilm outer surface; and simultaneous utilization and diffusion through the biofilm (Figure 2.2). The substrate concentrations in Figure 2.2 are S_b, the bulk concentration, S_s, the concentration at the biofilm-water interface, and S_f, the concentration within the biofilm. The transfer of BOM from the bulk to the biofilm surface is a diffusion process, referred to as external mass transfer, and occurs through a diffusion layer of thickness L. The transfer of BOM within the biofilm is referred to as internal mass transfer. Internal mass transfer occurs simultaneously with utilization through the biofilm of depth, L_f. The removal rate of a substrate (*i.e.* BOM) may be controlled by mass transfer or utilization kinetics. The slower of the two processes limits the overall rate at which BOM can be removed. It is possible to determine which process controls the removal rate, through the use of moduli, which determine the relative rates of reaction and mass transfer. Specific moduli are discussed in Chapter 6 with respect to the removal of BOM components in biological filters, in the present research.

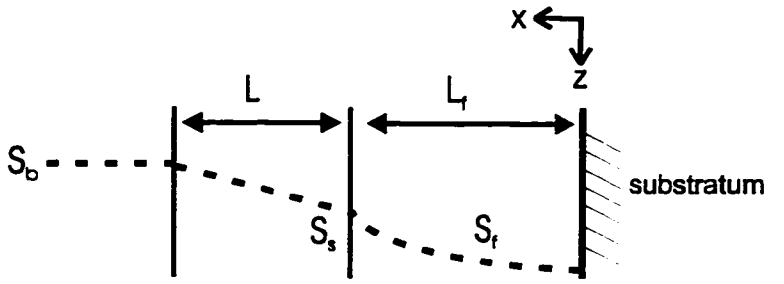

Figure 2.2: Schematic representation of an idealized planar biofilm.
(Rittmann and McCarty (1980), pp. 2346. © John Wiley & Sons, Inc. Reprinted by permission of John Wiley & Sons, Inc.)

Zhang and Huck (1996) have applied the Rittmann and McCarty (1980) steady-state biofilm model to biological drinking water treatment. An important contribution by Zhang and Huck (1996) was the development of an index for contact time. This was called the dimensionless EBCT and incorporated actual contact time, specific surface area, as well as the ease of diffusion and biodegradation of the organic matter. This allowed comparison of results among studies and for different parameters (AOC or BDOC) used to define BOM.

Billen and co-workers (1992) have developed the CHABROL model for BDOC removal. The model introduced the important aspect of dividing BDOC into rapidly and slowly biodegradable fractions, H_1 and H_2. A number of other processes are also included in the model including protozoan grazing of bacterial biofilms. Two parameters required in the model, k_d, which relates to bacterial mortality, and SP, a parameter which characterizes the media, are difficult to estimate. In particular k_d may be water specific and vary seasonally, indicating that care must be taken in choosing its value.

Another modeling approach was presented by Summers and co-workers (Wang and Summers, 1995), which assumes a sufficiently thin biofilm such that substrate utilization can be considered a surface reaction. They also divide DOC into easily and slowly biodegradable components, and allow biomass to decrease with filter depth. They included an empirical

equation expressing the amount of biomass as a function of EBCT. Their model provides the concentration of the DOC fractions with filter depth.

A much simpler approach developed by Huck and co-workers (Huck and Anderson, 1992; Huck *et al.*, 1994), showed that the amount of BOM removed in a given biofilter is directly proportional to the influent concentration. Thus, removals can be approximated as a first order process, and a biofilter with a given contact time will essentially achieve a constant percentage removal, as long as a steady state is maintained. This approach has been shown to hold for AOC, BDOC, trihalomethane formation potential, chlorine demand and carboxylic acids (Huck *et al.*, 1994; Gagnon *et al.*, 1997a).

Discussion of Modeling Approaches

The rigorous and mechanistic modeling approaches have been shown to be useful, however, a large number of parameters are usually required. These parameters may be dependent on the water source, water quality characteristics, and the season. Thus, a substantial amount of data may be required in order to begin parameter estimation. Furthermore, estimation procedures can be computationally intensive. Consequently, most models are used almost exclusively by their original developers. Also, none of the models attempt to account for potential microbially-mediated transformations among compounds or the production of specific ozonation by-product compounds within biofilters.

The simpler technique provided by Huck *et al.* (1994) is much easier to use, however, it does not explicitly account for differences in EBCT, the amount of attached biomass, or temperature. Clearly, further work is required to develop models which are reasonably easy to use, while providing adequate results. Models which make assumptions which eliminate or simplify certain computations, such as neglecting mass transfer within the biofilm, show promise in this regard.

REFERENCES

Allgeier, S. C., R.S. Summers, J.G. Jacangelo, V.A. Hatcher, D.M. Moll, S.M. Hooper, J.W. Swertfeger, and R.B. Green (1996). A simplified and rapid method for biodegradable dissolved organic carbon measurement. CD-ROM Proc. AWWA WQTC, Boston, Massachusetts, USA.

Anderson, W.B., P.M. Huck, I.P. Douglas, J. Van Den Oever, B.C. Hutcheon, B.C., J.C. Fraser, S.Y. Jasim, R.J. Patrick, H.E. Donison, and M.P. Uza (1994). Ozone by-product formation in three different types of surface waters. Proc. AWWA WQTC, San Francisco, California, USA.

Bailey, J.E. and D.F. Ollis (1986). Biochemical Engineering Fundamentals, 2nd Edition. McGraw-Hill Inc., New York, New York, USA.

Billen, G., P. Servais, P. Bouillot, and C. Ventresque (1992). Functioning of biological filters used in drinking water treatment - the chabrol model. *Jour. Water SRT-Aqua,* Vol. 41 (4), pp. 231-241.

Bull, R.J., and F.C. Kopfler (1991). Health Effects of Disinfectants and Disinfection By-Products. AWWA Research Foundation, Denver, Colorado, USA.

Carlson, K.H., G.L. Amy, G. Blais, and S. MacMillan (1996). The importance of soluble microbial products in drinking water biofiltration. Proc. AWWA WQTC, Boston, Massachusetts, USA.

Coffey, B.M., S.W. Krasner, M.J. Sclimenti, P.A. Hacker, and J.T. Gramith (1995). A comparison of biologically active filters for the removal of ozone by-products, turbidity and particles. Proc. AWWA WQTC, New Orleans, Louisiana, USA.

Gagnon, G.A., P.M. Huck, R.M. Slawson (1996). Evaluating and quantifying the rate of microbial utilization of specific biodegradable organic compounds in an annular reactor. Proc. AWWA WQTC, Boston, Massachusetts, USA.

Gagnon, G.A., S.D.J. Booth, S. Peldszus, D. Mutti, F. Smith, and P.M. Huck (1997a). Formation and removal of carboxylic acids in a full-scale treatment plant. *Jour. AWWA*, Vol. 89 (8), pp. 88-97.

Gagnon, G.A, P.J. Ollos, and P.M. Huck (1997b). Modelling BOM utilization and biofilm growth in distribution systems: review and identification of research needs. *Jour. Water SRT-AQUA*, Vol. 87 (1), pp. 90-105.

Huck, P.M. (1990). Measurement of biodegradable organic matter and bacterial growth potential in drinking water. *Jour. AWWA*, Vol. 82 (7), pp.78-86.

Huck, P.M. (1994). Biological drinking water treatment: concepts, issues, and performance. Proc. AWWA Annual Conference, New York, New York, USA.

Huck, P. M. and W. B. Anderson (1992). Quantitative relationships between the removal of NVOC, chlorine demand and AOX formation potential in biological water treatment, *Vom Wasser*, Vol. 78, pp. 281-303.

Huck, P.M., S. Zhang, M.L. Price (1994). BOM removal during biological treatment: a first order model. *Jour. AWWA*, Vol. 86 (6), pp. 61-71.

Joret, J.C. *et al.* (1988). Rapid method for estimating bioeliminable organic carbon in water. Proc. AWWA Annual Conference, Orlando, Florida, USA.

Kaplan, L.A., D.J. Reasoner, and E.W. Rice (1994). A survey of BOM in US drinking waters. *Jour. AWWA*, Vol. 86 (2), pp. 121-132.

Kaplan, L.A. and J.D. Newbold (1995). Measurement of streamwater biodegradable dissolved organic carbon with a plug flow reactor. *Wat. Res.*, Vol. 29 (12), pp. 2696-2706.

Krasner, S.W., M.J. Sclimenti, and B.M. Coffey (1993). Testing biologically active filters for removing aldehydes formed during ozonation. *Jour. AWWA*, Vol. 85 (5), pp. 62-71.

Matsuda, H., S. Takahito, H. Nagase, Y. Ose, H. Kito, and K. Sumida (1992). Aldehydes as mutagens formed by the ozonation of humic substances. *Sci. Tot. Env.*, Vol. 114, pp. 205-213.

Najm, I.N., and S.W. Krasner (1995). Effects of bromide and NOM on by-product formation. *Jour. AWWA*, Vol. 87 (1), pp. 106-115.

Niquette, P., M. Prévost, R. G. Maclean, D. Thibault, J. Collier, R. Desjardins, and P. Lafrance (1998). Backwashing first-stage sand-BAC filters. *Jour. AWWA*, Vol. 90 (15), pp. 86-97.

Prévost, M., P. Niquette, R.G. Maclean, D. Thibault, P. Lafrance, R. Desjardins (1995). Removal of various biodegradable organic compounds by first and second stage filtration. Proc. 12th Ozone World Congress, Lille, France, pp. 531-545.

Reckhow, D.A. and P.C. Singer (1985). Mechanisms of organic halide formation during fulvic acid chlorination and implications with respect to preozonation, in Water Chlorination: Chemistry, Environmental Impact and Health Effects, Vol. 5 pp. 1229-1257, R.L. Jolley (Ed.). Lewis Publishers, Chelsea, Michigan, USA.

Ribas, F., J. Frias, and F. Lucena (1991). A new dynamic method for the rapid determination of the biodegradable dissolved organic carbon in drinking water. *J. Appl. Bacteriol.*, Vol. 71, pp. 371-378.

Rice E.W., *et al.* (1991). Correlation of coliform growth response with other water quality parameters. *Jour. AWWA*, Vol. 83 (7) pp. 98-102.

Rittmann, B.E. and P.L. McCarty (1980). Model of steady-state-biofilm kinetics. *Biotechnol. Bioengr.*, Vol. 22, pp. 2343-2357.

Rittmann, B.E. and E. Namkung (1986). Soluble microbial products (SMP) formation kinetics by biofilms. *Wat. Res.*, Vol. 20 (6), pp. 795-806.

Sax, N.I. (1981). Basic carcinogens, in Cancer Causing Chemicals, N.I. Sax (Ed.). Van Nostrand Reinhold Company, New York, New York, USA.

Servais, P., A. Anzil, and C. Ventresque (1989). Simple method for determination of biodegradable organic carbon in water. *Appl. Environ. Microbiol.*, Vol. 55 (10), pp. 2732-2734.

Takahishi, M., H. Okamiya, F. Furuwaka, K. Toyoda, H. Sato, K. Imaida, and Y. Hayashi (1989). Effects of glyoxal and methylglyoxal administration on gastric carcinogenesis in wistar rats after initiation with N-methyl-N'-nitro-N-nitrosoguandine. *Carcinogenesis*, Vol. 10 (10), pp. 1925-1927.

Urfer, D., P.M. Huck, S.D.J. Booth, and B.M. Coffey (1997). Biological filtration for BOM and particle removal: a critical review. *Jour. AWWA*, Vol. 89 (12) pp. 83-98.

van der Kooij, D., A. Visser, and W.A.M. Hijnen, (1982). Determining the concentration of easily assimilable organic carbon in drinking water. *Jour. AWWA*, Vol. 74 (10) pp.540-545.

van der Kooij, D. and W.A.M. Hijnen, (1984). Substrate utilization by an oxalate-consuming *Spirillum* species in relation to its growth in ozonated water. *Appl. Environ. Microbiol.*, Vol. 47, pp. 551-559.

van der Kooij, D., W.A.M. Hijnen, and J.C. Kruithof (1989). The effects of ozonation, biological filtration and distribution on the concentration of easily assimilable organic carbon (AOC) in drinking water. *Ozone Sci. and Eng.*, Vol. 11, pp. 297-311.

Wang, J. Z., and R.S. Summers (1995). A heterogeneous biofiltration model for natural organic matter utilization. Proc. AWWA Annual Conference, Anaheim, CA.

Wang, J. Z., R.S. Summers, R.J. Miltner (1995). Biofiltration performance: part 1, relationship to biomass. *Jour. AWWA*, Vol. 87 (12), pp. 55-63.

Weinberg, H.S., W.H. Glaze, and S.W. Krasner (1992). Control of polar by-product formation in ozonation plants. Proc. AWWA WQTC, Toronto, Ontario, Canada.

Weinberg, H.S., W.H. Glaze, S.W. Krasner, and M.J. Sclimenti (1993). Formation and removal of aldehydes in plants that use ozonation. *Jour. AWWA*, Vol. 85 (5), pp. 72-85.

Woolschlager, J., and B.E. Rittmann (1994). Evaluating what is measured by the BDOC and AOC tests. Presented at International Seminar on Biodegradable Organic Matter, Montréal, Québec, Canada.

Xie, Y. and D.A. Reckhow (1992). Formation of ketoacids in ozonated drinking water. *Ozone. Sci. and Eng.*, Vol. 14, pp. 269-275.

Zhang, S. and P.M. Huck (1996). Removal of AOC in biological water treatment processes: a kinetic modeling approach. *Wat. Res.*, Vol. 30 (5), pp.1195-1207.

CHAPTER 3: MATERIALS AND METHODS

The purpose of this chapter is to describe the details of the batch bioreactors, bench-scale filter system, and also the analytical methods used in this research.

BATCH BIOREACTOR EXPERIMENTS

The batch bioreactor experiments were performed using synthetic waters in 500 mL Erlenmeyer shake flasks. These experiments were conducted at room temperature (20 ± 2 °C). Prior to beginning an experiment the shake flasks were washed with hot distilled water and detergent, then rinsed a minimum of ten times with deionized water prepared from a Milli-Q® system (Millipore Corp.; Bedford, MA). Three hundred mL of a mineral medium consisting of sodium nitrate ($NaNO_3$), potassium phosphates (K_2HPO_4 and KH_2PO_4) and magnesium sulfate ($MgSO_4$) was added to deionized water, the tops of the flasks were covered with aluminum foil, and the flasks were autoclaved. Autoclaving occurred for 20 minutes at 121°C and 15 psig, unless otherwise specified.

The concentrations of K_2HPO_4 and KH_2PO_4 in the mineral medium were established such that their ratio was 2.7:1 on a molar basis. The target concentration of $MgSO_4$ in the shake flasks was 0.1 mg/L. The necessary quantity of mineral medium was prepared from a concentrated stock using

freshly cleaned glassware that had also been rinsed a minimum of ten times with deionized water. The pH of the stock was 7.0 ± 0.2, and the final pH of the water in the flasks was between 6 and 7, depending on the BOM components added. Aseptic techniques (Brock and Madigan, 1997) were utilized whenever sampling from, or adding components to, the flasks.

The concentrations of the nitrogen and phosphorus containing components of the mineral medium were established such that the molar ratio of carbon (C), nitrogen (N) and phosphorus (P) was approximately 100:20:5. Camper (1994) found that the required C:N:P ratio for microbial growth in drinking water distribution systems was 100:10:1. The ratio selected for the present research provides excess nitrogen and phosphorus, and thus ensures that growth is limited by the organic carbon components added to the flasks. Because the amount of organic carbon was not consistent in all flasks, there was some variation in this ratio, however, even given these deviations, carbon was the limiting nutrient in all cases. Table 3.1 shows the C:N:P ratios for target concentrations of acetate and pyruvate, in example groupings. The target concentrations of the organic compounds were equal on a molar basis.

Table 3.1: Example C:N:P Ratios

Flask	Organic Components	Concentration		C:N:P
		µg/L	µmol/L	
1	acetate	236	4	100:38:10
2	pyruvate	348	4	100:25:7
3	acetate, pyruvate	236, 348	4, 4	100:15:4

The initial volume of 300 mL is greater than the 20% capacity often recommended for shake flask work (Brock and Madigan, 1997). The higher volume was selected to allow a greater number of liquid samples to be withdrawn. By starting with a volume of about 20% of the flask size, mixing and thus oxygen transfer, are maximized in shake flasks. However, under the conditions in which these experiments were performed, oxygen was not likely to be limiting. The dissolved oxygen of the liquid, one day after autoclaving,

was normally close to saturation (*i.e.* in the range of 7 to 8 mg/L), and did not significantly change during the course of an experiment. This was expected because of the low concentration of organic carbon, and consequently low theoretical oxygen demand, in the flasks. For example, a flask containing 236 μg/L of acetate and 348 μg/L of pyruvate would require only 0.58 mg O_2/L for complete mineralization. Thus, much more than sufficient oxygen was initially present in the liquid to accommodate the oxidation of these components, without considering the transfer of oxygen from the head space above the liquid.

The flasks were allowed to cool overnight, and then inoculated with a sample of filter (GAC/sand) effluent from a full-scale treatment plant, which had ozonation upstream of the filter. The source water for this plant was from the Grand River. A 20 L sample, which was stored at 4°C, was sufficient for all of the batch experiments. This inoculum was expected to contain a suspended microbial population representative of the filter biofilm population. The amount of inoculum added to the flasks was 3% on a volumetric basis. The flasks were inoculated two to three days prior to the addition of BOM to allow the population to adapt to the environmental conditions in the shake flasks. Without this acclimation period, it was found that little growth, nor organic component utilization, occurred within the first two days after inoculation. This initial lag was minimized by allowing an acclimation period, following which, specific ozone by-products were added to the flasks. Stock solutions of individual ozone by-products were prepared by adding the calculated amount of purchased stock solutions to autoclaved water. Two replicate flasks were included for each group of ozonation by-products investigated in a given experiment. Sterile rubber stoppers covered with teflon tape were placed in the tops of all flasks, and the flasks were placed on a shaker table at 120 RPM.

Samples for chemical analysis were aseptically removed from the flasks by decanting into sample vials. The sample vials were not normally

autoclaved, however, the tops of the vials were flamed several times prior to sampling. The samples for heterotrophic plate count analysis were aseptically withdrawn from the flasks with a pipettor. The pipette tips were autoclaved and cooled, prior to use.

Experimental Design

The goal of the batch experiments was to determine if the presence of specific ozonation by-products affected the utilization rate of a given ozonation by-product and to monitor for detectable transformation products. The utilization rates were compared by calculating kinetic parameters of each compound, in each group studied, with 95% confidence intervals. Utilization rates among compounds were considered to differ significantly if the confidence intervals did not overlap. The transformation products were reported, if any were detected.

BENCH-SCALE FILTER EXPERIMENTS

Bench-Scale Filters

The filter columns were of glass construction with an inside diameter of 5 cm (2 in.). An overflow port was present at the top of the filter which meant that the filters were operated with a constant head, which was normally 1.1 m above the top of the filter media. The depth of the media varied somewhat with each experiment and also over the course of a given experiment, because media was removed for analysis. A schematic of the filter system is shown in Figure 3.1. The flowmeter and flow direction at the effluent end were the same for all of the filters, however, in Figure 3.1, these are only shown for the first filter.

Wall effects and channeling are considered to be negligible when the ratio of the filter diameter to the media particle size is equal to or greater than 50 (Perry *et al.*, 1984). The anthracite used in this research had an effective size of 1 mm, therefore the ratio in this research was 50, which satisfies the criterion.

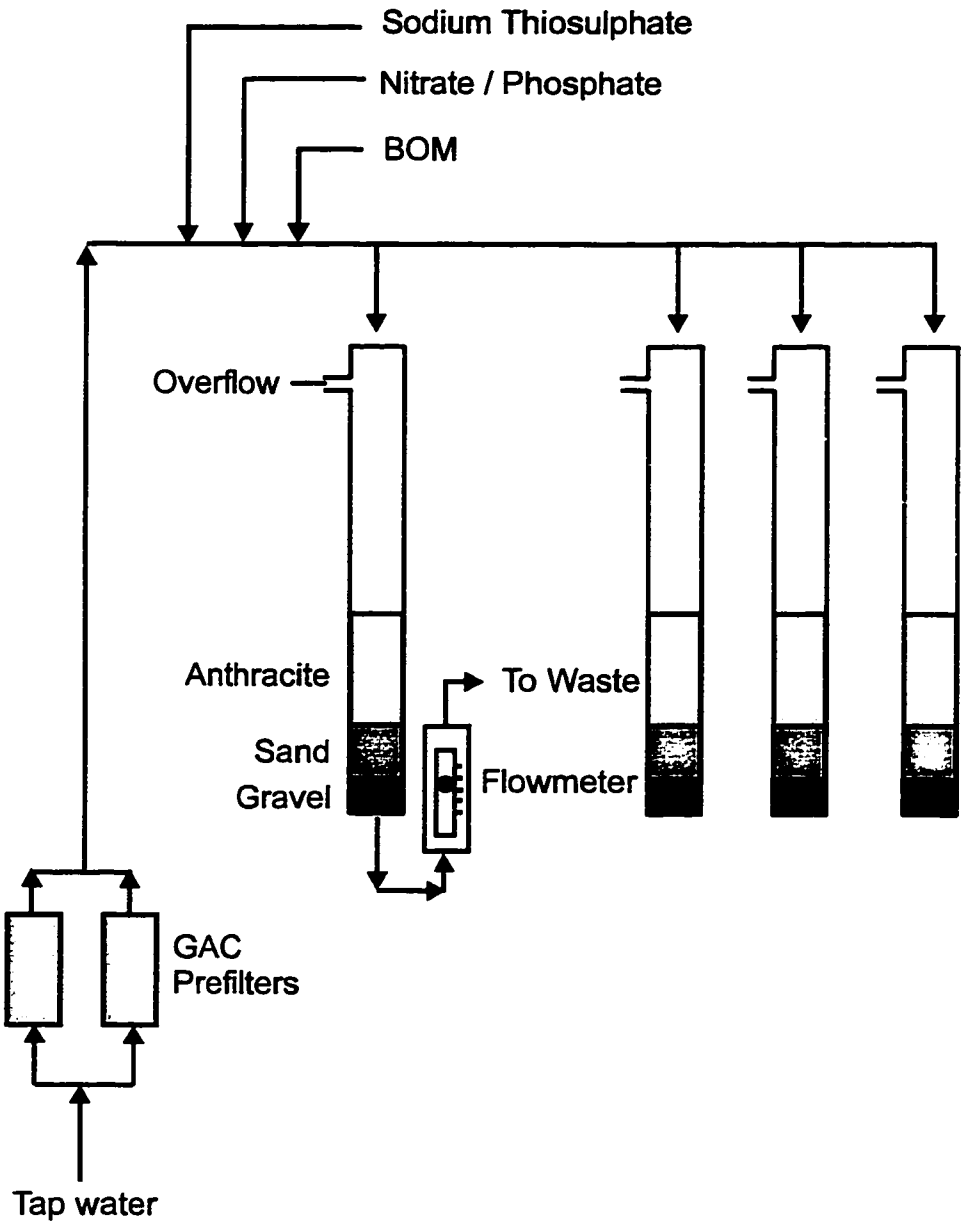

Figure 3.1: General schematic of filter apparatus.

Each filter had eight sample ports, the uppermost of which served as the filter influent sample port. The spacing of the sampling ports is given in Table 3.2. Samples were collected by piercing the sample port septum with a 50 mL glass syringe with a stainless steel needle, and extracting a sample from the centre of the filter. The septa were lined with teflon on the inside, and silicon on the outside. Effluent samples were obtained via a plug valve located on the effluent line, just below the filter.

Table 3.2: Sample Port Depths

Port	Media	Depth below top of media
Influent		(5 cm above media)
1	Anthracite	5 cm
2	Anthracite	10 cm
3	Anthracite	15 cm
4	Anthracite	25 cm
5	Anthracite	40 cm
6	Sand	55 cm
7	Sand	70 cm

The filter columns were filled with 25 cm of fresh sand and 50 cm of fresh anthracite at the start of each experiment, providing a total bed depth of 75 cm. The effective size and uniformity coefficients were 1 mm and 1.6 for the anthracite, and 0.5 mm and 1.5 for the sand. The media rested on about 15 cm of graded gravel which acted as a support, and also flow distributor when the filters were backwashed. The media was backwashed several times during the filling process, and three times prior to the start of an experiment to remove fines.

The flow rate through the filter was measured and controlled by a flowmeter with a valve, on the effluent line. The flow rate will normally decline during a filter run when the head is held constant, however, due to the low turbidity of the influent water the flow rate could usually be maintained at the target level throughout the filter run. The influent water was tap water from a ground water source, with a high alkalinity (300 to 325 mg/L as $CaCO_3$) and hardness (325 to 350 mg/L as $CaCO_3$), a total organic carbon concentration of about 1.0 to 1.5 mg-C/L, and a pH of about 7.5.

These filters had a media depth and type typical of drinking water treatment practice, while the surface area was much less than full-scale filters. These dimensions permitted experiments to be conducted using hydraulic loading rates and empty bed contact times (EBCTs) representative of full-scale practice, without using an excessive volume of water.

Physical Configuration

A general schematic for the filter experiments was presented in Figure 3.1. To summarize, tap water was fed to the filters directly from the tap through teflon tubing and stainless steel valves and fittings. The water then passed through one of two parallel glass GAC pre-filters, each with an inside diameter of 5 cm (2 in.), a length of 60 cm (24 in.), and providing an EBCT of 1.5 to 2 min, depending on the water flow rate for that experiment. The GAC had been exhausted with respect to TOC removal, and had been in use for over three years in a full-scale filter. The pre-filters were primarily designed to remove a free chlorine residual, although they may have also removed a small amount of BOM, if it was present. Normally a negligible chlorine residual (< 0.05 mg Cl_2/L) was measured in the pre-column effluent. After these pre-filters sodium nitrate ($NaNO_3$), potassium phosphate (K_2HPO_4), and BOM were added. These solutions were pumped from 3.8 L amber glass bottles. The nitrogen and phosphorus containing compounds were combined in one bottle, while separate bottles were used for each organic component. The C:N:P ratio was targeted at 100:20:5 on a molar basis.

All of these solutions were prepared by autoclaving 3.0 L of deionized water in the amber bottles, which had been previously washed and rinsed a minimum of six times with deionized water. After the bottles had cooled to room temperature the calculated quantity of pure component was added aseptically to the bottles and mixed well. These cocktails were pumped with peristaltic pumps using PharMed® tubing (Norton Co.). New tubing was used for each experiment. It was autoclaved prior to the start of an experiment, and every two to three weeks during the course of an experiment.

During the second and third filter experiments sodium thiosulphate ($Na_2S_2O_3$) was used to quench a monochloramine residual in the tap water. During this period, the tap water typically contained 0.5 mg Cl_2/L, about half of which was removed in the GAC pre-filters, with the remainder being quenched by thiosulphate according to the following reaction:

$$S_2O_3^{2-} + 4NH_2Cl + 5H_2O \rightarrow 4Cl^- + 2SO_4^{2-} + 4NH_4^+ + 2H^+ \qquad (3.1)$$

Both the residual monochloramine and thiosulphate were monitored during these two experiments.

In the third filter experiment the influent water for two of the filters was passed through a heat exchanger, to raise its temperature. The heating water flowing through the heat exchanger was passed through a recirculating heater (Model Lauda RM6; GmbH and Co., Germany).

Backwashing Protocol

Prior to backwashing the influent water valve was closed, and the filter was allowed to drain until the water level was a few centimetres above the top of the media. Water was then pumped in the upflow mode at 40% of the fluidization velocity, or 12 m/h. Air was also passed up through the filter, at 50 m/h (at standard temperature and pressure) such that air scouring occurred in a process termed "collapse-pulsing" (Amirtharajah *et al.*, 1991). During this process the media is cleaned due to the scouring action among the media grains. Collapse-pulsing was maintained for 3 minutes, following which, the air was turned off, and the water flow rate was increased to 35 m/h, to achieve a 20% bed expansion. This continued for 4 minutes to allow sufficient time for the dirty backwash water to be forced out the overflow at the top of the filter. Each filter was backwashed with its own effluent water, which had been previously collected and stored in glass carboys. Backwashing was performed every three to four days.

Experimental Design

The experimental design details of each of the three filter experiments are discussed in separate sections of Chapter 6. The third experiment was a two-level factorial experiment. The purpose of a factorial experiment is to determine which "factors" have a significant impact on the "response" of a process. In a two-level factorial experiment a trial must be conducted at high and low levels of each of the factors. The results of this experiment were

analyzed using the analysis of variance approach (ANOVA), as described by Box *et al.* (1978), which was used to determine the significant factors and interactions. Further details for all of the experiments are given in Chapter 6.

ANALYTICAL PROCEDURES

Carboxylic Acids

A recently developed ion chromatographic (IC) method (Peldszus *et al.*, 1996; Peldszus *et al.*, 1997) was used to analyze for carboxylic acids. Without any sample preparation, samples were injected directly into the IC using a large sample loop (740 μL). Utilizing a sodium hydroxide gradient (8 mM/10 min - 13 min - 125 mM/10 min) the organic acids were separated on an anion exchange column (AS 10, Dionex, Sunnyvale, CA) followed by conductivity detection. Low background conductivity was achieved with the use of an anion self generating suppresser (ASRS I, 4 mm, Dionex, Sunnyvale, CA), which was operated in the external water mode because of the relatively high sodium hydroxide concentration at the end of the gradient (125 mM). The carboxylic acids were identified by their retention time.

The samples for this research were preserved with 0.1% v/v chloroform ($CHCl_3$), stored at 4°C immediately after sampling, and measured within 2 weeks of their collection. Latex gloves were worn and all glassware and vials that came in contact with the samples were thoroughly rinsed with deionized water to minimize contamination. Fresh standards were prepared on the day of analysis by diluting a 100 mg/L stock to one or two dilutions in the range of 50 to 200 μg/L. The carboxylic acids included in this stock (with minimum reporting limits in parentheses) were hydroxybutyrate (2 μg/L), acetate (5 μg/L), glycolate (1 μg/L), butyrate (1 μg/L), formate (2 μg/L), pyruvate (3 μg/L), α-ketobutyrate (2 μg/L), and oxalate (9 μg/L). The standards were diluted in deionized water for the batch experiments and in tap water for the filtration experiments. The standards were run approximately every six injections in every sample queue. Method blanks were also included in every queue.

Aldehydes

Aldehydes were derivatized at room temperature overnight by oximation with *o*-(2,3,4,5,6-pentafluorobenzyl)-hydroxylamine hydrochloride (PFBHA), and extracted with hexane, as described by Sclimenti *et al.* (1990) and Eaton *et al.* (1995). The samples were analyzed by gas chromatography with electron capture detection (GC-ECD) (model HP 5890 series II, Hewlett-Packard; Sunnyvale, CA). The aldehydes were identified by their retention time. The extracted samples were stored at -10 °C for up to 30 days. One day prior to analysis fresh standards and method blanks were prepared. Standards and blanks were run after every 8 injections. The aldehydes contained in the standard (with minimum reporting limits in parentheses) were: formaldehyde (1.6 μg/L), glyoxal (3.5 μg/L), methylglyoxal (2.5 μg/L), and acetaldehyde (2.0 μg/L).

The hexane used for extracting the derivatized aldehydes contained an internal standard (dibromopropane). The areas of the aldehydes calculated from the chromatograms were not normalized for the dibromopropane area, however, its area was monitored in each sample. It was found that the coefficient of variation of the dibromopropane area was in the range of 2 to 7% for all sample queues. The fact that the dibromopropane concentration was reasonably constant, indicated that evaporative hexane losses and variability due to fluctuations in the injected sample volume were minimal.

Amino Acids

The amino acids were analyzed by precolumn derivatization with orthophthaldialdehyde (OPA) followed by analysis with high pressure liquid chromatography (HPLC), as described by Dossier-Berne *et al.* (1994). The mobile phase (mobile phase A was acetate/phosphate buffer, pH 7.4; mobile phase B was 75% methanol) was introduced to the column using a 600 E Multi-Solvent Delivery System (Waters Corp.; Milliford, MA). The sample was introduced to the system with a Waters 717 Autosampler (Waters Corp.; Milliford, MA), and quantified with a Waters 470 Scanning Fluorescence

Detector (Waters Corp.; Milliford, MA). Serine and glycine were the only amino acids investigated in this study, and their minimum reporting limits were both 5 μg/L. These samples were analyzed by Sigrid Peldszus and Andrea Chute, chemists within the Industrial NSERC Chair for Drinking Water Treatment.

Non-Purgeable Organic Carbon (NPOC)

Non-purgeable organic carbon (NPOC) was measured using a Xertex Dohrmann DC-180 Total Carbon Analyzer using Method 5310C in Standard Methods for the Examination of Water and Wastewater (Eaton *et al.*, 1995). Each reported value was typically the average of 3 determinations. The coefficient of variation for replicate measurements was normally smaller than the value of 2% cited for the method. These samples were analyzed by Andrea Chute and Val Goodfellow, chemists within the Industrial NSERC Chair for Drinking Water Treatment.

Chlorine

There was essentially no chlorine residual in the tap water for the first filter experiment. Early in the second filtration experiment a monochloramine residual appeared of approximately 0.5 mg Cl_2/L. About half of this residual was removed in the GAC pre-filters, and the remainder was quenched by thiosulphate, as explained above. Thus, the main purpose of the chlorine residual monitoring was to ensure that it was completely quenched, prior to the filter influent. Chlorine was measured using the colorimetric version of the N,N-diethyl-p-phenylenediamine (DPD) method (Eaton *et al.*, 1995). Measurements were made with a DR-200 UV-Visible spectrophotometer (HACH Co.; Loveland, CO) at a wavelength of 530 nm. The detection limit was 0.02 mg Cl_2/L.

Sodium Thiosulphate

Sodium thiosulphate was added during the second and third filtration experiments in order to quench a monochloramine residual, as explained in the

Physical Configuration section above. This quenching process essentially completely removed the chlorine residual, however, a measurable quantity of thiosulphate normally remained. Its concentration could be monitored by using the carboxylic acid method described above, without any modifications. Using this method the minimum reporting limit was 0.025 mg $Na_2S_2O_3$/L.

Heterotrophic Plate Counts

Bacterial numbers were determined by heterotrophic plate counts (HPCs) on R2A agar using the spread plate technique according to method 9215C of Standard Methods for the Examination of Water and Wastewater (Eaton *et al.*, 1995). Samples were serially diluted with autoclaved, deionized water. Dilutions were plated in duplicate and incubated at room temperature (20 ± 2°C) for 7 days. Plates which contained between 30 and 300 colony forming units (CFUs) were selected for counting, and the results were expressed as CFUs per mL.

Phospholipid Method

The amount of living biomass on the filter media was quantified by determining its phospholipid content using the method of Findlay *et al.* (1989), with minor modifications. Briefly, between 0.1 and 1.0 g of media was transferred to a 20 mL screw cap vial. The phospholipids contained in the cell membranes of the biofilm cells were extracted into a chloroform-methanol-water mixture, in a volumetric ratio of 1:2:0.8. This mixture was allowed to stand overnight, then separated into a lipid-containing chloroform phase and a methanol-water phase by the addition of chloroform and water, such that the final volumetric ratio of chloroform-methanol-water was 1:1:0.9. The chloroform was transferred to another vial and evaporated using nitrogen gas. The remaining lipids were then digested using potassium persulfate to liberate inorganic phosphate. The phosphate was quantified using ammonium molybdate and malachite green, as described by VanVeldhoven and Mannaerts (1987). The absorbance of the sample at 610 nm was measured using a UV-Visible spectrophotometer (model HP 8453, Hewlett-Packard;

Sunnyvale, CA). The absorbance was related to the inorganic phosphate concentration by the use of a standard curve. Duplicate samples were always obtained, with each being analyzed once. Blank samples were analyzed in order to monitor for possible phosphate contamination.

The standard curve was created by measuring the absorbance of standard solutions of K_2HPO_4 (Figure 3.2). As shown in Figure 3.2, at concentrations greater than approximately 55 nmol PO_4^{3-}/mL, the absorbance did not change with phosphate concentration. Therefore, only samples which fell into the linear range of the calibration curve could be successfully analyzed. By making the assumption that each mole of phospholipid contains one mole of inorganic phosphate, the results could be reported as nmol lipid-P per g dry filter media, or per cm^3 of filter bed. The minimum reporting limit for this method was 2 nmol lipid-P/g media.

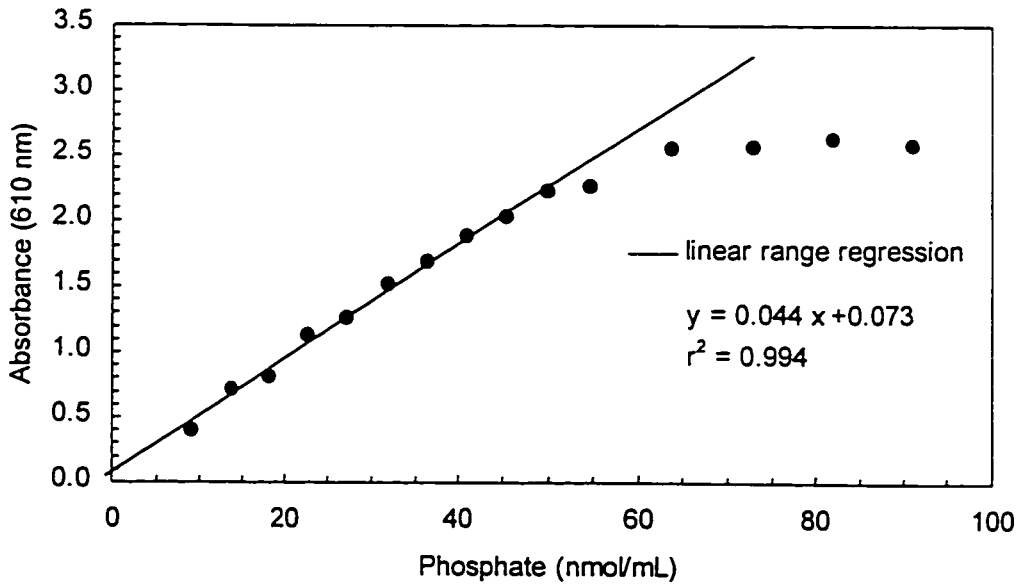

Figure 3.2: Calibration curve for phospholipid method.

Characterization of Microbial Communities

Some microbial communities used in the batch reactor experiments were characterized using the BIOLOG® system (Biolog, Inc.; Hayward, CA). This is a redox-based system for carbon source utilization testing of bacterial

isolates. Colour produced by the reduction of tetrazolium violet is used as an indicator of respiration of sole carbon sources. The commercially available microplates allow for simultaneous testing of 95 different carbon sources. After a 24 hour incubation period, the results from each well are entered into a software program which seeks to match the pattern with one in its database. Both Gram negative and positive plates were available. Although this system was originally intended for identifying pure strains, it has also been used for characterizing communities (*e.g.* Haack *et al.*, 1995; Garland and Mills, 1991). In this case the results represent a characteristic pattern, or "fingerprint", in carbon source use. This pattern can be monitored over time, or correlated with other relevant variables, to detect changes in the metabolic response of the population under study.

The communities for analysis were incubated on R2A agar for 7 days, or until sufficient CFUs had developed. Cells were then aseptically transferred to a dilution tube with a swab. Sufficient cells were transferred such that the turbidity of the cell suspension was in the specified target range. 150 μL of this suspension was then transferred to each well in the microplate, and incubated for 24 hours. An alternative method would have been to directly transfer samples from the shake flasks to the microplates. This method was not employed because the biomass concentration of the water in the shake flasks was far below the specified turbidity target range. Wells which developed no colour were considered negative, a purple colour were positive, and a light purple colour were identified as "borderline". For each sample the 8x12 matrix of results was saved for comparison with other analyses, or with other communities. All samples were analyzed in duplicate.

Other Measurements

Temperature and dissolved oxygen were measured with a portable meter (Orion model #835; Analytical Technologies Inc., Boston, MA). pH was monitored using a pH meter (Orion model #710A; Analytical Technologies Inc., Boston, MA).

All chemical products were purchased from Aldrich Chemical Company Inc. (Milwaukee, WI), and the microbiological media was purchased from BBL Products (Becton Dickinson Microbiology Systems; Cockeysville, MD).

REFERENCES

Amirtharajah, A., N. McNelly, G. Page, and J, McLeod (1991). Optimum Backwash of Dual Media Filters and GAC Filter-Adsorbers with Air Scour. AWWA Research Foundation, Denver, Colorado, USA.

Box, G.E.P., W.G. Hunter, and J.S. Hunter (1978). Statistics for Experimenters. John Wiley and Sons Inc., New York, New York, USA.

Brock, T.D. and Madigan, M.T. (1997). Biology of Microorganisms, 8th Edition. Prentice Hall, Upper Saddle River , New Jersey, USA.

Camper, A.K. (1994). Coliform regrowth and biofilm accumulation in drinking water systems: a review, in Biofouling and Biocorrosion in Industrial Water Systems, G.G. Geesy, Z. Lewandowski, and H.C. Flemming (Eds.). CRC Press Inc., Boca Raton, Florida, USA.

Dossier-Berne, F., B. Panais, N. Merlet, B. Cauchi, and B. Legube (1994). Total dissolved amino acids in natural and drinking waters. *Environ. Technol.*, Vol. 15, pp. 901-916.

Eaton, A.D., L.S. Clesceri, and A.E. Greenberg (Eds.) (1995). Standard Methods for the Examination of Water and Wastewater, 19th Edition. American Public Health Assoc., Washington, DC, USA.

Findlay, R.H., G.M. King, and L. Watling (1989). Efficacy of phospholipid analysis in determining microbial biomass in sediments. *Appl. Environ. Microbiol.*, Vol. 55, pp. 2888-2893.

Garland, J.L., and A.L. Mills (1991). Classification and characterization of heterotrophic microbial communities on the basis of patterns of community-level sole-carbon-source utilization. *Appl. Environ. Microbiol.*, Vol. 57, pp. 2351-2359.

Haack, S.K., H. Garchow, M.J. Klug, and L.J. Forney (1995). Analysis of factors affecting the accuracy, reproducibility, and interpretation of microbial community carbon source utilization patterns. *Appl. Environ. Microbiol.*, Vol. 61, pp. 1458-1468.

Peldszus, S., P.M. Huck, and S.A. Andrews (1996). Determination of short chain aliphatic, oxo- and hydroxy- acids in drinking water at low µg/L concentrations. *J. Chromatogr. A.*, Vol. 723, pp. 27-34.

Peldszus, S., P.M. Huck, and S.A. Andrews (1997). Quantitative determination of oxalate and other organic acids in drinking water at low µg/L concentrations. Submitted to *J. Chromatogr. A.*

Perry, R.H., D.W. Green, and J.O. Maloney (Eds.) (1984). Perry's Chemical Engineers' Handbook, 6th Edition. McGraw-Hill, New York, New York, USA.

Sclimenti, M.J., Krasner, S.W., Glaze, W.H. and Weinberg, H.S. (1990). Ozone disinfection by-products: optimization of the PFBHA derivitization method for the analysis of aldehydes. Proc. AWWA WQTC, San Diego, California, USA.

Van Veldhoven, P.P., and G.P. Mannaerts (1987). Inorganic and organic phosphate measurements in the nanomolar range. *Anal. Biochem.*, Vol. 161, pp. 45-48.

CHAPTER 4: CONCEPTUAL METABOLIC MODEL

A number of the ozonation by-products introduced in Chapter 2 are also naturally occurring microbial substrates or metabolites (Gottschalk, 1986). This implies that these compounds are expected to be readily biodegraded by microbes and moreover, that these compounds may be released by microbes as a part of normal metabolism, or as a result of death and cell lysis. It may be important to consider these possibilities when contemplating the removal efficiency of ozonation by-products in biologically active filters. In this chapter the pathways which involve the ozonation by-products of interest in this research are introduced, discussed, and then assembled into a simplified conceptual model.

REVIEW OF MAJOR MICROBIAL METABOLIC PATHWAYS

Tricarboxylic Acid and Glyoxylate Cycles

The tricarboxylic acid (TCA) and glyoxylate cycles are important metabolic pathways which can produce both energy and biosynthetic building blocks, and are called amphibolic pathways for this reason. Both the TCA and glyoxylate cycles are shown in Figure 4.1. The TCA cycle consists of the reactions represented in the outer circle, while the reactions in the interior of this circle are those of the glyoxylate cycle. The input to the TCA cycle is acetyl-coenzyme A or acetyl-CoA, which is often formed from the partial oxidation of pyruvate. This cycle forms four-, five- and six-carbon chains,

which can be used for biosynthesis, in addition to being intermediates in the cycle (Brock and Madigan, 1997). In an environment in which only two-carbon compounds are available, all cell constituents must be formed from two-carbon sub-units. The cycle can only continue, however if oxalacetate is formed during each turn of the cycle, and thus the cycle breaks down if intermediates are removed to provide biosynthetic building blocks. Under such conditions anaplerotic, or "filling in", reactions are required. The glyoxylate cycle provides such anaplerotic reactions, by replacing key intermediates, especially oxalacetate, which is the starting point for gluconeogenesis (*i.e.* carbohydrate synthesis) (Gottschalk, 1986).

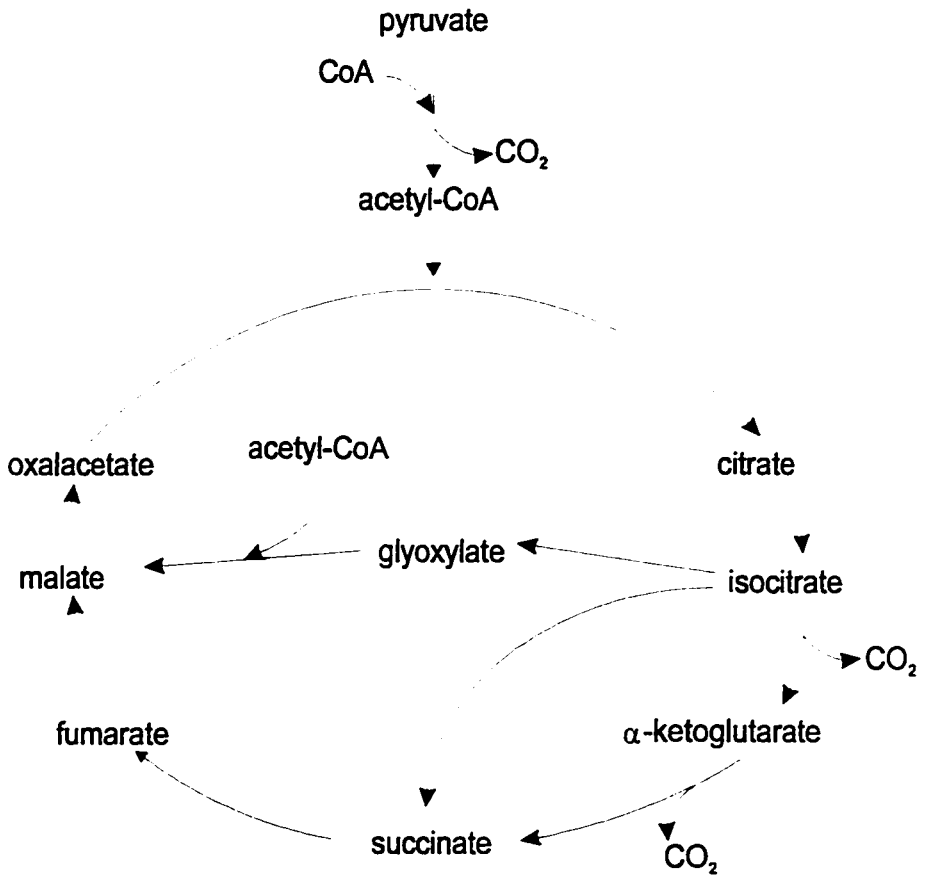

Figure 4.1: TCA and glyoxylate cycles.
(Madigan/Martinko, BROCK BIOLOGY OF MICROORGANISMS, 8/e, © 1997, pp. 136, 520. Reprinted by permission of Prentice-Hall, Upper Saddle River, New Jersey.)

Embden-Meyerhof-Parnas Pathway

The Embden-Meyerhof-Parnas (EMP) pathway describes the classic representation of the breakdown of glucose. The pathway from glucose to pyruvate is termed glycolysis, and is shown in Figure 4.2. The reactions from glucose to fructose-1,6-diphosphate do not involve oxidation-reduction reactions, nor do they release energy, but lead to the formation of glyceraldehyde-3-phosphate. The subsequent steps are oxidation reactions which result in the production of energy, and the formation of pyruvate from glyceraldehyde-3-phosphate. The reactions can continue from pyruvate to form fermentation products, such as ethanol and carbon dioxide. These anaerobic reactions are not shown because they are not likely to occur in biologically active drinking water filters. In the presence of molecular oxygen pyruvate is completely oxidized to carbon dioxide, with a much greater yield of energy. An important pathway for the complete oxidation of pyruvate is the TCA cycle, described above (Figure 4.1). However, Moll *et al.* (1998) found that sulfate-reducing bacteria and other anaerobes were more prevalent in a filter treating a synthetic ozonated water compared to a filter fed a non-ozonated, conventionally treated water. They speculated that these bacteria existed in anaerobic microniches, which may have been more prevalent in the filter treating the ozonated water, because it was known to have a much greater biomass. Therefore, although the possibility of anaerobic activity cannot be entirely excluded, aerobic metabolism is expected to be dominant, and was therefore the focus of the present research.

Also shown in Figure 4.2 is the so-called methylglyoxal bypass, which consists of the reactions on the left-hand side. This bypass is known to exist in *Escherichia coli* and *Pseudomonas saccharophila* (Gottschalk, 1986). An important aspect of these reactions is that they allow the formation of pyruvate from dihydroxyacetonephosphate, under conditions where low inorganic phosphate (P_i) concentrations limit the conversion of glyceraldehyde-3-phosphate to 1,3-diphosphoglycerate.

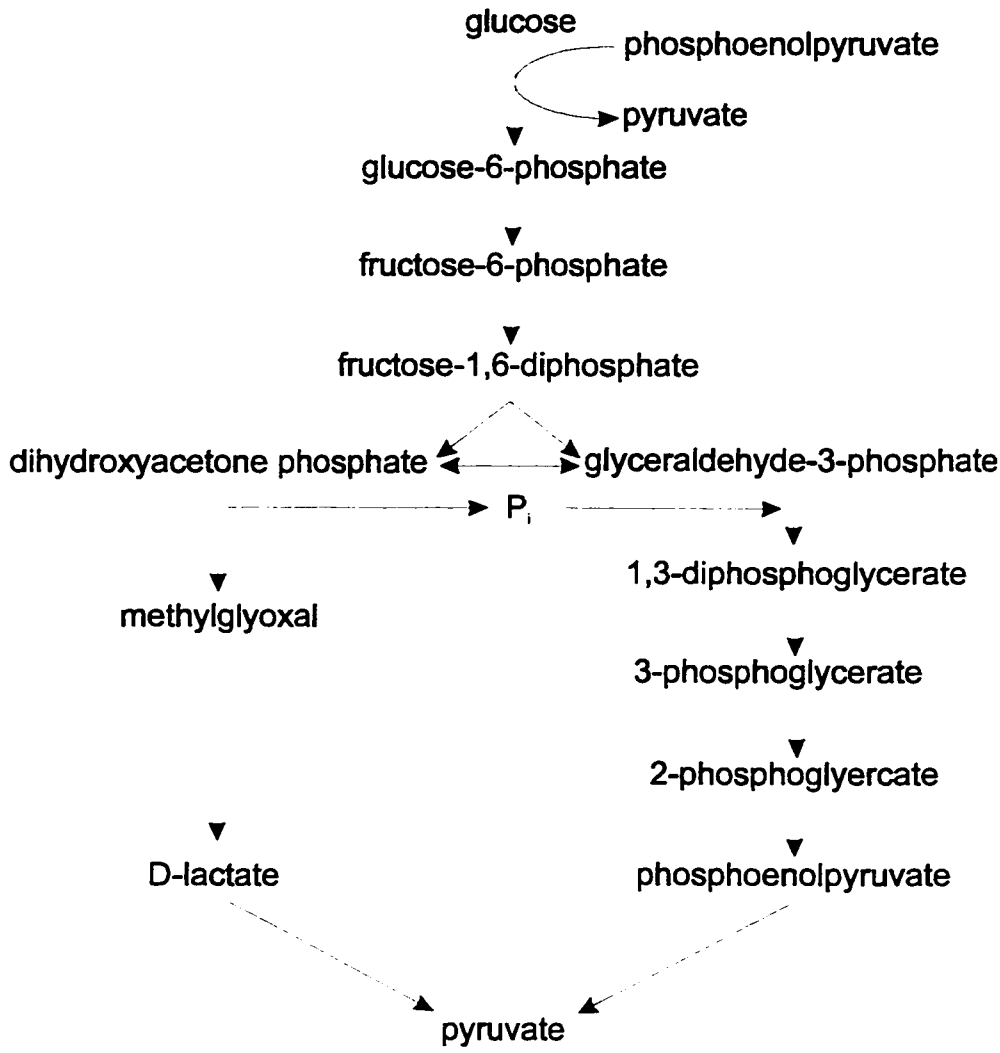

Figure 4.2: EMP pathway with methylglyoxal bypass.
(Reprinted with permission, from the Annual Review of Microbiology, Volume 38, © 1984, by Annual Reviews).

Methylglyoxal has been detected accumulating in the growth medium of mutant strains known to lack pyruvate kinase, the enzyme which produces pyruvate from phosphoenolpyruvate (shown at the bottom right of Figure 4.2), while growing on either maltose or lactose (Cooper, 1984). Although unconfirmed, it was speculated that the functioning of the methylglyoxal bypass may have been responsible for the methylglyoxal production. Also, mutants which cannot convert dihydroxyacetonephosphate to glyceraldehyde-3-phosphate (*i.e.* triosephosphate isomerase-negative) have been shown to produce methylglyoxal in the growth medium during growth on gluconate.

Thus, methylglyoxal can be a key intermediate in glucose metabolism, in addition to accumulating outside of cells. The methylglyoxal bypass is important because it shows the metabolic sequence by which pyruvate can be formed from methylglyoxal, and thus provides a possible means by which growth on methylglyoxal as sole substrate may be possible.

Serine and Ribulose Monophosphate Pathways

Methylotrophic bacteria are those which can oxidize single-carbon compounds for energy or as sole sources of carbon. Methylotrophs are generally considered aerobic. A specific sub-group of the methylotrophs are the methanotrophs, which are able to take advantage of the extensive supply of methane found in nature. Two special pathways are known which permit methylotrophs to utilize single carbon substrates. The serine pathway is possessed by Type II methylotrophic bacteria (Figure 4.3), while Type I methylotrophs possess the ribulose monophosphate cycle (Figure 4.4). The serine pathway results in the production of acetyl-CoA, while the output of the ribulose monophosphate cycle is glyceraldehyde-3-phosphate. Both of these intermediates are central biosynthetic building blocks.

It is not known which of these pathways, if either, is likely to be predominant in the bacteria inhabiting drinking water biologically active filters. The serine pathway may be more prevalent since it is possessed by facultative methylotrophs such as *Pseudomonas* (Brock and Madigan, 1997), which has been identified as a dominant bacterial genus inhabiting GAC and sand filters (Burlingame *et al.*, 1986). GAC and sand are common filter media in drinking water treatment plants. Also, since the single carbon compounds formate and formaldehyde have been shown to be readily removed in biofilters (*e.g.* Krasner *et al.*, 1993; Urfer and Huck, 1997) it is reasonable to assume that at least one of these common pathways is normally functional.

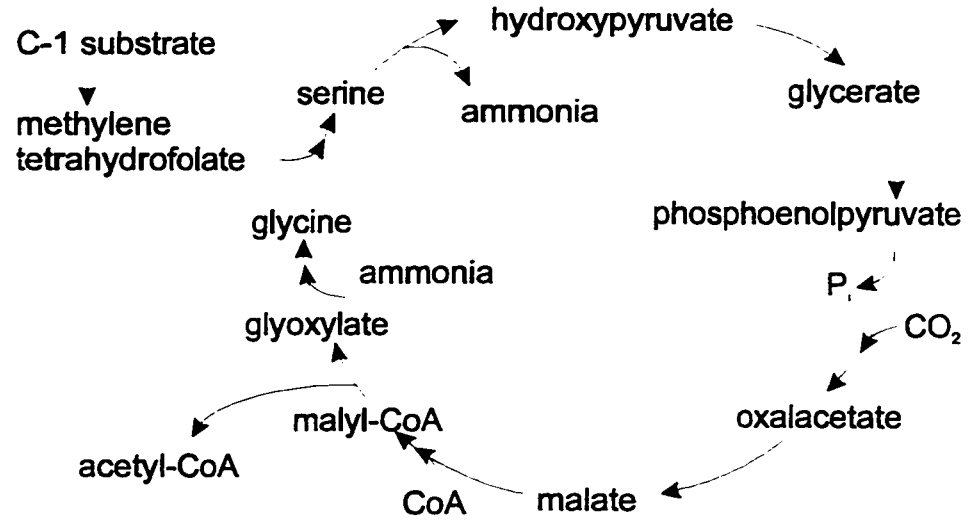

Figure 4.3: Serine pathway.

(Madigan/Martinko, BROCK BIOLOGY OF MICROORGANISMS, 8/e, © 1997, pp. 670. Reprinted by permission of Prentice-Hall, Upper Saddle River, New Jersey.)

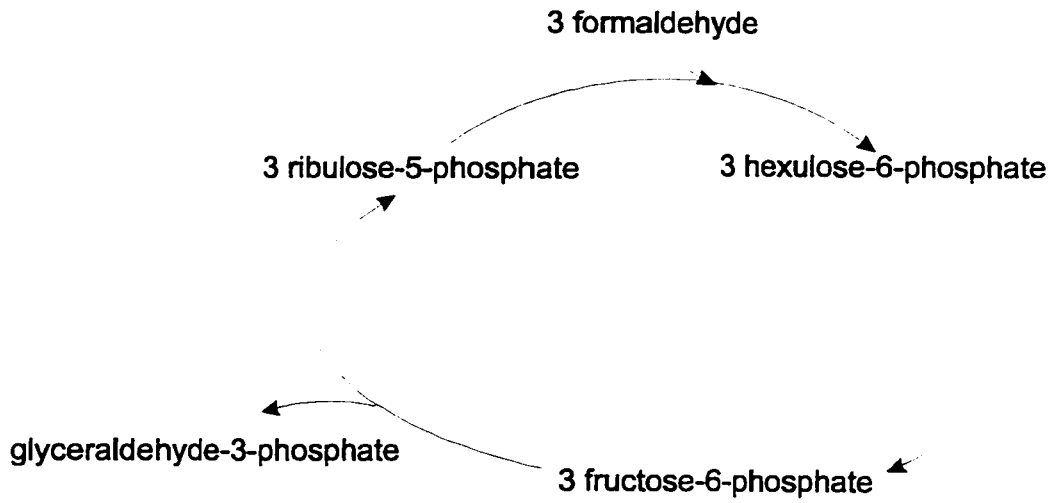

Figure 4.4: Ribulose monophosphate cycle.

(Madigan/Martinko, BROCK BIOLOGY OF MICROORGANISMS, 8/e, © 1997, pp. 671. Reprinted by permission of Prentice-Hall, Upper Saddle River, New Jersey.)

METABOLISM OF COMMON OZONATION BY-PRODUCTS

As mentioned in Chapter 2, the compounds investigated in this research were methylglyoxal, formaldehyde, pyruvate, acetate, oxalate, and formate. These compounds are listed in Table 4.1 along with their theoretical oxygen demand, and their structural formulae are shown in Figure 4.5. Although carboxylic acids are shown in Figure 4.5, these acids would normally exist as anions. This is because the pK_a of these acids is in the range of 2.39 to 4.76 (Lide, 1995) which is far below the pH of most natural waters.

Table 4.1: Theoretical Oxygen Demand of Ozonation By-Products

Ozonation By-Product	Theoretical Oxygen Demand (mole O_2/mole component)
methylglyoxal	3
pyruvate	2.5
acetate	2.0
formaldehyde	1.0
oxalate	0.5
formate	0.5

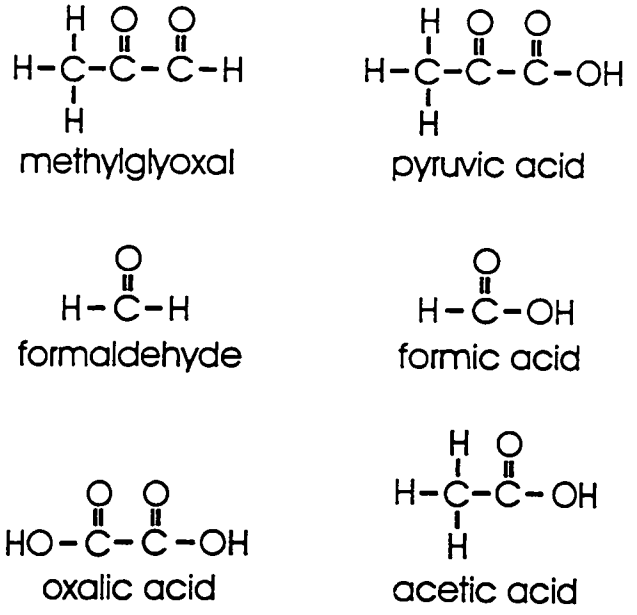

Figure 4.5: Structural formulae of the ozonation by-products investigated.

In the following sections the metabolism of these six compounds is discussed in terms of the metabolic pathways, introduced previously. The

intention is to describe likely routes of metabolism for these compounds, and to speculate on their possible fates in biologically active drinking water filters.

Acetate

Acetate is likely converted to acetyl-CoA and utilized via the TCA and glyoxylate cycles. Since both energy and biosynthetic building blocks can be produced by this pathway, growth on acetate as sole substrate is possible. No metabolic reactions have been presented which indicate that acetate could be readily produced from other ozonation by-products, although the possibility of acetate production cannot be entirely dismissed because acetogenic metabolic pathways do exist in microorganisms. The acetic acid bacterium *Gluconobacter*, for example, metabolizes glucose via the pentose phosphate cycle, and the glyceraldehyde-3-phophate produced is converted via pyruvate to acetate, which is excreted (Gottschalk, 1986). Acetate is also a common end product of other fermentation reactions (Gottschalk, 1986), although these anaerobic reactions are not likely to be of importance in drinking water biofilters, as discussed in the EMP pathway section. Acetate is expected to be well removed in biofilters, because of its easy conversion to acetyl-CoA, a very central metabolite which, for example, could be consumed in the TCA cycle. Indeed Gagnon *et al.* (1997) reported good, yet incomplete removals of acetate, in a full-scale study, as discussed in Chapter 2. However, in that study the filters were operated such that the empty bed contact time (EBCT) was relatively high, at about 24 minutes. At such a long EBCT complete removal would be expected. The possibility of acetate excretion by biofilm microbes remains a tenable explanation for the observed acetate in the filter effluent.

Pyruvate

Pyruvate is likely also converted to acetyl-CoA and utilized in the TCA and glyoxylate cycles, as discussed previously. Pyruvate is an important precursor for a wide variety of cellular materials, however, many of these are produced from the TCA and glyoxylate cycles. Pyruvate can also be converted to phospoenolpyruvate (PEP), and oxalacetate (Doelle, 1975), which are both

important biosynthetic building blocks. Pyruvate is also a precursor to the amino acids alanine, valine and leucine, through intermediates produced in the TCA cycle (Brock and Madigan, 1997). Therefore, pyruvate is important for both the construction of cell materials and the generation of energy to carry out metabolic functions. Pyruvate is expected to be readily biodegradable because of its key role in cell metabolism, and therefore accumulation of pyruvate is not expected. However, pyruvate can be formed from methylglyoxal in the methylglyoxal bypass of the Embden-Meyerhof pathway. Pyruvate formed in this pathway is likely to be required for energy or biosynthesis, however, the possibility of its accumulation cannot be completely ignored. Good pyruvate removals have been reported by Gagnon *et al.* (1997), as discussed in Chapter 2.

Methylglyoxal

The utilization of methylglyoxal likely involves its conversion to pyruvate, as in Figure 4.2. Since methylglyoxal is not normally considered a substrate, and its importance as a metabolic intermediate has only been relatively recently studied (Cooper, 1984), other metabolic roles have yet to be determined. It is certainly of importance that methylglyoxal can be converted to pyruvate, from which energy production and biosynthesis of cell constituents is possible. Therefore, growth on methylglyoxal as sole substrate may be possible, however, the enzymes required for these reactions may require induction, and some genera may not be able to perform these conversions at all. For these reasons it seems reasonable that methylglyoxal may be less readily biodegradable than the other ozonation by-products investigated, as observed in some studies (*e.g.* Niquette *et al.*, 1998). Also, the period during which enzyme induction occurs may result in a lag period prior to methylglyoxal utilization. Indeed in this research a lag phase was observed in experiments in which methylglyoxal utilization was studied in batch bioreactors. These experiments are discussed in Chapter 5.

Also, since Figure 4.2 showed that methylglyoxal formation can occur during glucose metabolism, it may be possible for methylglyoxal to accumulate in cells and the growth medium. If this were to occur, growth would eventually become inhibited, because methylglyoxal is toxic at high concentrations (Cooper, 1984).

Formaldehyde

Formaldehyde is a central intermediate in methylotrophic metabolism (Attwood and Quayle, 1984), and is incorporated into cellular matter via either the serine (Figure 4.3) or ribulose monophosphate cycles (Figure 4.4). Formaldehyde can also be catabolized by methylotrophs, providing energy for biosynthesis (Brock and Madigan, 1997), as follows:

$$methane \rightarrow methanol \rightarrow formaldehyde \rightarrow formate \rightarrow CO_2 \qquad (4.1)$$

Formaldehyde is expected to be well removed by incorporation into cellular materials via the serine or ribulose monophosphate cycle, or by oxidation for energy. In fact, formaldehyde is often very readily removed in drinking water biofilters, as discussed in Chapter 2. Thus, it would appear that methylotrophic bacteria commonly comprise a portion of the microbial population inhabiting a typical drinking water biofilter.

Oxalate

Oxalate has not appeared in the cycles mentioned thus far. Oxalate metabolism is closely related to formate metabolism in *Pseudomonas oxalaticus* (Doelle, 1975). For example, oxalate can be oxidized for energy as follows:

$$oxalate \rightarrow oxalyl-CoA \rightarrow formyl-CoA + CO_2 \rightarrow formate \rightarrow CO_2 \qquad (4.2)$$

Alternatively, oxalate can be converted via oxalyl-CoA to form glyoxylate (Doelle, 1975), which could then enter either of the serine or glyoxylate cycles. The serine pathway would only be operative if single

carbon compounds were being incorporated into cellular material. In the glyoxylate cycle, glyoxylate is converted sequentially to malate then oxalacetate. These compounds are important biosynthetic building blocks. In this way the glyoxylate cycle is used to build up cell materials, whereas the TCA cycle would provide cellular energy. Oxalate is expected to be readily biodegradable because it can be oxidized for energy, or converted to important biosynthetic building blocks. Good oxalate removals were reported by Niquette *et al.* (1998), as discussed in Chapter 2. However, since oxalate is already highly oxidized the energy yield from its oxidation is relatively low, and therefore other available substrates may be favoured in some instances. Also, no possible pathways for its formation are apparent, therefore, it is not likely to be excreted and to accumulate in the growth medium.

Formate

Formate can be oxidized, by the action of the enzyme formate dehydrogenase, to carbon dioxide (Doelle, 1975), as shown in the last step of equation 4.2. This would release energy for the production of biosynthetic building blocks. Also, the carbon dioxide produced could be fixed via a mechanism similar to the Calvin cycle (Doelle, 1975). The Calvin cycle is normally associated with autotrophic bacteria, which can produce organic matter from carbon dioxide and an external energy source, such as light, or an inorganic electron donor such as ammonium, dissolved hydrogen, ferrous ion, or a reduced form of sulfur. Alternatively, carbon dioxide can also be fixed into pyruvate, or phosphoenolpyruvate, to form malate, or oxalacetate, if either of these cosubstrates are available (Doelle, 1975).

Formate can also be incorporated into cellular material by its conversion to methylene tetrahydrofolate, followed by several subsequent conversions, which are shown in Figure 4.3. The output of this cycle is acetyl-CoA, which, as discussed previously, is an important intermediate for biosynthesis, and energy production via the TCA cycle.

Formate is expected to be readily removed, where either the serine or ribulose monophosphate cycle are available. Formate was shown to be amenable to biological filtration by Urfer and Huck (1997). However, since formate is an oxidation product of both oxalate and formaldehyde, it is possible that the presence of these compounds may result in the formation of formate. Significant accumulation of formate would not be expected because it can be readily oxidized to carbon dioxide.

The amino acids serine and glycine are involved in the serine pathway (Figure 4.3). Growth on amino acids as sole substrates is possible since these compounds can be oxidized for energy, or utilized directly in biosynthesis (Brock and Madigan, 1997). For example, these amino acids can be oxidized to pyruvate, via a process similar to glycolysis (Figure 4.2) or utilized in protein synthesis (Brock and Madigan, 1997). Also, if these amino acids could be directly incorporated into the serine pathway, this may increase the rate of formaldehyde utilization. The effect of amino acids on formaldehyde utilization was examined in the third filter experiment, described in Chapter 6.

CONCEPTUAL METABOLISM MODEL

The metabolic reactions presented in the previous section have been assembled into a single summary diagram, emphasizing the ozonation by-products investigated in this research (Figure 4.6). The ozonation by-products are shown in bold in Figure 4.6. As can be seen by comparing this diagram to the individual metabolic cycles presented earlier, several simplifications have been made. By simplifying the pathways the expected fate and potential interactions of these ozonation by-products is emphasized, not the individual enzyme reactions. Also, the biochemical reactions summarized in Figure 4.6 have been drawn from several sources, and not from a single comprehensive study, nor a single bacterial species, therefore the model summarizes a combination of metabolic capabilities. A single bacterial species is not necessarily expected to possess all of the enzymes necessary to carry out each of the reactions presented, however, a mixed community, such as those which

inhabit biologically active filters, may be capable of performing all of the bioreactions presented.

The serine pathway, and not the ribulose monophosphate cycle, is shown in Figure 4.6. If the ribulose monophosphate cycle had been shown, the diagram would be essentially the same, except that the ribulose monophosphate cycle produces glyeraldehyde-3-phosphate, instead of acetyl-CoA. Both of these compounds serve as biosynthetic building blocks.

It is clear from Figure 4.6 that the metabolism of many of these ozonation by-products is related, and often involves the same metabolic pathways. Also, metabolic processes may result in an impact on filter performance, with respect to the compounds in question, due to phenomena such as a preference for one compound over another, or the production of one compound via the metabolism of another. In order to have an effect on filter performance, formed compounds must accumulate outside the cells, since component concentrations can only be determined in the bulk liquid. Moreover, from an effluent quality point of view, the concentrations in the bulk liquid are of much greater concern than those within cells in drinking water treatment.

Non-steady state or upset conditions may result in a shift in the biofilm population inhabiting a biologically active drinking water filter. This population shift may result in a change in the overall mix of the metabolic capabilities of the population. This may lead to the temporary appearance of some substrates in the effluent of filters.

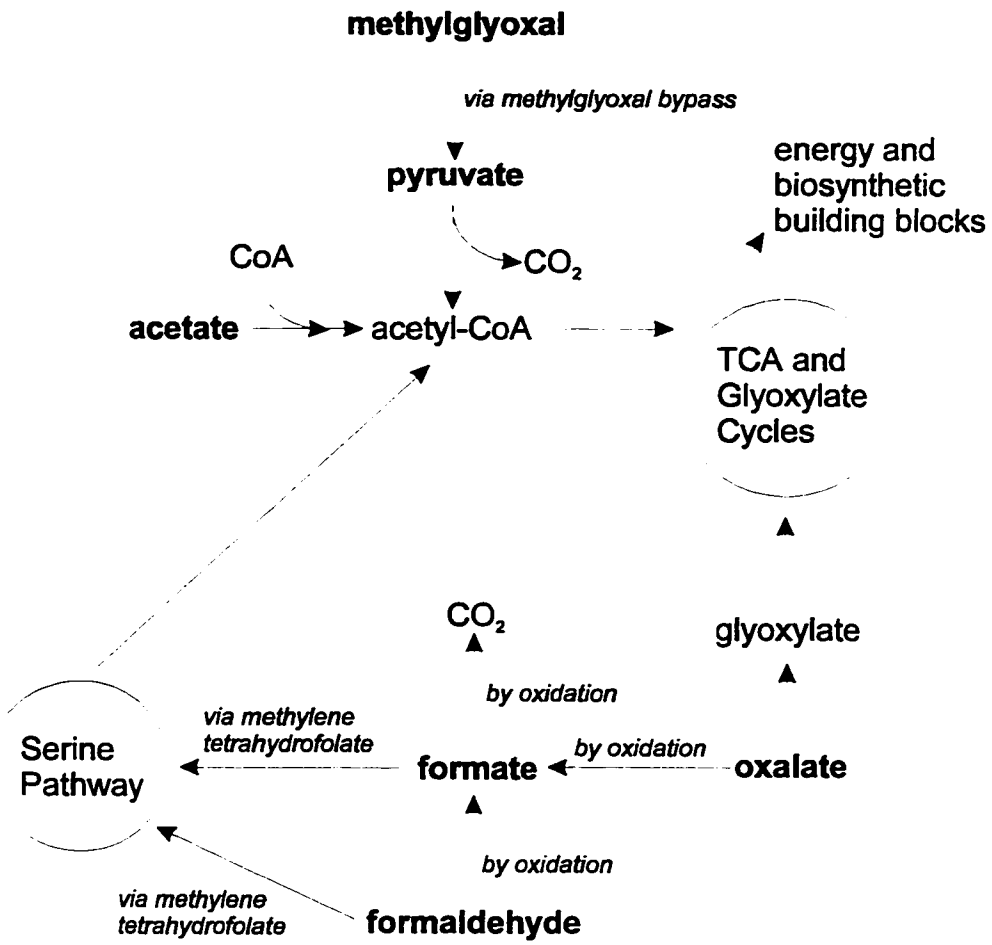

Figure 4.6: Conceptual metabolism model.

Utility of the Conceptual Metabolism Model

The conceptual metabolism model shows how the metabolism of the compounds of interest is related. For example pyruvate is formed during the metabolism of methylglyoxal, and formate is an oxidation product of both oxalate, and formaldehyde. An objective of this research was to determine if the utilization rate of any of these compounds was affected by the presence of other compounds, due to metabolic interactions. These possibilities were experimentally tested by monitoring the loss of a given compound in the presence of various groups of other compounds. Compounds whose metabolism appeared to be related according to the conceptual metabolism model were selected for these experiments. The batch bioreactors, used in these experiments, initially contained the selected compounds at the desired

concentrations and microbiota from a drinking water filter. The possible formation of one compound from another was monitored, and the effect of the presence of a compound on the biodegradation rate and/or transformation products of other compounds was tested.

Because this work focuses on specific ozonation by-products the experimental systems for their investigation have excluded or limited the presence of other organics. Organics such as humic and fulvic acids, carbohydrates, and possibly proteins would be present in natural waters. The effect of the presence of these other organics on the utilization rate of ozonation by-products was not an objective of this work. Since the ozonation by-products of interest are generally readily biodegradable, the other organic components are likely relatively recalcitrant by comparison, and thus would not likely have a sufficient effect on the removal of these ozonation by-products to alter the basic trends identified in the conceptual metabolism model and examined in this research.

REFERENCES

Attwood, M.M. and J.R. Quayle (1984). Formaldehyde as a central intermediary metabolite of methylotrophic metabolism, in Microbial Growth on C-1 Compounds, 4th International Symposium of the American Society for Microbiology, pp. 315-323, R.L. Crawford and R.S. Hanson (Eds.). Washington, DC, USA.

Brock, T.D. and M.T. Madigan (1997). Biology of Microorgansims, 8th Edition. Prentice Hall, Upper Saddle River, New Jersey, USA.

Burlingame, G.A., I.H. Suffet, W.O. Pipes (1986). Predominant bacterial genera in granular activated carbon water treatment systems. *Can. J. Microbiol.*, Vol. 32, pp. 226-230.

Cooper R.A. (1984). Metabolism of methylglyoxal in microorganisms. *Ann. Rev. Microbiol.*, Vol. 38, pp. 49-68.

Doelle, H.W. (1975). Bacterial Metabolism, 2nd Edition. Academic Press, New York, New York, USA.

Gagnon, G.A., S.D.J. Booth, , S. Peldszus, D. Mutti, F. Smith, and P.M. Huck (1997). Formation and removal of carboxylic acids in a full-scale treatment plant. *Jour. AWWA*, Vol. 89 (8), pp. 88-97.

Gottschalk, G. (1986). Bacterial Metabolism, 2nd Edition. Springer-Verlag, New York, New York, USA.

Krasner, S.W., M.J. Sclimenti, and B.M. Coffey (1993). Testing biologically active filters for removing aldehydes formed during ozonation. *Jour. AWWA*, Vol. 85 (5), pp. 62-71.

Lide, D.R. (Ed.) (1995). CRC Handbook of Chemistry and Physics, 76th Edition. CRC Press, Boca Raton, Florida, USA.

Moll, D.M., R.S. Summers, and A. Green (1998). Microbial characterization of biological filters used for drinking water treatment. *Appl. Environ. Microbiol.*, Vol. 64 (7), pp. 2755-2759.

Niquette, P., M. Prévost, R. G. Maclean, D. Thibault, J. Collier, R. Desjardins, and P. Lafrance (1998). Backwashing first-stage sand-BAC filters. *Jour. AWWA*, Vol. 90 (15), pp. 86-97.

Urfer, D. and P.M. Huck (1997). Effects of hydrogen peroxide residuals on biologically active filters. *Ozone Sci. and Eng.*, Vol. 19, pp. 371-386.

CHAPTER 5: BATCH EXPERIMENTS

INTRODUCTION

Groups of ozone by-products were studied in batch bioreactors, as described in Chapter 3. The by-product groupings were based on the positions of the compounds in the conceptual metabolic model (Figure 4.6), presented and discussed in Chapter 4. As Figure 4.6 illustrates the metabolism of acetate, pyruvate, and methylglyoxal appear to be linked. Also, formaldehyde, formate, and oxalate appear to be similarly related. For this reason most of the batch experiments were divided into investigations of these two groups of compounds, representing the top and bottom of Figure 4.6, respectively. The combinations of compounds tested are presented in Table 5.1.

The purpose of these experiments was to determine the kinetics of biodegradation of individual ozonation by-products, and the possible formation of one compound from another. Also, the effect of the presence of a particular compound on the biodegradation rate and/or transformation products of other compounds was investigated. In these experiments both carboxylic acids and aldehydes were monitored at all sampling times, thus the biodegradation rates of the added compounds, in addition to detectable transformation products, could be monitored.

Table 5.1: Groups of Compounds Investigated

Relevant Portion of Figure 4.6	Components of Group
top	acetate
	pyruvate
	methylglyoxal
	acetate and pyruvate
	methylglyoxal and pyruvate
	methylglyoxal, pyruvate, and acetate*
bottom	formaldehyde
	formate
	oxalate
	formaldehyde and formate
	formate and oxalate
	formaldehyde, formate, and oxalate
whole	formaldehyde, formate, oxalate, acetate and pyruvate

*An unidentified contaminant in the methylglyoxal was found to interfere with acetate quantification. The methylglyoxal-acetate and formaldehyde-oxalate pairs were not tested.

INOCULUM

As discussed in Chapter 3, the inoculum for these experiments was a sample of a GAC/sand filter effluent from a full-scale treatment plant, which had ozonation upstream of the filter. HPCs were performed on the inoculum, indicating it contained an average of 5.4×10^6 CFU/mL, with a coefficient of variation of 2.3%, on a log-scale. This analysis was performed in duplicate, three different times during the course of these experiments. The coefficient of variation indicates that the HPCs were reasonably stable in the inoculum over the duration of these experiments. It was important that the HPCs remained relatively consistent in order to ensure that previously established protocols remained applicable from experiment to experiment. A given experiment was normally completed prior to obtaining any results, therefore, the sampling times had to be established from previous experience. Large deviations in the HPCs, and presumably the viable biomass, would have resulted in sampling at inappropriate times.

Because the inoculum was a filter effluent from an operating treatment plant, it was likely to contain some organic carbon and possibly some readily BOM. Analyses indicated that reasonably low concentrations of some compounds were indeed present (Table 5.2). Upon dilution of the inoculum into the experimental flasks, the concentration of these components would normally be reduced to less than the detection limit.

Table 5.2: Component Concentrations of Inoculum

Component	Concentration (µg/L)* Average	Range
acetate	82	37 - 120
glycolate	9.1	4.1 - 15
formate	16	7.8 - 25
pyruvate	3.0	0 - 6.1
ketobutyrate	44	40 - 51
formaldehyde	5.8	1.6 - 8.3

* Chemical analyses were performed on the inoculum three different times over the course of these experiments.

The microbial population of the inoculum was characterized using the BIOLOG® system (Biolog Inc.; Hayward, CA), as described in Chapter 3. This analysis was used as qualitative indicator of the consistency of the metabolic capabilities of the inoculum. The inoculum was analyzed on two occasions, five months apart and these results are in Appendix A.3. The same general substrate utilization pattern was observed for these two sampling days. An average of 10 out of 95 wells were different between these samples on the gram negative microplates, and 8 were different on the gram positive microplates. Typically duplicate analyses of the same population differed by 6 wells for this method. The differences of 8 and 10 are only slightly greater than the variability observed between duplicates, and therefore indicate a small change in the pattern of sole carbon source utilization by the inoculum. In some cases the variation between duplicates involved different wells compared to the variation observed between the two sampling days. However, differences often involved borderline wells, while very few wells were found

to be positive on one plate and negative on another. These analyses provide some assurance that the metabolic capabilities of the inoculum did not drastically change over this period. The consistency of the inoculum was important in order to make meaningful comparisons among experiments conducted at different times.

EXPERIMENTAL CONTROLS

Two types of controls were included with every experiment. A control flask which was not amended with ozone by-products, but was inoculated with bacteria, termed a "biological control" (see data in Appendix A.5). Also, "chemical controls" which contained ozone by-products, but were not inoculated were included (see data in Appendix A.4). One chemical control was included for each group of by-products investigated in a given experiment.

Chemical Controls

The chemical controls were not inoculated and therefore no growth was expected in these flasks. These controls were included to verify that the concentration of the ozone by-products did not vary due to a non-biological mechanism, such as evaporation. HPCs were performed on these flasks at all sampling times. Normally no CFUs were observed, and the minimum number for counting, thirty, was never observed. The slope of the concentration versus time data for these flasks was tested for significance for each of the chemical controls. In each instance the slope was not significantly different from zero at the 1% level. Figure 5.1 shows data for the chemical controls which contained acetate and pyruvate. The data are averages from two experiments, which each included a single chemical control for this pair of components. This indicates that the concentrations of the components were constant when biological activity was prevented, and thus evaporative or other non-biologically mediated losses were negligible.

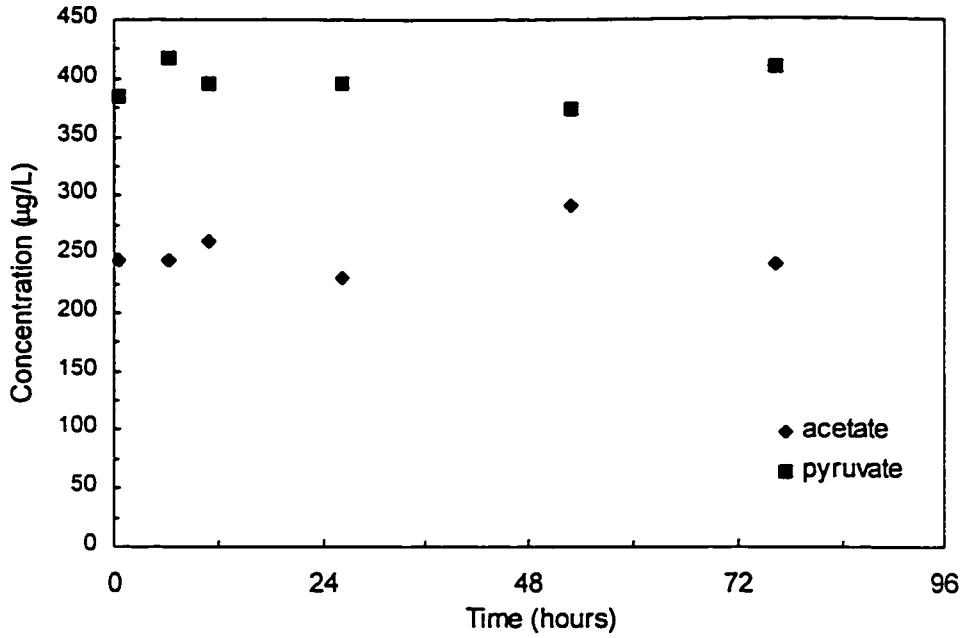

Figure 5.1: Chemical control data for acetate-pyruvate pair.

Biological Controls

The biological controls were included to determine the amount of microbial growth which occurred without any BOM amendment. The inoculum contained some BOM, as discussed above, and therefore a small increase in HPC numbers might have been expected in the biological controls. Experiments ranged from 5 to 10 days in duration which included an initial acclimation period, as discussed in Chapter 3. An inspection of the HPC data from the biological controls at the start and end of the experiments indicates an apparent increase in the measured values, in some cases. However, when the HPC data for all of the biological controls were pooled, the average starting and ending values were not found to be significantly different (5% level) in a paired comparison. Also, there was no significant difference at the 5% level between the mean HPCs in the biological controls and the mean value for the experimental flasks, just prior to ozone by-product addition, as expected. Figure 5.2 shows the average HPC values, with 95% confidence intervals, used in these comparisons. The observed variation in HPC numbers in the

biological controls likely resulted from random error, and not from an actual increase in cell numbers.

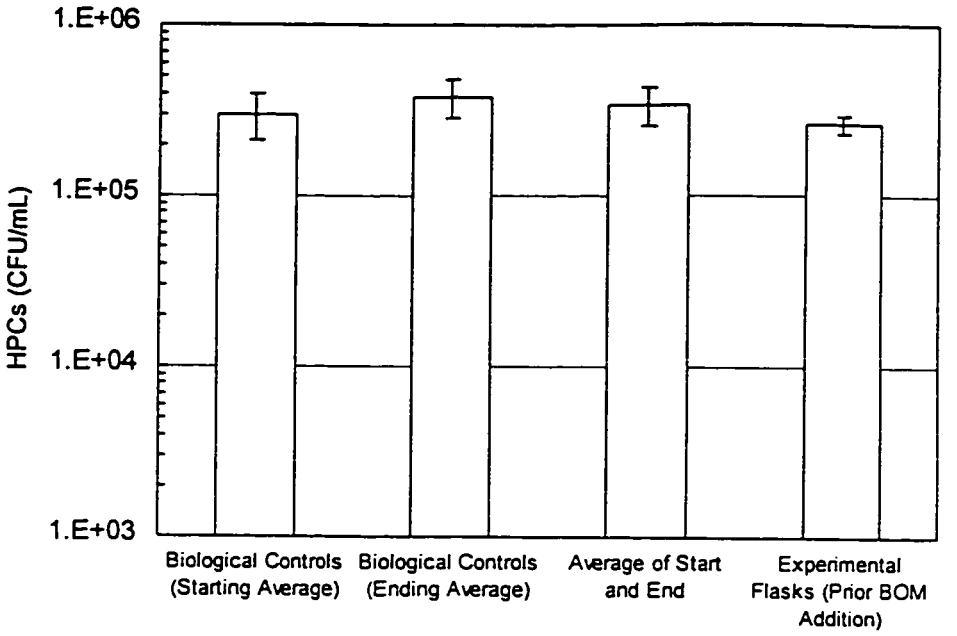

Figure 5.2: Comparison of HPCs in biological controls (error bars represent 95% confidence intervals).

ANALYSIS OF BATCH DATA

Biodegradation rates were calculated for each investigated component in every experiment. A zero-order kinetic model was assumed for this purpose, because it provided a good empirical fit to the data, based on the correlation coefficient, and an inspection of the model residuals. Other researchers have used other kinetic orders to model the removal of easily biodegradable components in biological drinking water processes. Gagnon (1997) showed that the flux of the ozonation by-products formaldehyde, glyoxal, formate, and acetate was directly proportional to their loading rates, indicating first order kinetics in a model distribution system. Also, Zhang and Huck (1996) have shown that the half saturation constant for AOC was much larger than its concentration in drinking water filters, and therefore, AOC degradation fell into the first-order kinetic region. Thus, first order kinetics may be applicable

in some circumstances. However, since the quality of the zero-order fit was generally good, it has been applied throughout to facilitate comparisons among experiments. Moreover, there was insufficient data to definitively demonstrate the statistical superiority of one kinetic model over the other. Also, in the next chapter, data from bench-scale filter experiments are used to contend that zero-order kinetics were applicable in that system also. A comparison of calculated kinetic parameters from each system is presented in Chapter 6.

Lag Phase

A lag phase, in which little or no substrate utilization occurs is often observed at the start of biological studies in batch reactors (Brock and Madigan, 1997). Significant lag phases were usually observed for formaldehyde and methylglyoxal, but not for the other components investigated in this research. Data points corresponding to the lag phase were omitted from regression calculations. The duration of the lag phase is dependent on the quantity of initial biomass, kinetic utilization and growth parameters, and other factors (Simkins and Alexander, 1984). Therefore, some variation in the lag phase was expected among different substrates and from experiment to experiment. The duration of the lag phase was subjectively determined by inspection of the data in each case.

Approach for Comparisons Among Experiments

To facilitate meaningful comparisons among the calculated kinetic parameters they were normalized for the amount of biomass. A higher biomass is expected to provide a higher apparent removal rate. The biomass was not directly measured in the present research, as no reasonable method for its direct determination could be identified in the relevant literature. Also, the biomass concentrations were too low to be measured using the phospholipid method, described in Chapter 3. HPCs were performed to estimate the number of viable cells, although only those which are culturable on R2A agar were enumerated. The fraction of the total population which could grow on R2A agar is difficult to determine, however, R2A agar has become a standard

medium for microbial analysis of drinking waters. Therefore, its use was considered appropriate for this purpose.

HPCs were measured 2 to 4 times during each experiment. In most cases this provided insufficient data for a detailed examination of the kinetics of HPC accumulation in these bioreactors. Instead, the HPC data were examined by making two calculations: the net increase in HPCs and the average HPC number. Each was calculated from sampling times which corresponded, as closely as possible, to the beginning and end of the degradation of the compound of interest.

Figure 5.3 shows the correlation of the net increase in HPCs with the theoretical oxygen demand of the components added to the flasks. The data shown are average values for each of the different groups of components studied. The regression shown on the figure was significant at the 1% level. A correlation between the biomass gain and the theoretical oxygen demand was expected. The theoretical oxygen demand of a compound is proportional to the amount of energy that can be derived from oxidizing it. The energy required for the biosynthesis of cellular materials is derived from the oxidation of organic substrates by heterotrophic microorganisms. The observed relationship between CFU increase and oxygen demand is not necessarily expected, because growing cells can become larger without dividing. However, the close linkage of biomass increase and cell division is characteristic of the exponential growth phase. Because of the strong correlation between observed increase in HPCs and the theoretical oxygen demand, the use of HPCs for the normalization of kinetic parameters seems justified.

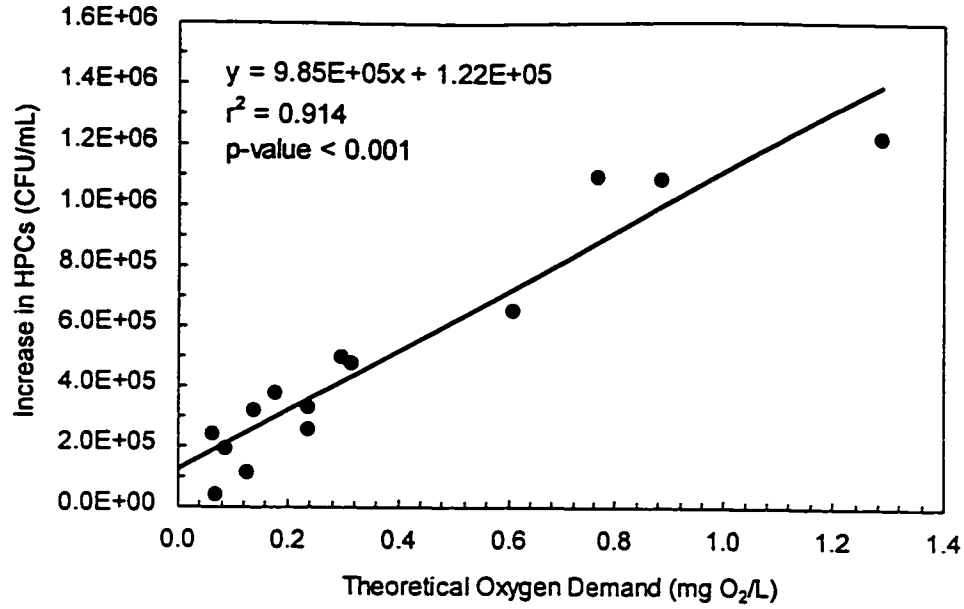

Figure 5.3: Relationship between increase in HPCs and initial theoretical oxygen demand for shake flasks in batch experiments.

By making a number of assumptions the approximate yield of biomass from each of the components studied can be determined. The necessary assumptions are: all of the cells are culturable on R2A agar; each CFU developed from one cell; the average mass of each cell was 10^{-6} μgram; and the carbon content of a cell is 0.3 gram carbon per gram of cell (Brock and Madigan, 1997). The value for the cell mass was the approximate mean of a range given by Brock and Madigan (1997) for procaryotes. By making these assumptions the yields for each of the components studied were calculated; and presented in Table 5.3. Example yield calculations for pyruvate follow:

$$\frac{5.00 \times 10^{8}\ \text{CFU}}{\text{L}} \times \frac{1\ \text{cell}}{1\ \text{CFU}} \times \frac{10^{-6}\ \mu g}{\text{cell}} \times \frac{0.3\ \mu g\text{-C}}{\mu g\ \text{cells}} = 150\ \frac{\mu g\text{-C}}{\text{L}} \qquad (5.1)$$

$$\frac{322\ \mu g\ pyruvate}{L} \times \frac{\mu mol\ pyruvate}{87\ \mu g\ pyruvate} \times \frac{3\ \mu mol - C}{\mu mol\ pyruvate} \times \frac{12\ \mu g - C}{\mu mol - C} = 133 \frac{\mu g - C}{L} \quad (5.2)$$

$$Y_{x/s} = \frac{150\ \mu g - C\ cells}{133 \mu g - C\ pyruvate} = 1.13 \frac{\mu g - C\ cells}{\mu g - C\ pyruvate} \quad (5.3)$$

The values given in Table 5.3 are not expected to be greater than unity, because the units are µg-C biomass per µg-C component. Therefore, the values calculated for formaldehyde, methylglyoxal, and pyruvate are higher than expected, while the remaining values may be reasonable. Literature values for acetate ranged from 0.27 to 0.59 (Bailey and Ollis, 1986), which are somewhat lower than calculated for acetate in this research.

Table 5.3: Yield Coefficients for Examined Components

Component	$Y_{x/s}$ (µg-C/µg-C)
formaldehyde	1.77
methylglyoxal	1.22
pyruvate	1.13
acetate	0.89
formate	0.86
oxalate	0.12

The calculation of the yields required a number of assumptions, as discussed above. The assumed cell mass value may have been too high to represent the cells which were studied under oligotrophic conditions in this investigation. A lower cell mass would have resulted in lower values for the yields.

The assumptions used in the conversion of the CFU numbers to biomass apply to all of the calculated yields equally, and therefore relative comparisons among them may be valid. With the exception of formaldehyde,

the order of the components given in Table 5.3 is essentially the same as that given in Table 4.1, which listed the components in decreasing order of theoretical oxygen demand. Thus, the calculated yields generally follow the expected trend that more biomass would result from substrates which provide a greater amount of theoretical oxygen demand. Moreover, the validity of relative comparisons is strengthened by the fact that the order of the components in the two tables corresponds so closely. Given these factors, the calculated yield values seem reasonable and also support the use of HPCs as a surrogate for biomass in these experiments.

The measured biodegradation rate is expected to vary directly with biomass. In order to account for differing amounts of biomass that existed in the different flasks the zero-order kinetic parameters, calculated for each component, were divided by the average HPC value in a given flask. The sampling times chosen for averaging corresponded, as closely as possible, to the beginning and end of the degradation of the compound of interest. This calculation approximately normalized the kinetic parameter, calculated for a given compound, for the amount of biomass that was involved in the biodegradation of that compound.

Top Portion of Conceptual Metabolic Model

The relevant chemical component and HPC data for the batch experiments are in Appendix A.1 and A.2, respectively. The calculated values for pyruvate, acetate, and methylglyoxal are discussed individually, below.

The only transformation product occurrence that could be detected was the formation of pyruvate from methylglyoxal. A discussion of the results from groups of compounds involving methylglyoxal follows an examination of those for pyruvate and acetate. The calculated kinetic values for pyruvate and acetate are summarized in Tables 5.4 and 5.5 respectively. The p-value given in these tables refers to the statistical significance of the regression slope. For example, a p-value of 0.045 is significant at the 4.5% level. This

means that it would be found significant at the 5% level, but not at the 1% level.

Table 5.4: Normalized Zero-Order Kinetic Parameters for Pyruvate

Added Compounds	$k_0 \times 10^8$ ($\mu g\ CFU^{-1}\ hr^{-1}$) [a]	p-value of slope
pyruvate	2.16 ± 1.02	0.012
pyruvate and acetate	3.02 ± 1.96	0.022
formaldehyde, acetate, pyruvate, formate, and oxalate	1.69 ± 1.44	0.037

[a] Average plus or minus 95% confidence interval, calculated from confidence interval of the slope.

It can be seen from Table 5.4 that none of the zero-order kinetic parameters (k_0), calculated for pyruvate, fell outside of the confidence intervals of any other. This is a strong indication that no statistically significant differences among these values exists. The same was true for acetate (Table 5.5). The regression slope for acetate in the acetate-pyruvate-methylglyoxal group was not significantly different from zero. This was mainly due to an interfering peak which prevented quantification of some of the acetate values, as mentioned in the introduction to this chapter.

Table 5.5: Normalized Zero-Order Kinetic Parameters for Acetate

Added Compounds	$k_0 \times 10^8$ ($\mu g\ CFU^{-1}\ hr^{-1}$) [a]	p-value of slope
acetate	2.09 ± 1.98	0.045
acetate and pyruvate	1.37 ± 1.29	0.045
acetate, pyruvate, and methylglyoxal	1.22	>0.05
formaldehyde, acetate, pyruvate, formate, and oxalate	1.56 ± 1.07	0.024

[a] Average plus or minus 95% confidence interval, calculated from confidence interval of the slope.

The k_0 for methylglyoxal was independent of the other compounds present (Table 5.6), however, the biodegradation of methylglyoxal resulted in the formation of pyruvate (Figure 5.4). This formation process might be

expected to reduce the apparent removal rate of pyruvate, although the values given for pyruvate did not significantly differ from those given in Table 5.4, since their confidence intervals overlap. The pyruvate values were calculated by omitting a lag period of about 10 hours in the methylglyoxal-pyruvate and methylglyoxal-pyruvate-acetate groups. The pyruvate lag for the former group can be seen in Figure 5.5. This lag had not been observed for pyruvate in the absence of methylglyoxal. This lag phase may have been due to pyruvate formation from methylglyoxal, although the methylglyoxal concentration did not substantially decrease during this period.

Table 5.6: Normalized Zero-Order Kinetic Parameters for Methylglyoxal

	$k_0 \times 10^8$ ($\mu g\ CFU^{-1}\ hr^{-1}$) [a]	
Added Compounds	methylglyoxal	pyruvate
methylglyoxal	0.41 ± 0.18[b]	-
methylglyoxal and pyruvate	0.47 ± 0.35[c]	2.08[e]
methylglyoxal, pyruvate, and acetate	0.55 ± 0.45[d]	0.960 ± 0.44[f]

[a] Average plus or minus 95% confidence interval, calculated from confidence interval of the slope. P-value of slope equal to [b]0.005, [c]0.029, [d]0.041, [e]>0.05, [f]0.023.

In order to further investigate the process of pyruvate formation from methylglyoxal, it was modeled as a two step sequence of reactions using AQUASIM® (Swiss Federal Institute for Environmental Science and Technology (EAWAG), Dübendorf, Switzerland). The first step was the utilization of methylglyoxal by zero-order kinetics, which resulted in the direct production of pyruvate. This step may, in reality, represent many steps including the uptake of methylglyoxal, at least two metabolic steps (see Figure 4.2), and the release of pyruvate to the bulk water. The second step was the zero-order utilization of pyruvate. The kinetic parameters for methylglyoxal alone and pyruvate alone, given in Tables 5.6 and 5.4, respectively, were used in these calculations. The pyruvate concentration in the bulk liquid in these simulations never increased above zero. This was due to the fact that pyruvate utilization was about one order of magnitude faster than for methylglyoxal, therefore, pyruvate produced from methylglyoxal was essentially

instantaneously degraded. Other processes must be involved, in order to explain the experimentally observed transient pyruvate accumulation.

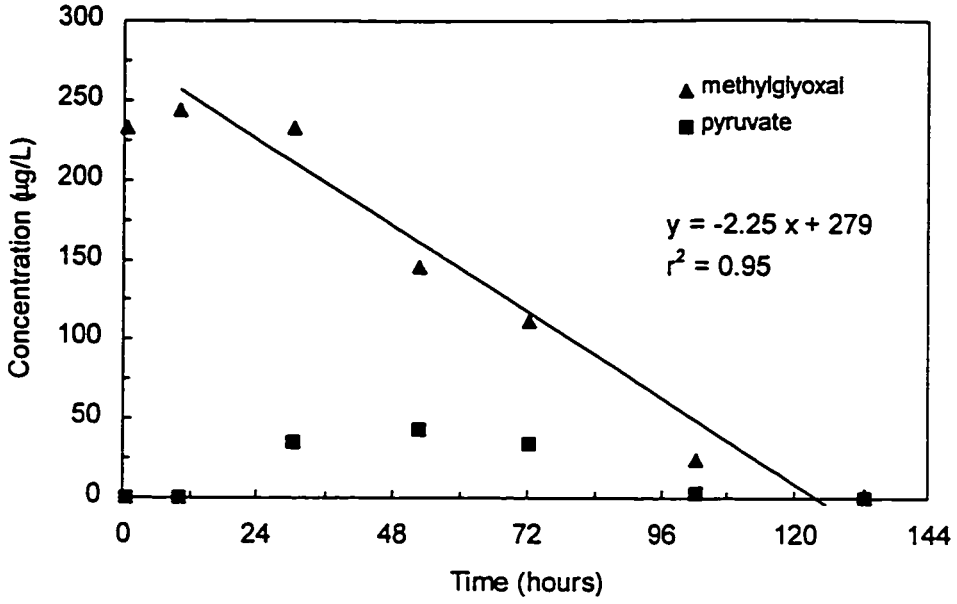

Figure 5.4: Component concentrations for flasks with only methylglyoxal initially present.

A possible hypothesis to explain the observed pyruvate formation is that two distinct populations develop when methylglyoxal is provided as the substrate. At first methylglyoxal-users develop, which excrete pyruvate, upon methylglyoxal uptake. The establishment of this population exhibited a lag phase of approximately 24 hours, as noted earlier. As the methylglyoxal concentration diminishes, the population shifts to pyruvate-users. During the shift between these two populations pyruvate temporarily accumulates in the bulk liquid. This hypothesis was not confirmed, although the utilization of methylglyoxal and pyruvate in biologically active filters is discussed in Chapter 6.

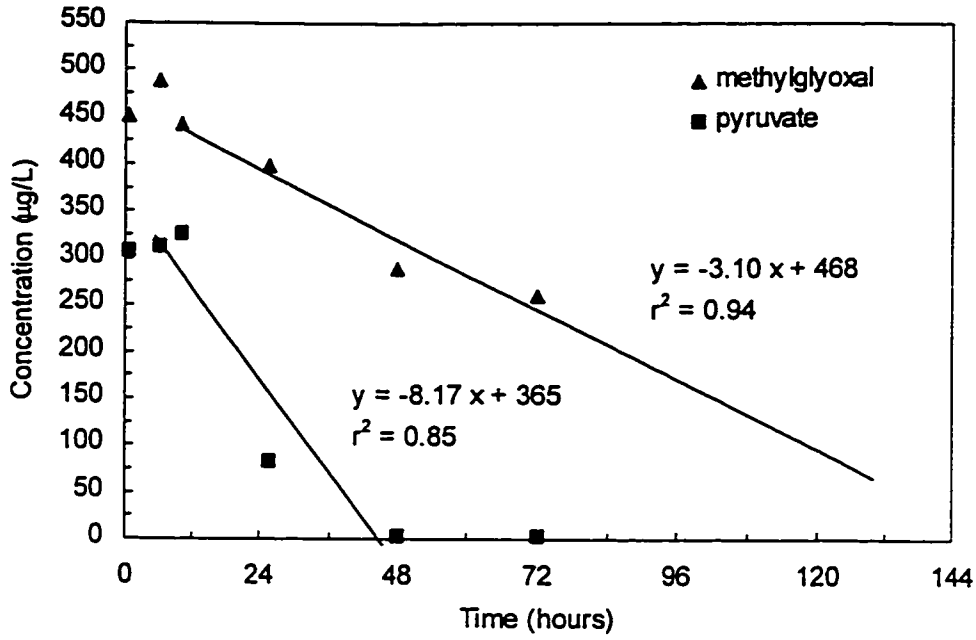

Figure 5.5: Component concentrations for flasks with methylglyoxal and pyruvate initially present.

Bottom Portion of Conceptual Metabolic Model

In this section the results for formaldehyde, formate and oxalate are presented and discussed. No transformation products could be identified, using the aldehyde and organic acid methods, for any of the compounds or groups of compounds examined. The discussion therefore focuses on biodegradation rates only.

Tables 5.7, 5.8 and 5.9 present the k_0 values for formaldehyde, formate, and oxalate, respectively. It can be observed from Table 5.7 and 5.8 that none of the k_0 estimates appear to differ from the others. Figures 5.6 to 5.9 show the data and regressions, for the formaldehyde-containing groups. As shown in these figures, the zero-order kinetic model provided a good fit to the formaldehyde data.

Table 5.7: Normalized Zero-Order Kinetic Parameters for Formaldehyde

Added Compounds	$k_0 \times 10^8$ ($\mu g\ CFU^{-1}\ hr^{-1}$)[a]	p-value of slope
formaldehyde	0.32 ± 0.26	0.033
formaldehyde and formate	0.41 ± 0.098	< 0.001
formaldehyde, formate, and oxalate	0.41 ± 0.16	0.002
formaldehyde, acetate, pyruvate, formate, and oxalate	0.33[b]	NA[b]

[a] Average plus or minus 95% confidence interval, calculated from confidence interval of the slope.
[b] Neither the confidence interval nor the significance level could be determined, because only two data points were included in the regression.

Two different kinetic parameter values were calculated for formate in Table 5.8 The separate values are included because these two experiments were conducted at substantially different initial concentrations (*i.e.* 500 μg/L and 180 μg/L), and thus it was not appropriate to average these values.

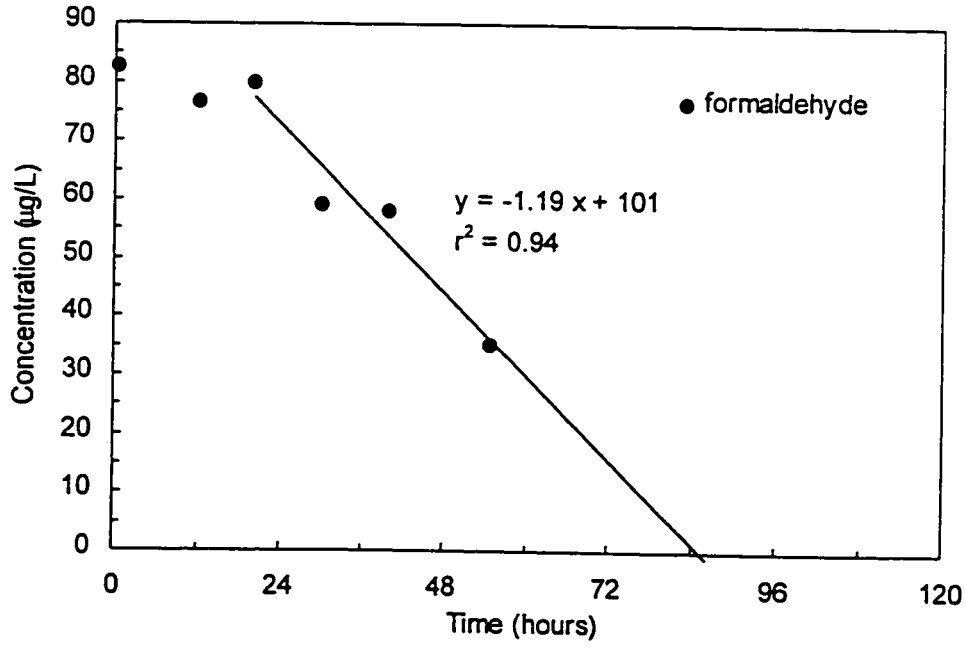

Figure 5.6: Formaldehyde concentrations for flasks with only formaldehyde initially present.

Table 5.8: Normalized Zero-Order Kinetic Parameters for Formate

Added Compounds	$k_0 \times 10^8$ ($\mu g\ CFU^{-1}\ hr^{-1}$)[a]	p-value of slope
formate (at high initial concentration)	1.41 ± 1.29	0.046
formate (at low initial concentration)	1.66 ± 0.16	< 0.001
formate and formaldehyde	1.59 ± 1.56	0.049
formate and oxalate	1.03 ± 0.57	0.010
formate, formaldehyde, and oxalate	1.28 ± 0.74	0.012
formate, formaldehyde, acetate, pyruvate, and oxalate	1.28 ± 1.0	0.031

[a] Average plus or minus 95% confidence interval, which was calculated from confidence interval of the slope.

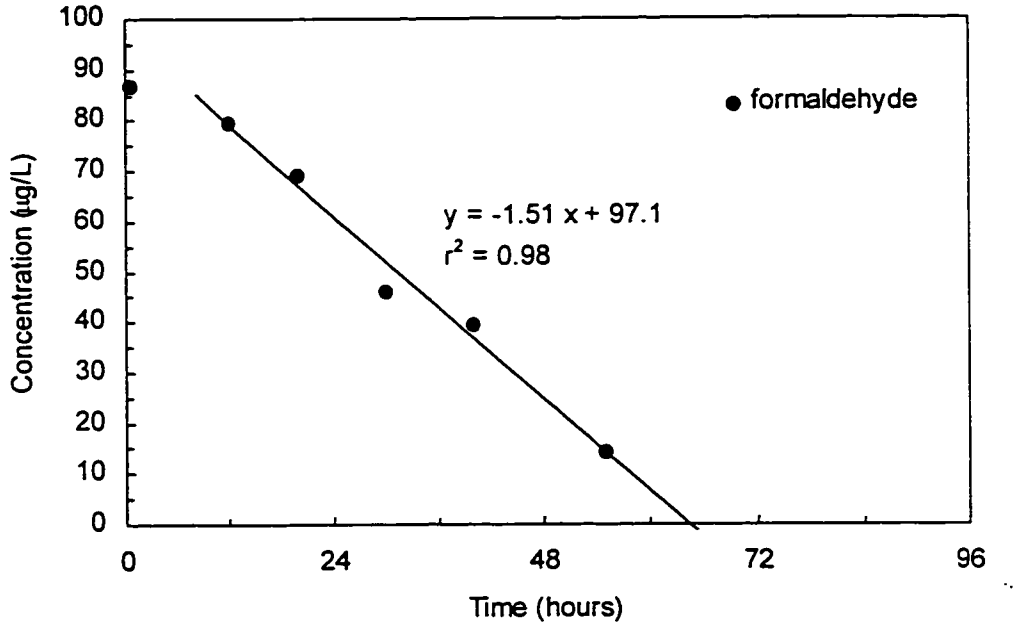

Figure 5.7: Formaldehyde concentrations for flasks with formaldehyde and formate initially present.

The first two k_0 values, listed in Table 5.9, appear to be significantly different. This was primarily due to the fact that the calculated oxalate value for the oxalate-formate pair, was lower than for most of the other cases. Also, the regressions for oxalate alone and oxalate with formate had very little scatter associated with them, resulting in very narrow confidence intervals for these two cases. The oxalate value for the oxalate-formate-formaldehyde

group was the highest, although it was not significantly different from the value calculated for the oxalate-formate group. A difference between these two groups was not expected. If metabolic processes resulted in slower degradation of oxalate in the presence of formate, this should also be observed in the presence of formaldehyde. A lag period of about 20 hours occurred prior to formaldehyde utilization, while about three quarters of the oxalate and formate had disappeared in this same interval. Therefore, formaldehyde was expected to have little impact on the removal of oxalate, under the conditions of this experiment. Furthermore, because of the conflicting results between the oxalate-formate and oxalate-formate-formaldehyde groups, it is unlikely that formate had any significant impact on oxalate degradation.

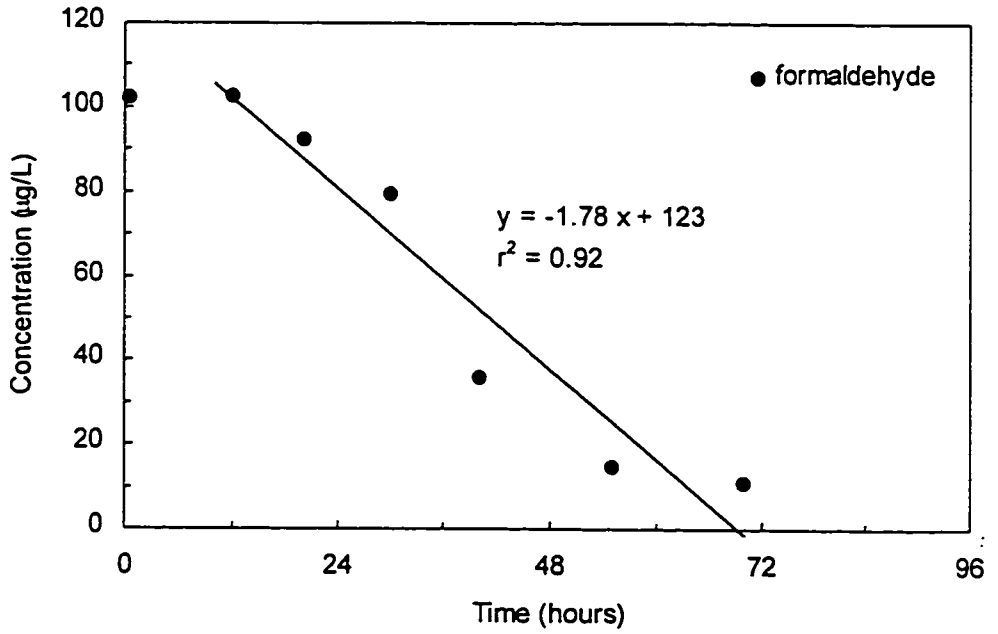

Figure 5.8: Formaldehyde concentrations for flasks with formaldehyde, formate, and oxalate initially present.

Table 5.9: Normalized Zero-Order Kinetic Parameters for Oxalate

Added Compounds	$k_0 \times 10^8$ ($\mu g\ CFU^{-1}\ hr^{-1}$)[a]	p-value of slope
oxalate	2.26 ± 0.12	< 0.001
oxalate and formate	1.50 ± 0.14	< 0.001
oxalate, formate, and formaldehyde	3.75 ± 2.32	0.014
oxalate, formate, formaldehyde, acetate, and pyruvate	1.76 ± 1.14	0.022

[a] Average plus or minus 95% confidence interval, which was calculated from confidence interval of the slope.

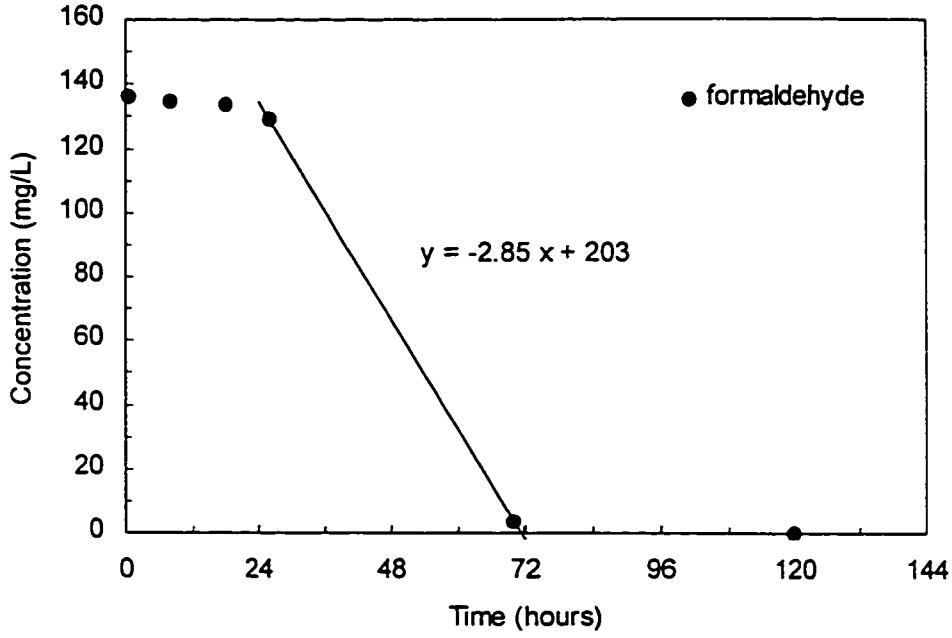

Figure 5.9: Formaldehyde concentrations for flasks with formaldehyde, formate, oxalate, acetate, and pyruvate initially present.

Table 5.10 lists the components studied in this research in order of decreasing overall average k_0 value, therefore ranking the components by biodegradability. Because of the variability in these values and the fact that many of them were quite close to each other, demonstration of statistically significant differences among most them was not possible. It is reasonable, however, to conclude that all of the organic acids investigated were highly biodegradable. Also, the order of the components in Table 5.10 seems reasonable, based on the findings of other drinking water biofilter studies,

which were cited and discussed in Chapters 2 and 4. It was expected that formaldehyde would have been more readily biodegradable than methylglyoxal, because it is often well removed in biologically active filters, as discussed in Chapter 2.

Table 5.10: Average Normalized Kinetic Parameters

Component	$k_0 \times 10^8$ ($\mu g\ CFU^{-1}\ hr^{-1}$)
oxalate	2.32
pyruvate	2.29
acetate	1.56
formate	1.27
methylglyoxal	0.48
formaldehyde	0.37

SEQUENCED BOM ADDITION EXPERIMENTS

Introduction

In these experiments flasks were amended sequentially with BOM. The purpose was to examine the lag phase observed for formaldehyde and methylglyoxal. It was hypothesized that these lags were due to an acclimation period which possibly involved enzyme induction. If this is true, the second amendment of BOM should be utilized with no lag phase, because the necessary enzymes would have previously been assembled, during the first BOM addition.

Utilization Kinetics

Two experiments were performed for each of the methylglyoxal- and formaldehyde-containing flasks. A single experiment in which methylglyoxal was sequentially added to flasks which contained tap water was also carried out. In this experiment the inorganic mineral medium stock (see Chapter 3) was diluted into tap water, instead of deionized water. This experiment was conducted to determine if the utilization of methylglyoxal would be different in a water with a more substantial background organic content. The chemical

and HPC data for these experiments are in Appendices A.1 and A.2, respectively.

Figures 5.10 and 5.11 show the average results for the formaldehyde, and methylglyoxal experiments, respectively. The regression calculations often included only three or four data points (see Figures 5.10 and 5.11). A greater number of data points would have improved the statistical significance of the regressions, however, the maximum number of total sampling events was limited to about 10, due to the initial water volume in the flasks. In all three cases the normal lag phase of about 20 hours was observed for the first amendment of BOM, and disappeared for the second.

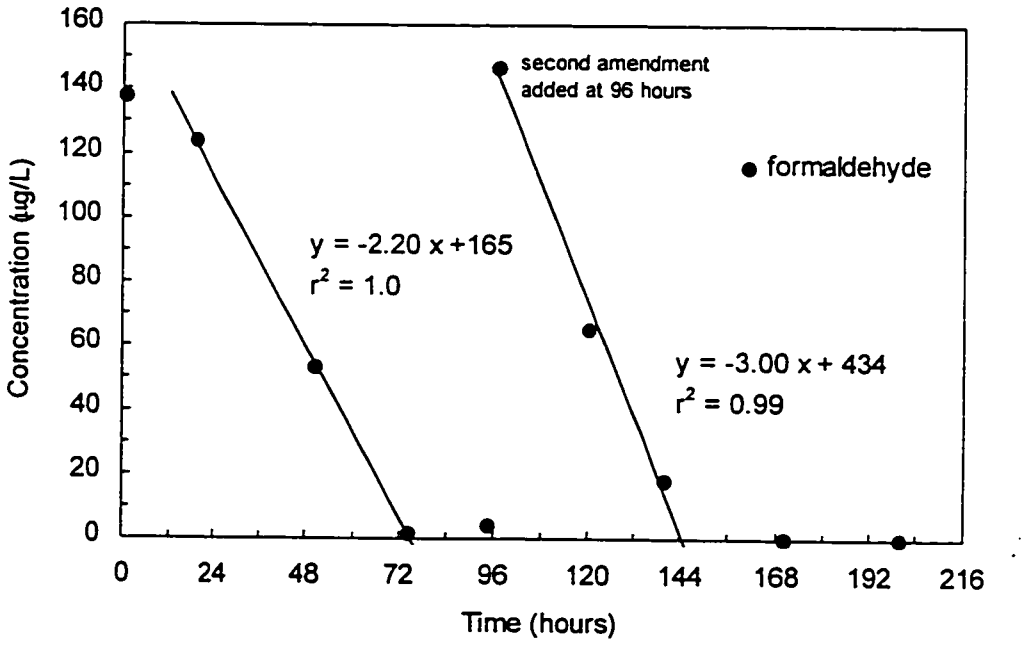

Figure 5.10: Formaldehyde concentrations for flasks sequentially amended with formaldehyde.

Pyruvate formation from methylglyoxal was observed for both additions of BOM, and in both the deionized and tap water experiments (Figures 5.11 and 5.12). In the tap water case, the second amendment of methylglyoxal was completely utilized, prior to the complete utilization of the

formed pyruvate. If this were to be observed in a filter, it could result in the appearance of pyruvate in the effluent when none was present in the influent.

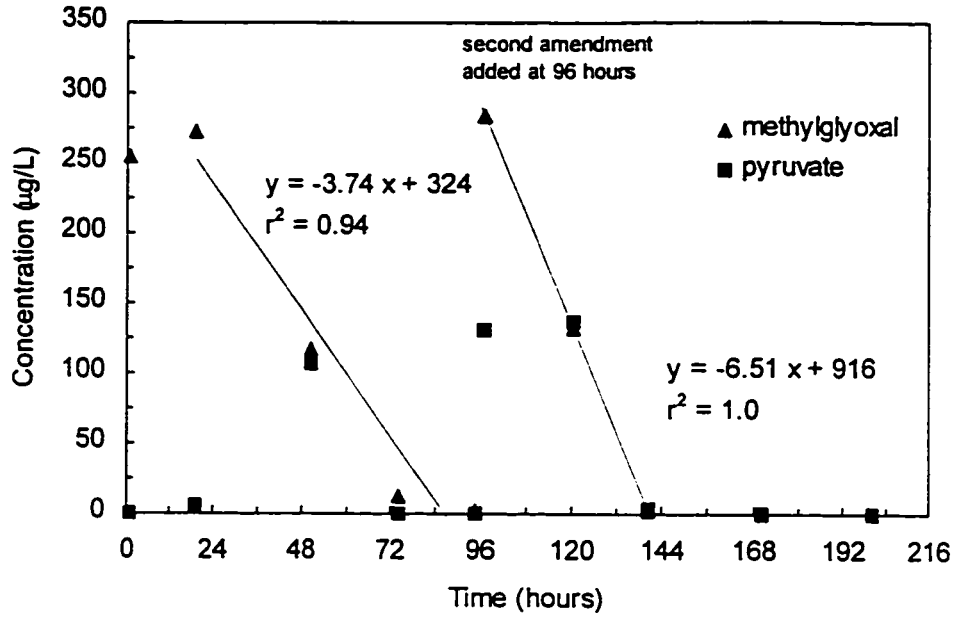

Figure 5.11: Component concentrations for flasks sequentially amended with methylglyoxal.

Table 5.11 summarizes the average normalized zero-order kinetic parameters, k_0, calculated for these experiments. The calculated values are similar to those calculated previously for formaldehyde and methylglyoxal (see Tables 5.6 and 5.7, respectively). Also, the k_0 values indicate that the utilization rate of formaldehyde and methylglyoxal was about the same in both amendments.

Table 5.11: Zero-Order Kinetic Parameters for Sequenced Experiments

	$k_0 \times 10^8$ ($\mu g\ CFU^{-1}\ hr^{-1}$)[a]	
Component Added	1st amendment	2nd amendment
formaldehyde	0.55 ± 0.085[b]	0.53[c]
methylglyoxal	0.38 ± 0.29[d]	0.43 ± 0.031[e]
methylglyoxal (tap water)	0.42[f]	0.55[g]

[a] Average plus or minus 95% confidence interval, calculated from confidence interval of the slope. P-value of slope equal to [b]0.0077, [c]>0.05, [d]0.031, [e]0.004, [f]>0.05, [g]not determined (only two data points in regression).

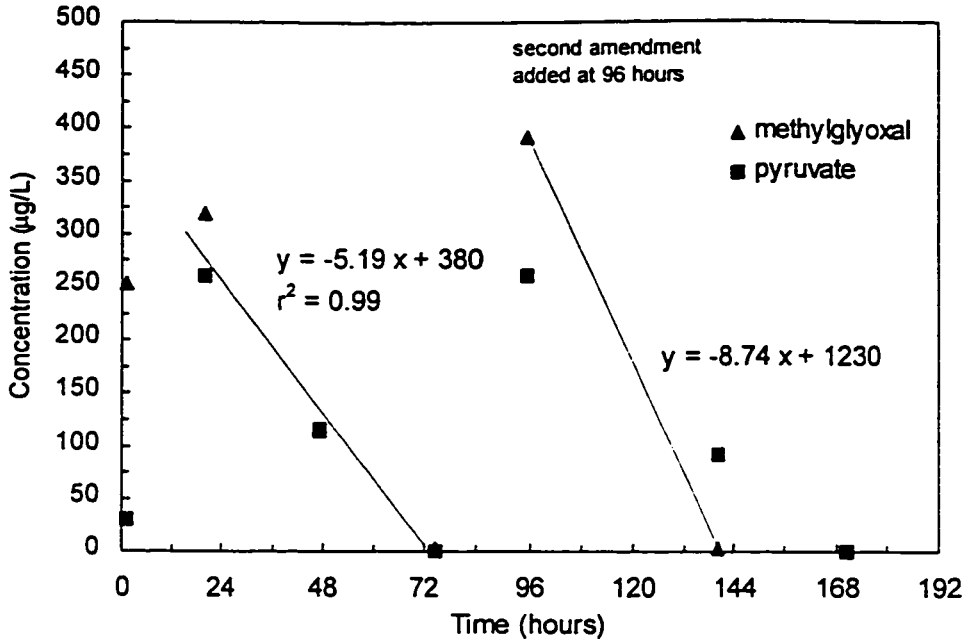

Figure 5.12: Component concentrations for tap water flasks sequentially amended with methylglyoxal.

Characterization of Microbial Communities in Sequenced Experiments

The microbial population of methylglyoxal and formaldehyde containing flasks were characterized using the BIOLOG® system (Biolog Inc.; Hayward, CA), as described in Chapter 3. Samples were collected at the end of the experiments, and the results are in Appendix A.3. This analysis was used as a means of comparing microbial communities grown on formaldehyde versus those grown on methylglyoxal.

An average of 52 out of 95 wells were different between the formaldehyde and methylglyoxal communities on the gram negative microplates, and 25 were different on the gram positive microplates. Differences of this magnitude likely represent significant differences in these communities, because the differences between duplicate analyses of a single community averaged 6 wells, for this method. Also, the methylglyoxal community differed from the inoculum by an average of 57 and 25 wells on gram negative and positive microplates, respectively. However, average differences of only 10 and 11 wells, on gram negative and positive

microplates, respectively, were observed between the formaldehyde community and the inoculum.

These results indicate that provision of methylglyoxal resulted in much greater changes to the pattern of sole carbon source utilization than did formaldehyde, suggesting a considerable shift in the makeup of the microbial community in the former case. These results support the finding that methylglyoxal has been found to be less readily biodegradable in some studies (*e.g.* Krasner *et al.*, 1993), as discussed in Chapter 2. However, in the following chapter it will be shown that biofilters can efficiently remove methylglyoxal, when few other carbon sources are available. When methylglyoxal is the sole carbon source a population can be acclimated to its utilization, however, this acclimation process may be less favorable when more readily biodegradable carbon sources are available.

CONCLUSIONS

The utilization rate of several representative ozonation by-products was calculated alone, and in the presence of other ozonation by-products, in batch bioreactors. The ozonation by-products investigated were acetate, formate, pyruvate, oxalate, formaldehyde, and methylglyoxal. Samples were also taken to monitor for the appearance of detectable transformation products during the biodegradation of these compounds. The ozonation by-product groupings were based on the positions of the compounds in the conceptual metabolic model (Figure 4.6), presented and discussed in Chapter 4.

When methylglyoxal was provided as the sole substrate, pyruvate was transiently detected during methylglyoxal utilization. No other transformation products could be identified in the other groups tested. Also, the utilization rates of the compounds tested were not found to be dependent on the other added ozonation by-products. This statement was also true of pyruvate when methylglyoxal was also initially present. The utilization of pyruvate may have been expected to be slower, due to the additional pyruvate formed from

methylglyoxal. These experiments indicate the possibility of pyruvate formation from methylglyoxal, within biologically active drinking water filters.

All of the organic acids investigated were found to be highly biodegradable. The two aldehydes investigated appeared to be less readily biodegradable than the organic acids, and both of these compounds exhibited a lag phase of about 24 hours. This lag phase was found to disappear upon a second aldehyde amendment to flasks which had been acclimated to that aldehyde. Omitting the initial lag phase, both amendments of aldehydes were utilized at about the same rate, for both formaldehyde and methylglyoxal.

The formaldehyde-using population was found to have a substantially different pattern of sole carbon source utilization (as determined using the BIOLOG® system) than the methylglyoxal-users. The BIOLOG® results also suggested that methylglyoxal utilization resulted in a considerable shift in the composition of the microbial community, compared to the starting population (*i.e.* the inoculum). The formaldehyde-using population appeared to be much more similar to the inoculum. These results provide a possible explanation for the observation that methylglyoxal has often appeared to be less readily biodegradable than formaldehyde, in biologically active drinking water filters.

REFERENCES

Bailey, J.E. and D.F. Ollis (1986). Biochemical Engineering Fundamentals, 2nd Edition. McGraw-Hill Inc., New York, New York, USA.

Brock, T.D. and M.T. Madigan (1997). Biology of Microorgansims, 8th Edition. Prentice Hall, Upper Saddle River, New Jersey, USA.

Gagnon, G.A. (1997). Utilization of Biodegradable Organic Matter by Biofilms in Drinking Water Distribution Systems. Ph.D. thesis, Department of Civil Engineering, University of Waterloo, Waterloo, Ontario, Canada.

Krasner, S.W., M.J. Sclimenti, and B.M. Coffey (1993). Testing biologically active filters for removing aldehydes formed during ozonation. *Jour. AWWA*, Vol. 85 (5), pp. 62-71.

Simkins, S., and M. Alexander (1984). Models for mineralization kinetics with the variables of substrate concentration and population density. *Appl. Environ. Microbiol.*, Vol. 47 (6), pp. 1299-1306.

Zhang, S. and P.M. Huck (1996). Removal of AOC in biological water treatment processes: a kinetic modeling approach. *Wat. Res.*, Vol. 30 (5), pp.1195-1207.

CHAPTER 6: FILTER EXPERIMENTS

INTRODUCTION

The purpose of the research described in this chapter was to further examine some of the key findings of the batch experiments in biologically active filters. Some of these aspects were: the removal of methylglyoxal at different hydraulic loading rates (HLRs); the removal of methylglyoxal with pyruvate also present in the influent; a comparison of the steady-state removals of formaldehyde and methylglyoxal; and an initial examination of the effect of amino acids on formaldehyde removals. Three filter experiments were performed, and each of these is described separately and sequentially. The possibility of mass transfer limitations in the filters is discussed, and the development of modeling equations, which are later applied to specific experimental results, is also presented. The data discussed in this chapter have been tabulated, and appear in Appendix B.1 (chemical component data), Appendix B.2 (phospholipid data), and Appendix B.3 (sodium thiosulphate data).

Mass Transfer Considerations

The utilization of BOM by suspended bacteria was considered to be negligible compared with that of the biofilm. This assumption was validated by data presented later in the chapter, which shows that little removal of BOM occurred until a biofilm had developed. This normally required about 20 days,

under the conditions investigated. The possibility of mass transfer limitations to and within the biofilm are discussed in this section.

Measured removal rates may be controlled by mass transfer or utilization kinetics. The slower of the two processes limits the overall rate at which BOM can be removed. It is possible to determine which process controls the removal rate, through the use of moduli. An external mass transfer modulus has been suggested (Karel *et al.*, 1985), and is defined as follows:

$$\phi = \frac{R_{obs} L_c}{k_L S_b} \tag{6.1}$$

where, R_{obs} is the observed reaction rate, $M_{BOM}L^{-3}T^{-1}$
L_c is the characteristic length, L
k_L is the external mass transfer coefficient, LT^{-1}
S_b is the bulk BOM concentration, $M_{BOM}L^{-3}$

If the value of this modulus is much less than unity, then utilization kinetics control the rate of reaction, and if the value approaches or exceeds unity, mass transfer becomes limiting (Karel *et al.*, 1985). The advantage of this modulus is that it does not require prior knowledge of specific kinetic parameters, and thus was selected for this analysis. A more rigorous approach would require prior determination of the kinetic parameters for which the chosen modulus is defined, and the determination of specific mass transfer parameters, however, that was beyond the scope of the present research.

R_{obs} was calculated using data presented and discussed later in this chapter, for the three compounds studied. These values were calculated from averaged data from filters in which each component was the sole carbon source fed to the filters. R_{obs} was calculated by dividing the amount of BOM removed by the corresponding EBCT. Data from experiments operated under similar conditions were averaged for this calculation. The data used were measured at the filter influent and the sample port which corresponded, as closely as possible, to the point at which complete removal of the BOM

component occurred. S_b was taken as the average of these two values, which is approximately the average concentration exposed to the biofilm.

The external diffusion layer thickness was selected for L_c. The external diffusion layer thickness was not directly measured in this research. An empirical formula presented by Jennings (1975) was used to provide an estimate:

$$L = \frac{DN_{Re}^{0.75} Sc^{0.667}}{5.7HLR} \qquad (6.2)$$

where, $N_{Re} = \frac{2\rho D_p HLR}{(1-\varepsilon)\mu}$, and $Sc = \frac{\mu}{\rho D}$

L is the external diffusion layer thickness, L
D is the diffusivity, L^2T^{-1}
ρ is the density of water, $M_{water}L^{-3}$
D_p is the diameter of the filter media, L
ε is the porosity of the filter bed
μ is the dynamic viscosity of water, $M_{water}L^{-1}T^{-1}$

The HLR was 7.5 m/h. The diffusivity of acetate (D = 1.24×10^{-9} m^2/s, Perry *et al.*, 1984) was used as a model compound for the BOM components of interest to the present research. The effective size of the anthracite media, 1 mm, was used for D_p, and the other values were known or obtained from appropriate handbooks. A value of 3.91×10^{-5} m was calculated for L, which agrees closely with that calculated for AOC (Zhang and Huck, 1996) in a dual media filter. k_L is equal to D/L, or 3.17×10^{-5} m/s. This value is also in good agreement with values, calculated by Zhang and Huck (1996), of 9.65×10^{-6} m/s and 1.47×10^{-5} m/s, for AOC in a dual media filter. Also, Rittmann and McCarty (1980a) calculated a value of approximately 1×10^{-5} m/s, for acetate. The compounds investigated in this research are components of AOC, and likely have similar mass transfer characteristics. Because both k_L and L are in good agreement with literature values, the assumed value for D must also be reasonable.

Using the above values, the external mass transfer modulus was calculated for the three BOM components studied in this research. These results are presented in Table 6.1. Since the value of the modulus was much less than unity in each case, it is very unlikely that external mass transfer limits the removal of BOM, under these conditions.

Table 6.1: Calculated Values of External Mass Transfer Modulus

BOM Component	External Mass Transfer Modulus (ϕ)
pyruvate	0.0386
methylglyoxal	0.0140
formaldehyde	0.0149

An internal mass transfer modulus has been suggested by Weisz (1973), and is defined as follows:

$$\Phi = \frac{R_{obs} L_c^2}{D_f S_b} \qquad (6.3)$$

where, D_f is the diffusivity of BOM within the biofilm, L^2T^{-1}

As for the external mass transfer modulus, if the value of this modulus is much less than unity, than utilization kinetics control the rate of reaction, and if the value exceeds unity, mass transfer is limiting. This modulus also does not require prior knowledge of specific kinetic parameters, and thus is very useful for the present purpose.

R_{obs} and S_b were calculated in the same way as for the external diffusion modulus, above. The biofilm thickness, L_f, was selected for L_c, because it represents the distance over which mass transfer occurs. The biofilm depicted in Figure 2.2 implies a homogeneous layer of microbes. It has been shown that oligotrophic biofilms actually exist as sparse clusters of colonies (Costeron *et al.*, 1994). The biofilm depicted in Figure 2.2 is more likely to be diffusion limited, and thus a uniform biofilm thickness is assumed, in order to conservatively calculate the internal mass transfer modulus.

Choosing a value for the biofilm thickness was complicated by the fact that it could not be directly measured and few values are available in the literature. Rittmann and McCarty (1980b) reported calculated values in the range of 25 to 320 μm, for filter influent concentrations of 500 to 4400 μg acetate/L. These influent concentrations range from approximately 2 to 15 times greater than employed in the present research, based on theoretical oxygen demand. Also, L_f is expected to be greatest at the top of the filter and diminish with filter depth, as the bulk substrate concentration, and hence flux, also reduces with depth. Therefore, an average value for L_f must be chosen. A conservative estimate of 25 μm was chosen for these calculations.

The value of D_f was assumed to be half the value of D, as suggested by Zhang and Huck (1996), which is $5x10^{-10}$ m^2/s. D_f may actually be closer to the diffusivity of the bulk liquid, given that the biofilm is probably a collection of small, sparse clusters, as discussed above. However, this assumption was considered to be conservative, in that, a lower value of D_f is more likely to result in internal diffusion limitations.

Using the above values, the internal mass transfer modulus was calculated, for the three BOM components studied in this research. These results are presented in Table 6.2. Since the value of the modulus was much less than unity in each case, it is very unlikely that internal mass transfer limits the reaction rate of BOM, under these conditions. Thus, neither internal or external mass transfer limits the reaction rate of BOM in this experimental system. This conclusion is supported by Wang (1995), who showed that the rate of removal of BDOC in biological filtration was controlled by reaction rate, and not mass transfer.

Table 6.2: Calculated Values of Internal Mass Transfer Modulus

BOM Component	Internal Mass Transfer Modulus (Φ)
pyruvate	0.0391
methylglyoxal	0.0142
formaldehyde	0.0151

Development of Modeling Equations

A general equation which describes diffusion and bioreaction in a packed bed, adapted from Fogler (1992), is:

$$D_a \frac{d^2 S_b}{dz^2} - HLR \frac{dS_b}{dz} + \Omega r = 0 \qquad (6.4)$$

where, D_a is the effective axial dispersion coefficient, L^2T^{-1}
z is depth within the filter, L
Ω is the overall effectiveness factor
r is a general bioreaction term, $M_{BOM}L^{-3}T^{-1}$

The overall effectiveness factor is defined as follows:

$$\Omega = \frac{\text{actual overall substrate removal rate}}{\text{rate that would exist if the entire biofilm were exposed to the bulk substrate concentration}} \qquad (6.5)$$

This factor is calculated from internal and external mass transfer coefficients, reaction kinetic coefficients, the surface area available for biofilm development, and other system variables. The mathematical form of the equation used to calculate it depends on the kinetic reaction order, and thus a general expression is not available. Numerical values for this factor vary from 0 to 1. Values near zero indicate that the process is highly mass transfer limited, and values of unity indicate that reaction kinetics control the rate. Thus, this factor takes into account possible mass transfer limitations, however, it inherently assumes that the activity of the biomass does not vary with depth. An important feature of this factor is that it allows the equation to be written in terms of the bulk substrate concentration.

The equation could be greatly simplified if the first term could be eliminated. Young and Finlayson (1973), have shown that axial dispersion can be neglected when the following is true:

$$\frac{-r\rho_b D_p}{HLR\, S_{b_o}} << \frac{HLR\, D_p}{D_a} \qquad (6.6)$$

where, ρ_b is bulk density of the bed, $M_{bed}L^{-3}$

S_{b_o} is filter influent bulk BOM concentration, $M_{BOM}L^{-3}$

The observed rate of reaction for pyruvate, calculated previously for the internal and external mass transfer moduli, was used for r, the effective size of the media, 1 mm, was used for D_p, and the average influent pyruvate concentration was used for S_{b_o}. The value for D_a is expected to be of the same order of magnitude as D, and thus a reasonable assumption is that D_a is equal to D, which is $1x10^{-9}$ m^2/s. A value of 7.5 m/h was used for the HLR. Using these values the left and right sides of equation 6.6 were calculated. It was found that the left side of equation 6.6 was about 5 orders of magnitude smaller than the right. Thus, axial dispersion can safely be neglected. Because the left and right sides of equation 6.6 differed so greatly, this conclusion is not sensitive to the value of D_a. It is improbable that the assumed value of D_a was several orders of magnitude too small. The conclusion that dispersion is not likely to be important in drinking water filters because of the high flow rates normally employed, has also been drawn by other researchers (*e.g.* Wang, 1995).

Therefore the equation can be simplified to:

$$\frac{dS_b}{dz} = \frac{\Omega r}{HLR} \qquad (6.7)$$

Further, assuming zero-order kinetics, and representing the reaction rate per unit surface area of bed:

$$r = -k_0 X \rho_b A \qquad (6.8)$$

where, k_0 is the zero-order rate coefficient, $M_{BOM}L^{-2}T^{-1}M_{biomass}^{-1}M_{media}$

X is biomass, $M_{biomass}M_{media}^{-1}$

A is the specific surface area of the filter bed, $M_{bed}^{-1}L^2$

The biomass measurement that was used in this research was the phospholipid method, which provided units of nmol lipid-P per gram of media. These units result in inconvenient units for k_0. Most of the results in this chapter are discussed in these units. Approximate conversion factors were applied to convert k_0 into more traditional units, for comparison with the batch results. This analysis is discussed in the "Comparison of Kinetic Parameters to Batch Results" section.

Biomass was expected and, as will be shown later, observed to decrease with depth in the filter. The following exponential function provided a good empirical fit to the biomass data. The data and analysis which justify this are presented later in the chapter. Thus, the following equation is proposed,

$$X = X_0 \exp(-k_{biomass} z) \tag{6.9}$$

where, X_0 is the biomass at the top of the filter $M_{biomass}M_{media}^{-1}$
$k_{biomass}$ is the exponential coefficient for biomass, L^{-1}

By substituting the rate and biomass expressions into equation 6.7, and integrating, the following equation was determined:

$$S_b = S_{b_0} - \frac{\Omega k_0 \rho_b A X_0}{HLR\, k_{biomass}} \left[1 - \exp(-k_{biomass} z)\right] \tag{6.10}$$

The above equation is applied to data from specific filter experiments later in the chapter. The overall effectiveness factor is set equal to one, in further calculations, because as shown above, mass transfer limitations are negligible under the conditions investigated. The ability of this equation to describe specific data sets is also discussed. It is presented here to show the relationship of BOM concentrations to the major operating and system variables in a biofilter.

FILTER EXPERIMENT #1

Purpose and Experimental Design

It was shown in Chapter 5 that pyruvate is formed from methylglyoxal in batch bioreactors. An objective of this experiment was to examine the biodegradation of methylglyoxal in biologically active filters, and to determine whether measurable pyruvate concentrations would be observed. This was investigated at two different HLRs, and when various perturbations were applied to the filters. Also, a third filter which was not fed any BOM, was operated as a control. The experimental operating conditions of the three filters used in this experiment are given in Table 6.3. Measured influent and effluent dissolved oxygen (D.O.) values are also provided in Table 6.3. A comparison of these measured values to the theoretical oxygen demand, and also to the biomass measured in the filters, is provided in the "Correlation of Biomass with Dissolved Oxygen" section together with data from the other two filter experiments.

Table 6.3: Experimental Conditions for Filter Experiment #1

	Filter #1	Filter #2	Filter #3
methylglyoxal (μg/L)	0	150	150
theoretical oxygen demand (mg O_2/L)	0	0.20	0.20
HLR (m/h)	5	5	10
bed depth (mm):			
anthracite	490	490	490
sand	250	250	250
EBCT (min)	8.9	8.9	4.4
D.O. (mg/L)[a]:			
influent	6.10	6.11	6.00
effluent	6.05	5.89	5.80
temperature (°C)[b]:	16.4	16.4	16.2

[a] The given D.O. measurements refer to steady-state conditions.

[b] The average of the influent and effluent temperatures is given. The water temperature rose by 0.4 to 1.3 °C through the filters.

Filter #1 (Control Filter): Results and Discussion

Sampling of Filter #1, the control filter, indicated insignificant concentrations of most carboxylic acids and aldehydes. Formate

concentrations in the range of 4.2 to 26.4 μg/L and formaldehyde concentrations of 2.2 to 11.9 μg/L were observed in the filter influent. Background concentrations in this range were also observed in the other filter influents. Some of the detected formate and formaldehyde was likely from the tap water itself, although random contamination could also account for a portion of these amounts.

There was no significant difference between the average influent and effluent concentrations of these compounds, at the 1% level, by comparing paired influent and effluent values, from day 43 onward. It was assumed that pseudo-steady state removal of the added methylglyoxal had been achieved by the 43rd day in Filters #2 and #3, as discussed below. The average and standard deviation of the Filter #1 data are shown in Table 6.4. Also, negligible biomass accumulated on the media (< 4 nmol lipid-P/cm^3 filter) in Filter #1, after 81 days of operation. Much higher biomass values were measured in the filters with added BOM in the influent, as discussed below. Furthermore, the Filter #1 backwash water was found to remain essentially clear in colour throughout the experiment. This differed from filters with added BOM, for which the backwash water changed from almost clear to a yellowish brown, after a biofilm had been established.

Table 6.4: BOM Data for Filter #1 (Control Filter)

	Influent (μg/L)		Effluent (μg/L)	
	average	standard deviation	average	standard deviation
formate	11.7	7.7	9.4	6.4
formaldehyde	5.1	3.3	4.5	3.8

Non-Purgeable Organic Carbon Removal

NPOC was also measured in the influent and effluent of all filters several times throughout the experiment. The NPOC of the tap water was about 1.3 mg-C/L. It was not possible to demonstrate a significant difference between the influent and effluent concentrations for any of the three filters, at the 1% level. A difference was expected for Filters #2 and #3, which

accumulated a measurable biomass, but not for Filter #1, the control filter. The difference between influent and effluent values would consist of the added BOM, and any background NPOC which was removed. One explanation for the lack of an observed difference is the low concentration of added BOM, when expressed on a carbon mass basis. The added methylglyoxal was approximately 0.075 mg-C/L, or about 6% of the NPOC of the tap water. This amount is likely too small a difference to be detected. Also, little biomass was detected in Filter #1, thus indicating that the background NPOC was highly stable. This was expected for a high quality ground water.

Steady-State Results and Discussion

Complete removal of methylglyoxal was observed in Filters #2 and #3 after about 20 days (Figure 6.1). It appeared that a "pseudo-steady-state" had been achieved by day 23.

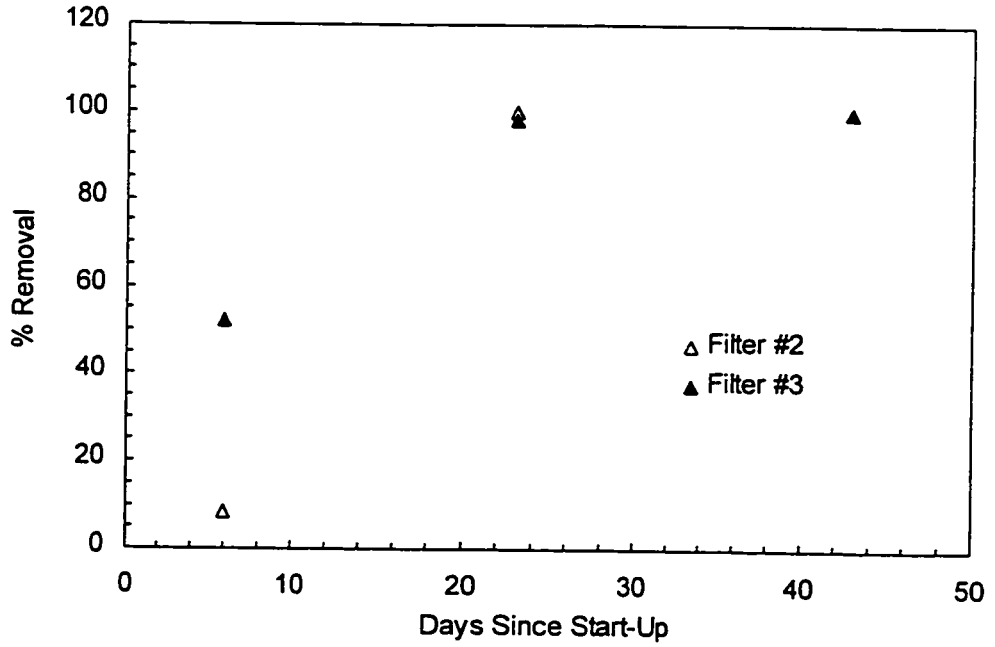

Figure 6.1: Percent removal of methylglyoxal in first 43 days of filter experiment #1.

Figure 6.2 shows the concentration profile of methylglyoxal in Filter #2, on day 43. Pyruvate was observed at a depth of 4 cm, or about 0.5 min of EBCT. Also, Figure 6.3 shows the corresponding data for Filter #3. In this

filter pyruvate was also observed, although at lower concentrations and at three different depths. On day 6 pyruvate was not observed in either filter, but was observed on day 23, in a similar pattern as shown in Figures 6.2 and 6.3. Therefore the formation of pyruvate coincided with the development of a biomass and the utilization of methylglyoxal, as observed in the batch experiments (*e.g.* Figure 5.4).

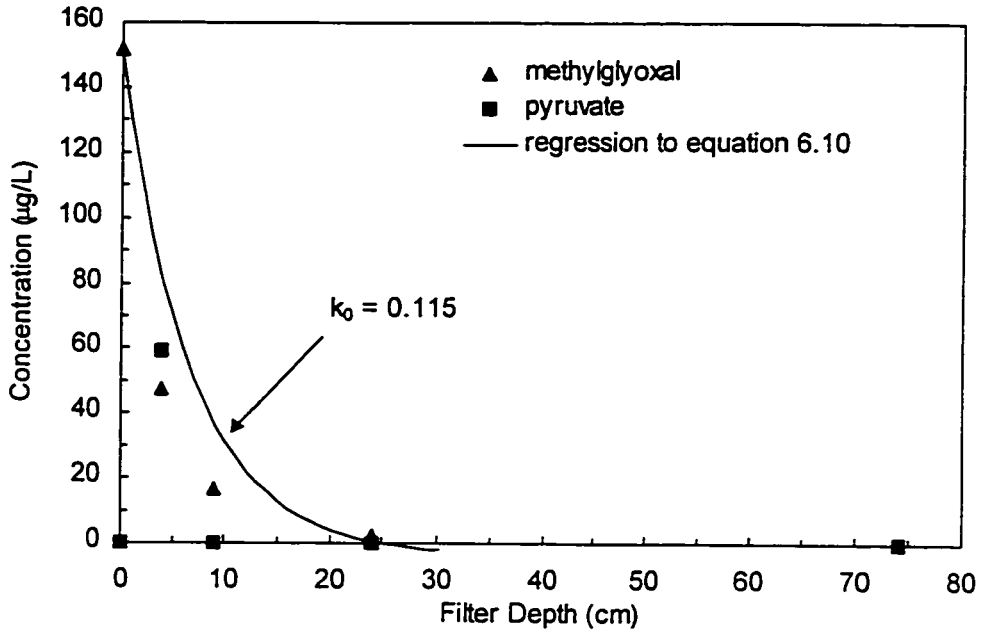

Figure 6.2: Methylglyoxal and pyruvate concentration profiles in Filter #2 on day 43. The units of the zero-order kinetic parameter (k_o) are the same as those given in Table 6.5.

Because Filter #3 was operated at a higher HLR the methylglyoxal concentrations appear higher at a given depth than in Filter #2. This is because there is less removal in a given length of filter at the higher HLR. However, the concentration profiles would appear much more similar if plotted versus EBCT. Servais *et al.* (1992) showed that any combination of HLR and depth which provide a given EBCT, will give the same BDOC removal. It is reasonable to extend this to the removal of specific BOM components. Since pyruvate formation is linked to methylglyoxal utilization, the pyruvate concentration profile is also shallower for Filter #3, compared to Filter #2.

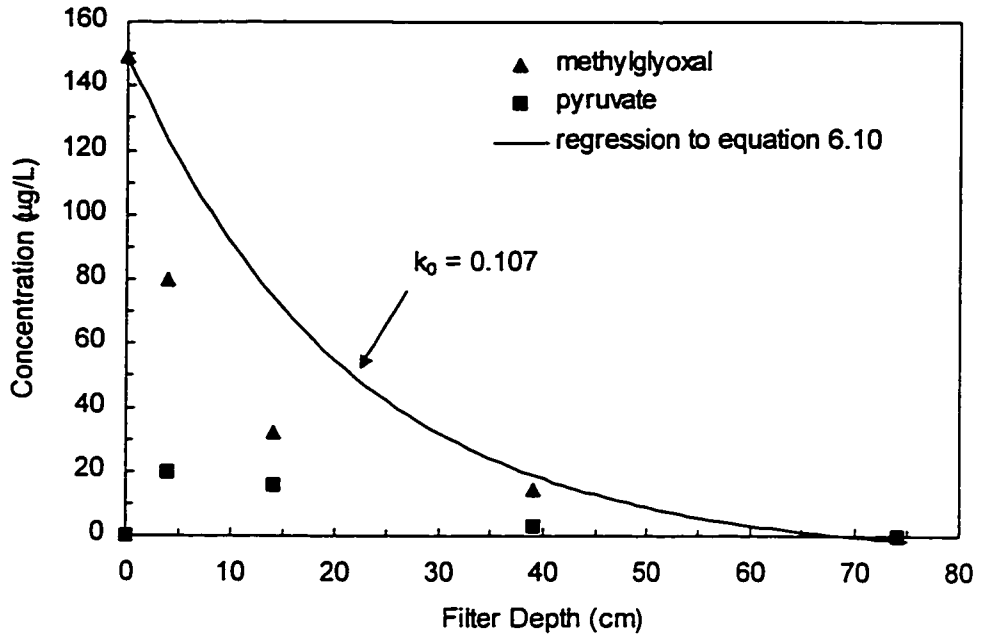

Figure 6.3: Methylglyoxal and pyruvate concentration profiles in Filter #3 on day 43. The units of the zero-order kinetic parameter (k_o) are the same as those given in Table 6.5.

Also shown in Figures 6.2 and 6.3 are regression lines. These lines were obtained by first fitting the applicable biomass data to the exponential decay function given in equation 6.9, by non-linear regression. The regressions for Filter #2 and #3 on day 43, shown in Figure 6.4, were found to have little scatter, and both had p-values < 0.001, with no pattern to the model residuals. From this it was concluded that the biomass profiles could be adequately described by this exponential decay function. The calculated regression values for X_0, the biomass at the top of the filter, and $k_{biomass}$, the exponential coefficient for biomass, were then substituted into equation 6.10. A value of k_o, the zero-order rate constant could then be determined by performing linear regressions of equation 6.10 to the methylglyoxal data, which are shown on Figures 6.2 and 6.3. Values of 0.115 and 0.107 $\frac{\mu g \text{ methylglyoxal g media}}{\text{L hr nmol lipid - P}}$ were calculated for Filters #2 and #3, respectively. These regressions had p-

values of 0.033, 0.072 for Filters #2 and #3, respectively. The regression on the Filter #3 data was less significant than for Filter #2, and would have been improved had the biomass profile been less shallow. This biomass profile was shallower than expected, even considering the difference in the HLRs of the two filters.

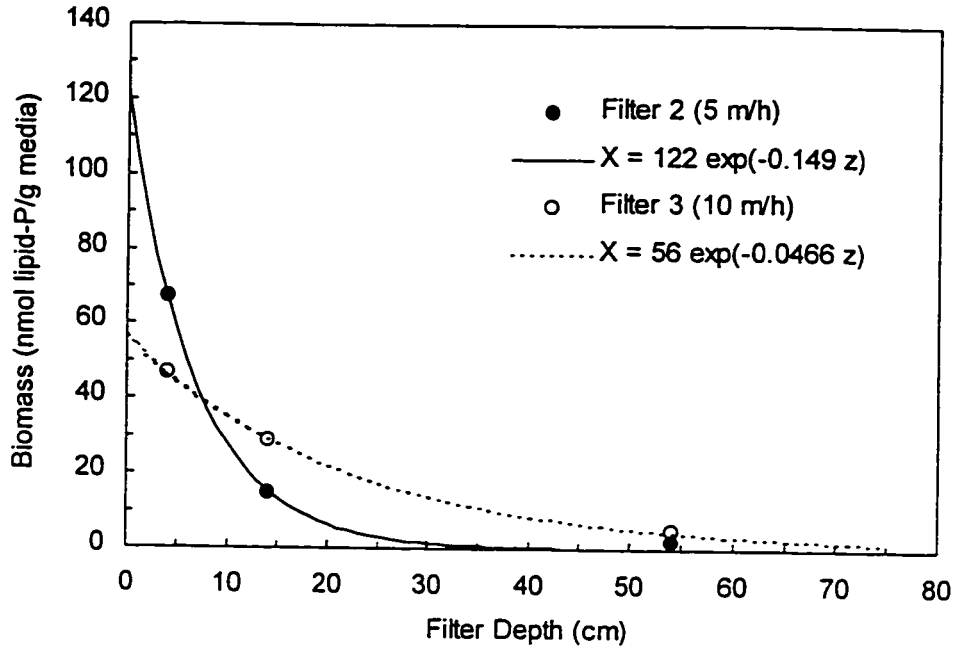

Figure 6.4: Biomass profiles in Filters #2 and #3 on day 43.

Effect of Backwashing

Under steady-state conditions neither methylglyoxal nor pyruvate were observed in the filter effluent, of either Filter #2 or #3. On day 43, sampling for methylglyoxal and pyruvate was conducted about one hour after backwashing. The backwashing protocol consisted of a water and air wash under "collapse-pulsing" conditions, followed by a water wash at 20% bed expansion, as described in detail in Chapter 3.

Similar patterns were found in both filters for the methylglyoxal and pyruvate concentration profiles. The profiles did not appear to differ significantly from those taken just before backwashing, except that small yet distinguishable quantities of methylglyoxal were observed in the effluents.

These concentrations were below 2.5 μg/L, the minimum reporting limit of methylglyoxal for this method. Values for k_o were determined, as discussed above, assuming the same biomass profile as just prior to backwashing. The values are given in Table 6.5. The calculated values for before and after backwashing agreed very closely. This indicates that the biomass activity was not adversely affected by backwashing, and that the methylglyoxal removal rate was unchanged by the backwashing process.

Table 6.5: Zero-Order Kinetic Parameters Before and After Backwashing

	$k_0 \left(\frac{\mu g \text{ methylglyoxal g media}}{\text{L hr nmol lipid - P}} \right)^a$	
	before backwashing	following backwashing
Filter #2 (5 m/h)	0.115 ± 0.093^b	0.102 ± 0.024^d
Filter #3 (10 m/h)	0.107 ± 0.072^c	0.097 ± 0.034^e

[a] Parameter estimates shown with 95% confidence intervals.
The p-values of the regressions were [b]0.033, [c]0.072 (90% confidence interval shown), [d]0.012, and [e]0.0175.

Some biomass may have been removed during the backwashing process, contrary to the assumption made in the calculation of the kinetic parameters. A visual inspection of the backwash water indicated that it likely contained some biomass. Also, Urfer-Frund (1998) found that biomass values, as measured by the phospholipid method, were about 50% lower at the top of biofilters, immediately following backwashing. However, it was also observed in that study that removals of formate and acetate were not impaired at the beginning of the subsequent filter run, when the backwash water did not contain chlorine or other oxidants. If the biomass concentration was indeed lower following backwashing in the present study, the calculated kinetic parameters would be higher following backwashing than before. It would be highly unexpected to find that the backwashing process improved the efficiency of the biomass for the removal BOM. It is more likely, as suggested by Urfer-Frund (1998) that the phospholipid method does not adequately quantify the BOM removal capability of the biofilm.

Other studies have also examined BOM removals before and after backwashing. Prévost *et al.* (1995) observed that after backwashing, removals of DOC, BDOC, oxalate, and most aldehydes were better than at the end of the previous filter run. They argued that the build-up of floc and particles reduced the flux of BOM to the biomass. This build-up is expected to worsen over the filter run. This was not observed, nor was it expected, in the present study because of the lack of particles, coagulant, and hence floc, in the feed water.

Miltner *et al.* (1995) examined the effect of backwashing on biofilters. They found that the biomass concentration, as measured by the phospholipid method, did not significantly change after backwashing with water that contained no chlorine residual, although air scour was not employed in that study. Moreover, the removals of aldehydes, AOC, TOC, and DBP precursors, were not affected by backwashing under those conditions. The results of the present study are in agreement with this finding.

Effect of Spike in Influent Concentration

A spike of approximately four times the normal methylglyoxal concentration, 24 hours in duration, was introduced to Filters #2 and #3. Methylglyoxal removals dropped from complete removal to about 60% at the beginning of the spike (Table 6.6). Both filters had the same overall removal percentage, despite being operated at different HLRs. The methylglyoxal concentration profile within Filter #2 appeared to follow an exponential decay, with most of the removal occurring in the first 4 minutes of EBCT. Very little biomass accumulated in the bottom half of Filter #2, since very little BOM was normally available in that portion of the filter. In contrast, the methylglyoxal concentration profile in Filter #3 was essentially linear, because more biomass had accumulated at lower depths of this filter (Figure 6.4). Since most of the removal in each filter occurred in the first 4 minutes of contact time, the overall performance of the filters was similar. This 4 minutes occupied only about half of the depth of Filter #2, but the entire depth of Filter #3.

Table 6.6: BOM Concentrations at Start of 24 hour Spike Increase

	Methylglyoxal (μg/L)			Pyruvate (μg/L)	
	Influent	Effluent	% Removal	Influent	Effluent
Filter #2 (5 m/h)	523	203	61.2	0	28.6
Filter #3 (10 m/h)	487	180	63.0	0	109

At the end of the 24 hour spike, nearly complete removals of methylglyoxal were observed in both filters, as shown in Table 6.7. A measurable quantity of pyruvate continued to be present in the effluent of Filter #3, which was operated at the higher HLR. It was unexpected that a near complete recovery of BOM removal would be obtained after only 24 hours. This was mainly due to the formation of additional biomass (Figure 6.5). In Filter #2 the biomass at a depth of 4 cm was significantly higher, at the 10% level, at the end of the spike compared to that observed prior to the spike. This biomass comparison was not statistically significant in Filter #3, however, the biomass at a depth of 14 cm was found to be significantly higher after the spike, at the 10% level, compared to before the spike. Also, there was little additional biomass observed in the lower half of Filter #2 (data not shown).

Table 6.7: BOM Concentrations at End of 24 hour Spike Increase

	Methylglyoxal (μg/L)			Pyruvate (μg/L)	
	Influent	Effluent	% Removal	Influent	Effluent
Filter #2 (5 m/h)	644	12.0	98.1	0	0
Filter #3 (10 m/h)	615	23.8	96.1	0	5.8

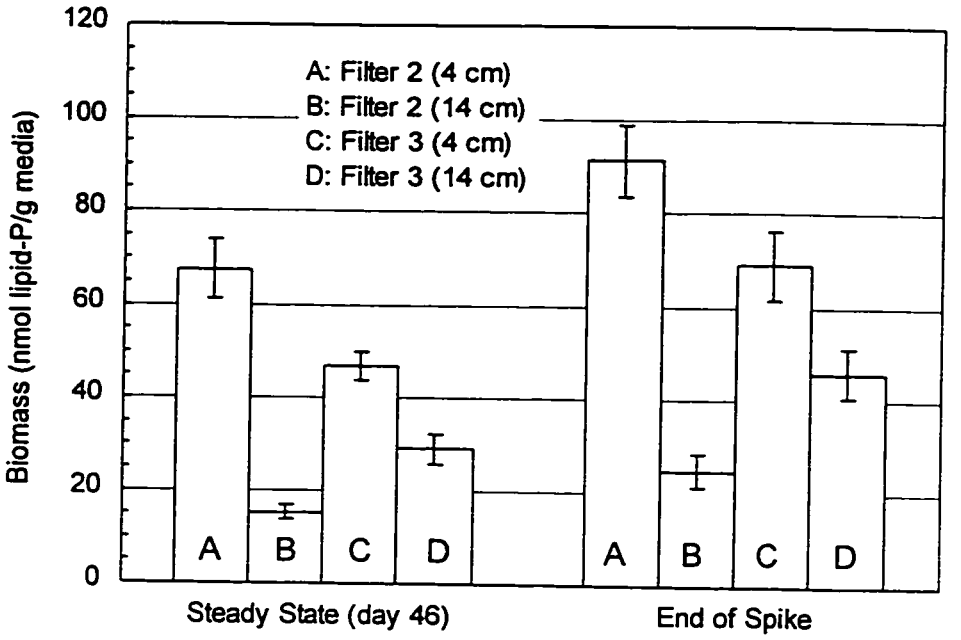

Figure 6.5: Biomass comparison prior to and at the end of a 24 hr spike in the influent methylglyoxal concentration (error bars represent ± 1 standard deviation).

About 4 hours after the normal influent concentration of methylglyoxal was re-established, superior removals were observed in both filters, compared to the steady-state values observed on day 43. Values for k_o were determined, as discussed above, and are shown in Table 6.8. These values were not significantly different than those calculated for day 43, at the 5% level. This was because the better removals were accompanied by higher biomass levels (see Figure 6.5), and therefore the removal rates were not greater once normalized for biomass.

Table 6.8: Zero-Order Kinetic Parameters After Spike Increase

	k_0[a]
Filter #2 (5 m/h)	0.073 ± 0.058[b]
Filter #3 (10 m/h)	0.115 ± 0.045[c]

[a] The units used are the same as given in Table 6.5 and 90% confidence intervals are shown. The p-values of the regressions were [b]0.088 and [c]0.065.

The spiking experiment was repeated, after allowing the filters to run at normal conditions for about two weeks. In this trial the higher concentration was maintained for three days, and hence was termed a step increase. Table 6.9 summarizes these results, which were similar to those given in Table 6.7. The improvement in methylglyoxal removals in the first 24 hours, was not followed by any further improvement after the next 2 days. The fact that pyruvate remained in the effluent of Filter #3, indicates that recovery of BOM control took longer at the higher HLR. Moreover, the presence of pyruvate in the effluent of Filter #3 may be unavoidable, under these conditions. This hypothesis would need to be confirmed in an experiment of greater duration. Sampling at intermediate depths indicated that the methylglyoxal concentration profiles in Filters #2 and #3 had the appearance of exponential decay curves. About 66% removal was achieved at a depth of 9 cm, or 0.5 minutes of EBCT, in Filter #3, and 75% removal had occurred at this depth in Filter #2, which corresponded to 1 minute of EBCT. This was a further indication that biomass development continued in the top portion of the filters, with less new growth in the bottom portions.

Table 6.9: BOM Concentrations at End of 3 Day Step Increase

	Methylglyoxal (μg/L)			Pyruvate (μg/L)	
	Influent	Effluent	% Removal	Influent	Effluent
Filter #2 (5 m/h)	646	2.5	99.6	0	0
Filter #3 (10 m/h)	634	41.5	93.5	0	13.3

Effect of Period out of Service

The filters were shut down for 48 hours after 81 days of operation and about 10 days after returning to the normal influent methylglyoxal concentration. The water level was maintained at the level of the overflow during the shut-down. Just prior to re-starting the filters the dissolved oxygen of the water in the filters had dropped to about 2.0 mg/L in Filters #2 and #3, and about 4.8 mg/L in Filter #1. Samples for BOM analysis were taken within an hour of re-starting the filters. Values for k_o were determined, as discussed

above, assuming the same biomass profile as at steady-state, and are tabulated in Table 6.10. These values agreed closely with steady-state values, from day 43, indicating that methylglyoxal removals were not strongly affected by the shut-down. A concentration of methylglyoxal less than the method detection limit of 2.5 μg/L was observed in the effluent of Filter #3. Pyruvate profiles were generally similar to what had been observed at steady-state, although pyruvate was detected about 5 cm deeper in both filters. Pyruvate was not observed in the filter effluents.

Table 6.10: Zero-Order Kinetic Parameters After Shut-Down

	k_0[a]
Filter #2 (5 m/h)	0.094 ± 0.029[b]
Filter #3 (10 m/h)	0.104 ± 0.039[c]

[a] The units used are the same as given in Table 6.5 and 95% confidence intervals are shown. The p-values of the regressions were [b]0.005 and [c]0.008.

Summary

The formation of pyruvate within biologically active filters was observed when methylglyoxal was the sole BOM component in the influent. At higher HLRs both methylglyoxal and pyruvate were measured at lower depths in the filter, as expected. At some higher HLR it may be possible that both methylglyoxal and pyruvate would appear in the filter effluent.

An exponential decay model provided a good fit to the steady-state biomass versus depth data. Also, the proposed modeling equation, given in equation 6.10, adequately described the methylglyoxal concentrations in this experiment. This equation showed that the biomass profile had a significant impact on the order of the apparent biodegradation kinetic expression.

Backwashing and a 48 hour period out of service did not have a significant effect on methylglyoxal removals in this experiment. This indicates that these processes did not impair the performance of the biomass, under the conditions of this experiment. A spike in the influent concentration of

methylglyoxal resulted in measurable concentrations of both methylglyoxal and pyruvate in the filter effluents. Also, the filter operated at the lower HLR re-established complete removal of both methylglyoxal and pyruvate after 24 hours of operation at the higher methylglyoxal influent concentration. However, complete removal of pyruvate was not observed in the filter operated at the higher HLR after three days of operation at the higher influent methylglyoxal concentration.

It was only when the filters were disturbed from steady-state that pyruvate appeared in the effluent. The presence of pyruvate in the effluent of filters which are fed only methylglyoxal, may be an indication of unsteady-state behavior.

FILTER EXPERIMENT #2

Purpose and Experimental Design

The purpose of this experiment was to further investigate the formation of pyruvate from methylglyoxal. For this purpose three filters, with three different influent BOM cocktails were compared. The first contained only methylglyoxal, the second only pyruvate, and the third both methylglyoxal and pyruvate. A fourth filter was also included, which had formaldehyde as its sole BOM component in the influent. This filter provided a means of directly comparing methylglyoxal and formaldehyde removals. This comparison was of interest because methylglyoxal removals have often been reported as being lower than that of formaldehyde (*e.g.* Krasner *et al.*, 1993). The experimental and operating conditions are given in Table 6.11.

Table 6.11: Experimental Conditions for Filter Experiment #2

	Filter #1	Filter #2	Filter #3	Filter #4
BOM (μg/L):				
methylglyoxal	200		100	
pyruvate		290	145	
formaldehyde				250
theoretical oxygen demand (mg O_2/L)	0.267	0.267	0.267	0.267
HLR (m/h)	8	8	8	8
bed depth (mm):				
anthracite	500	500	500	500
sand	250	250	250	250
EBCT (min)	5.6	5.6	5.6	5.6
D.O. (mg/L)[a]:				
influent	7.08	7.00	7.11	7.12
effluent	6.60	6.62	6.81	6.70
temperature (°C)[b]	15.3	15.3	15.3	15.4

[a] The given D.O. measurements refer to steady-state conditions.

[b] The average of the influent and effluent temperatures is given. The water temperature rose by about 0.6 °C through the filters.

Effect of Monochloramine Residual in Influent

For about the first 30 days of this experiment a monochloramine residual, of approximately 0.5 mg Cl_2/L, was present in the tap water.

Approximately half of this was removed in the GAC pre-filters, leaving a residual of about 0.25 mg Cl_2/L in the influent of the filters. This residual was sufficient to prevent any significant removal of BOM in all filters, in the first 18 days of operation (Table 6.12). It was expected, based on the results of filter experiments #1 and #3 (to be discussed below), that removals of ≥ 90% would be established for methylglyoxal and formaldehyde, after about 20 days of operation. Similar results have been obtained by other researchers. Urfer-Frund (1998) found that the continuous presence of a combined chlorine residual of 0.1 to 0.3 mg Cl_2/L was sufficient to inhibit the removal formate and other easily biodegradable components in a 3 month biofilter study.

Table 6.12: BOM Concentrations after 18 Days of Operation

Filter #	Added BOM	Concentration (μg/L) Influent	Effluent	% Removal
1	methylglyoxal	198	196	1.0
2	pyruvate	293	291	0.5
3	methylglyoxal	120	106	11.0
	and pyruvate	158	144	9.3
4	formaldehyde	254	226	11.0

Achieving Steady-State: Results and Discussion

Beginning on day 31, sodium thiosulphate was introduced to the feed water, after the GAC pre-filters, to quench the monochloramine residual. The concentration of thiosulphate was increased step-wise, from day 31 to 37, to obtain a concentration which would provide essentially complete quenching, while also minimizing the thiosulphate residual, which remained in the influent water. After quenching began, the BOM removals in the filters steadily improved, and steady-state values were obtained in about the same time as expected from the other filter experiments, as shown for Filter #2, in Figure 6.6. The thiosulphate concentration was measured in the filters, and concentration profiles for all four filters on Day 75, are shown in Figure 6.7. The thiosulphate represented about 10 to 15% of the total theoretical oxygen demand in the filter influents.

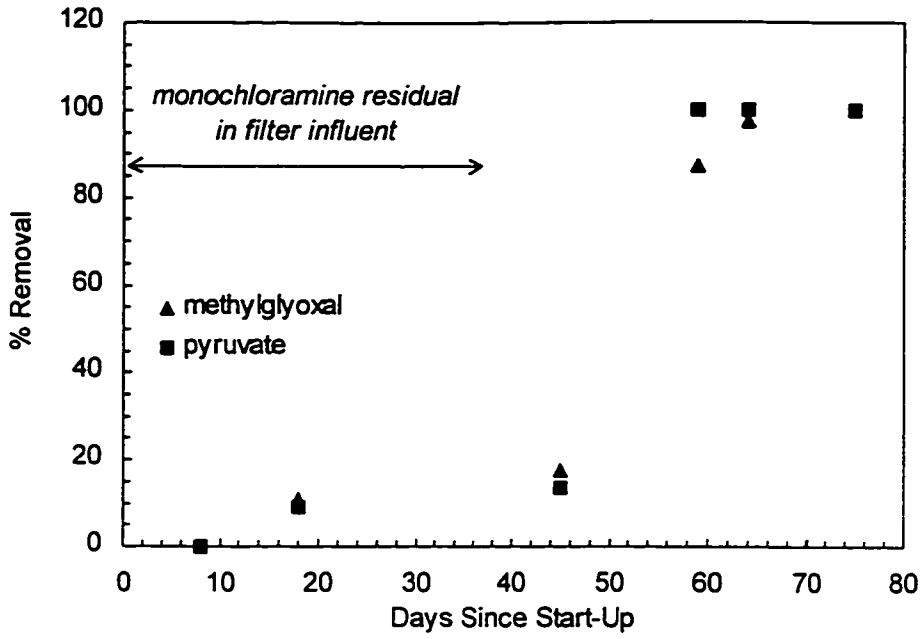

Figure 6.6: Removal of pyruvate and methylglyoxal in filter #2, over the duration of experiment #2.

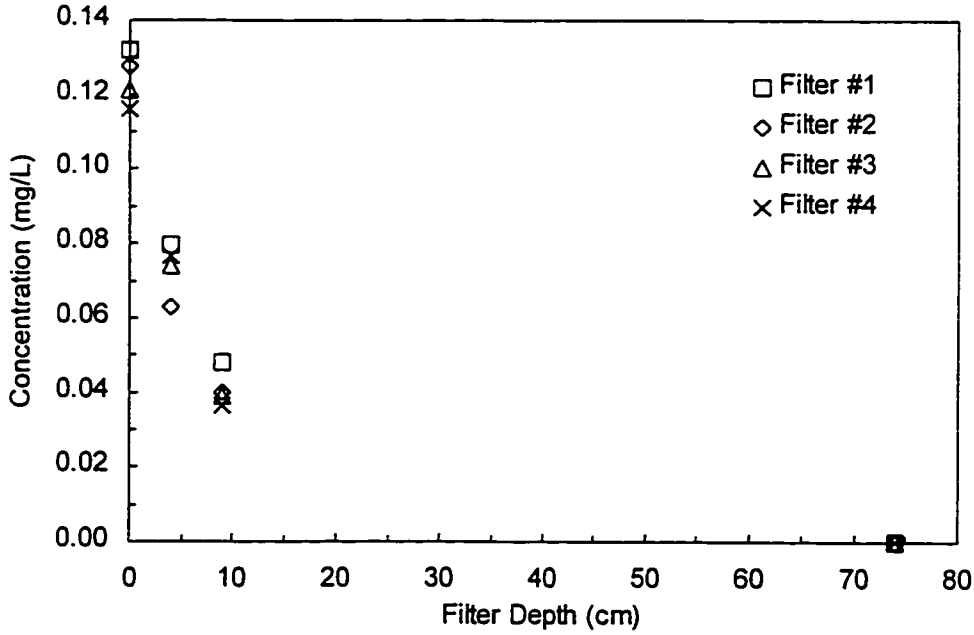

Figure 6.7: Sodium thiosulphate concentration profiles for all four filters on day 75 (38 days since quenching began).

The presence of thiosulphate in the filter influents my have altered the composition of the biofilm population, compared to the first experiment for

which no thiosulphate was dosed. However, the thiosulphate may have been oxidized to sulphate by the biofilm cells, in order to provide additional cellular energy. If the thiosulphate was oxidized in this manner a shift in the population toward sulphate metabolism would not be likely. It was thus assumed that comparisons with the results from filter experiment #1 remained valid.

Results for Filters #1, #2, and #3 for day 64 (27 days after thiosulphate quenching began) are presented in Table 6.13. These data indicate that good removals had been achieved in all the filters, except for Filter #1. It is significant to note that pyruvate was detected in the effluent of Filter #1, which was only fed methylglyoxal. The formation of pyruvate during methylglyoxal utilization was observed in the first filter experiment, discussed previously. The presence of pyruvate in the effluent of methylglyoxal-fed filters was also observed in that experiment, when perturbations were introduced to the filters. These data provide further evidence that the appearance of pyruvate in methylglyoxal-fed filters is an indication of unsteady state behaviour.

Table 6.13: Selected BOM Data after 64 Days of Operation

	methylglyoxal (µg/L)			pyruvate (µg/L)		
	Influent	Effluent	% Removal	Influent	Effluent	% Removal
Filter 1	203	46.6	77.1	-	18.7	-
Filter 2	-	-	-	309	0	100
Filter 3	96.6	2.5	97.4	144.5	0	100

Sampling at intermediate sampling ports of Filter #2 showed that nearly complete pyruvate removal occurred in just over 1 minute of EBCT. Complete pyruvate removal was also observed in Filter #3, which is an indication that it may be more readily biodegradable than methylglyoxal. A comparison of the data for Filters #1 and #3 also indicate that methylglyoxal removal was higher in the presence of pyruvate. This may be due to the fact that a biomass was established more quickly, due to the utilization of pyruvate.

This biomass must have also been able to utilize methylglyoxal. The possibility of observing pyruvate formation from methylglyoxal in this filter was limited because both compounds were essentially completely removed at the same filter depth.

By day 75 good removals had been well established in all four filters. Figures 6.8 to 6.11 show the BOM concentration profiles for these filters, along with regressions of equation 6.10. The calculated zero-order kinetic parameters are listed in Table 6.14. The kinetic parameter calculated for the methylglyoxal data was greater than that calculated in the previous filter experiment (Figures 6.2 and 6.3). The 95% confidence intervals of this value overlaps with both the values given in Figures 6.2 and 6.3, and therefore the apparent difference is not significant. The value calculated for methylglyoxal in Filter #3 was more typical of the values calculated in the first filter experiment. The calculated values for pyruvate in Filters #2 and #3 were found to differ significantly, at the 5% level. This is likely due to the formation of pyruvate from the methylglyoxal which was also fed to Filter #3.

Table 6.14: Steady-Sate Zero-Order Kinetic Parameters

			95% Confidence Interval	
Filter #	Added BOM	k_0[a]	lower	upper
1	methylglyoxal	0.283	0.160	0.407
2	pyruvate	0.393	0.226	0.560
3	methylglyoxal	0.0741	0.0595	0.0887
	and pyruvate	0.154	0.139	0.168
4	formaldehyde	0.290	0.221	0.359

[a] The units used are the same as given in Table 6.5.

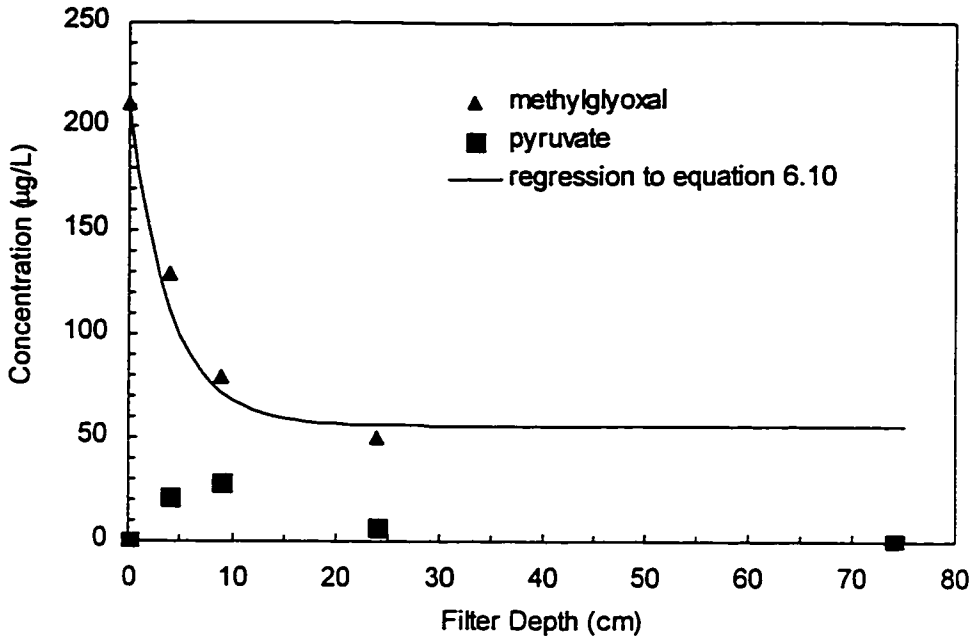

Figure 6.8: Methylglyoxal and pyruvate concentration profiles in Filter #1 on day 75 (38 days after quenching began).

The kinetic parameters for methylglyoxal and formaldehyde were very close to those observed in filter experiments #1 and #3, discussed below, respectively. The value calculated for formaldehyde was greater than those calculated for methylglyoxal in experiment #1, but not significantly different from that calculated for methylglyoxal in this experiment. Pyruvate appeared to be the most readily biodegradable component, while formaldehyde and methylglyoxal were comparable.

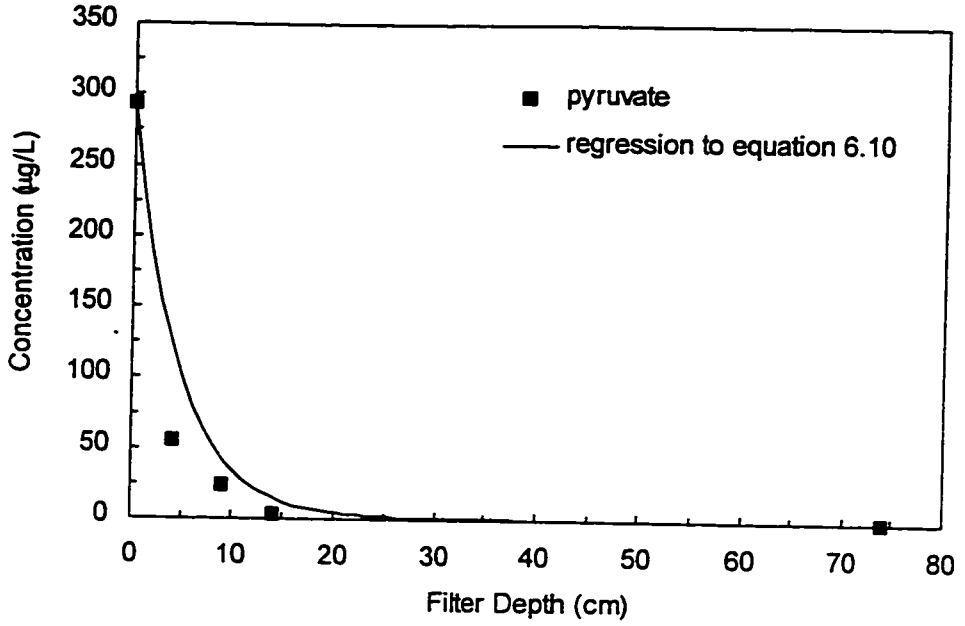

Figure 6.9: Pyruvate concentration profile in Filter #2 on day 75 (38 days after quenching began).

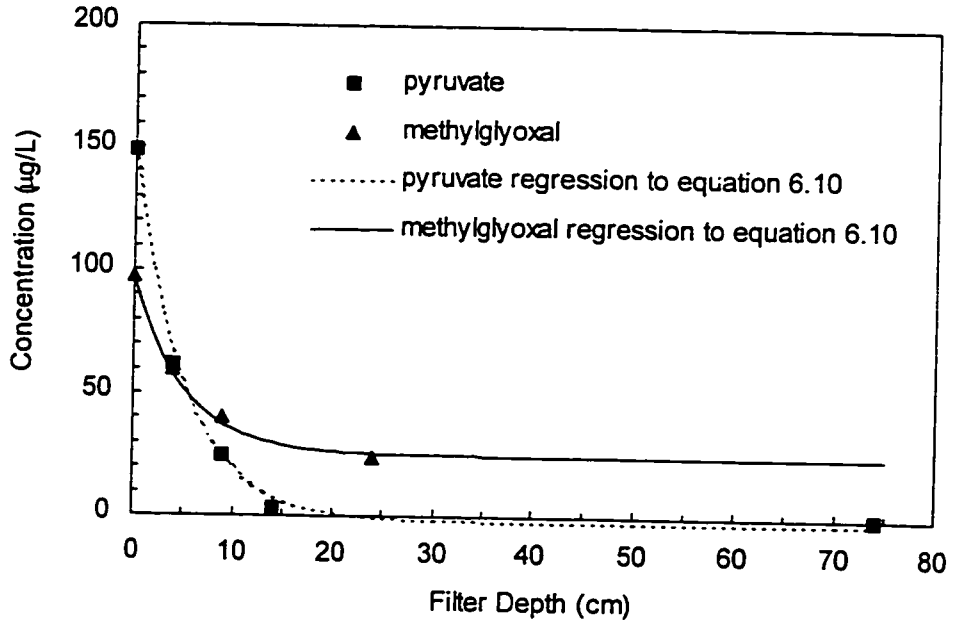

Figure 6.10: Methylglyoxal and pyruvate concentration profiles in Filter #3 on day 75 (38 days after quenching began).

Some of the regression curves asymptotically approach a minimum concentration which is well above the lowest concentration actually achieved (*e.g.* methylglyoxal regressions in Figures 6.8 and 6.10, and the formaldehyde regression in Figure 6.11). This is most apparent by comparing the measured effluent concentration to that predicted by the modeled curve. This is due to the exponential decay model used to regress the biomass data. These regression curves often approached a value near zero at a depth of about 30 cm in the filter. The modeling equation given in equation 6.10 predicts that once the biomass has been reduced to zero, no further removal of BOM is possible. This is reasonable except that biomass and BOM should diminish to zero simultaneously. A possible explanation is that the small amount of biomass in the lower portions of the filters was sufficient to remove some BOM. Alternatively, the phospholipid method, used for measuring biomass, as described in Chapter 3, was not sufficiently sensitive to detect the small amounts which had accumulated deeper in the filter. This is an indication that this biomass measurement method detects biomass which is not actively involved in the utilization of the measured BOM components. The phospholipid method is further discussed in the "Correlation of Biomass with Dissolved Oxygen" section at the end of this chapter.

It was expected that pyruvate would be very readily biodegradable, as demonstrated for it and other carboxylic acids at a full-scale installation (Gagnon *et al.*, 1997). The lack of a difference between formaldehyde and methylglyoxal removal rates was consistent throughout the present study. It was shown that both compounds were biodegradable in batch bioreactors in Chapter 5. Other researchers have observed that formaldehyde tends to be more easily removed than methylglyoxal (*e.g.* Niquette *et al.*, 1998; Weinberg *et al.*, 1993; Krasner *et al.*, 1993). Although, in those studies the methylglyoxal resulted from ozonation, while in the present study it was added from a feed solution. This may account for some of the difference, however, Wang *et al.* (1995) reported removals similar to those reported here, for methylglyoxal in a pilot-scale study. This suggests that it is possible to obtain

good removals of methylglyoxal, and that further study is required to determine why this has not been consistently observed by other researchers.

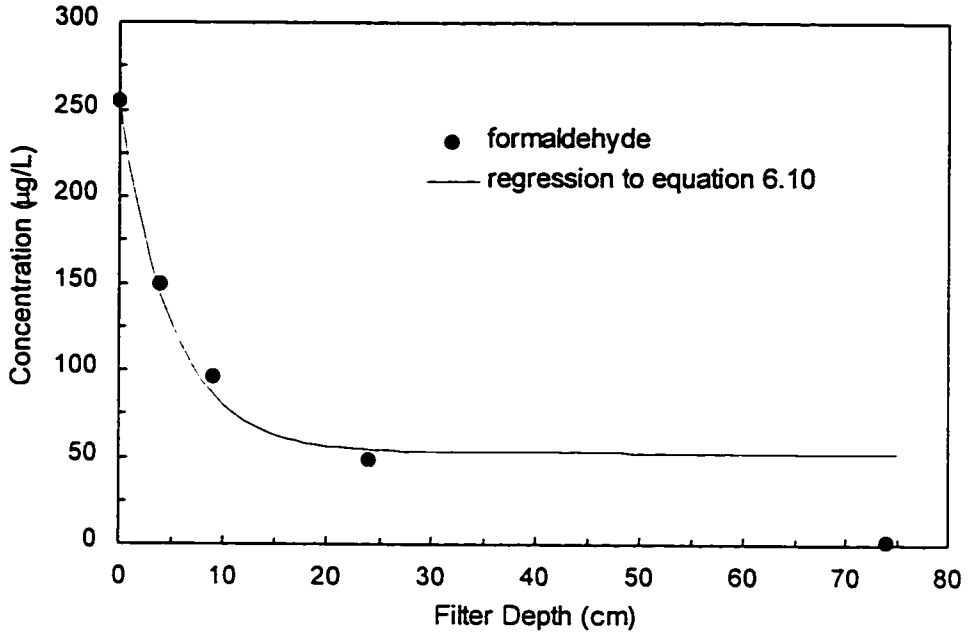

Figure 6.11: Formaldehyde concentration profile in Filter #4 on day 75 (38 days after quenching began).

Summary

A relatively small monochloramine residual in the filter influents impaired the biological removal of methylglyoxal, pyruvate, and formaldehyde, for the first 30 days of this experiment. This emphasizes the importance of eliminating oxidant residuals in the influent of biological filters, especially during the start-up phase where a negligible initial biomass is attached to the media.

The presence of methylglyoxal significantly reduced the apparent removal rate of pyruvate during biological filtration. This was caused by the additional pyruvate which was formed from methylglyoxal, as observed in this and the previous experiment.

The removal rates of formaldehyde and methylglyoxal were found to be comparable, when each was the sole BOM component in the filter influent.

Pyruvate appeared to be more readily biodegradable than either formaldehyde or methylglyoxal.

FILTER EXPERIMENT #3

Purpose and Experimental Design

The purpose of this experiment was to make a preliminary investigation into the effect of temperature and amino acids on formaldehyde removals. A 2^2 factorial experiment with temperature and amino acid concentration as the two factors, was designed for this purpose. The experimental and operational details are given in Table 6.15. In this experiment Filters #2 and #4 received amino acids, and Filters #1 and #2 were operated at an elevated water temperature. The theoretical oxygen demand of the organics fed to Filters #2 and #4 was double that fed to Filters #1 and #3. The variation of temperature throughout the experiment is shown in Figure 6.12.

Table 6.15: Experimental Conditions for Filter Experiment #3

	Filter #1	Filter #2	Filter #3	Filter #4
formaldehyde (μg/L)	250	250	250	250
amino acids:				
serine (μg/L)	0	175	0	175
glycine (μg/L)	0	200	0	200
temperature (°C)[a]	24.6	24.6	13.6	13.6
theoretical oxygen demand (mg O_2/L)	0.267	0.528	0.267	0.528
HLR (m/h)	7.5	7.5	7.5	7.5
bed depth (mm):				
anthracite	500	500	500	500
sand	250	250	250	250
EBCT (min)	6	6	6	6
D.O. (mg/L)[b]:				
influent	5.80	5.78	5.94	5.90
effluent	5.35	5.08	5.44	5.14

[a] The average of the influent and effluent temperatures is given. The water temperature decreased by about 0.3 °C through filters 1 and 2, and increased by about 1 °C through filters 3 and 4.

[b] The given D.O. measurements refer to steady-state conditions.

The amino acids serine and glycine were investigated because they are involved in formaldehyde metabolism in the serine pathway (Figure 4.3). The serine pathway is one of two common metabolic pathways by which microbes

can utilize single carbon compounds, as discussed in Chapter 4. The amino acid concentrations used in this research are likely greater than found in actual drinking water treatment plants (Berne, 1994). However, if these amino acids are "rate-limiting" components in the metabolism of formaldehyde, their presence at elevated concentrations may increase the rate of formaldehyde utilization. This assumes that uptake of these amino acids would occur by methylotrophic microorganisms.

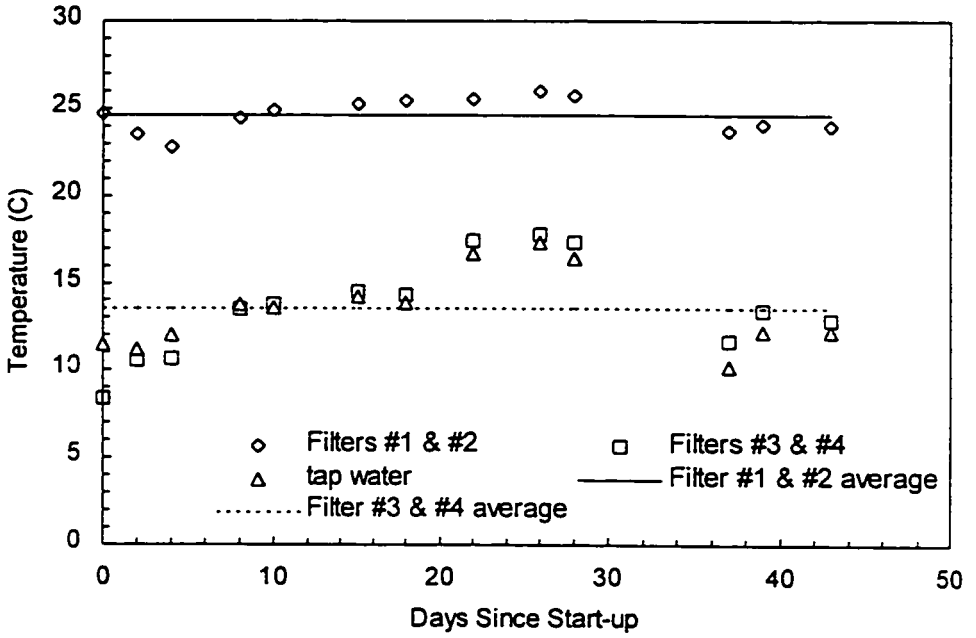

Figure 6.12: Water temperatures for duration of filter experiment #3.

Serine can be oxidized to form pyruvate (Brock and Madigan, 1997), as mentioned in Chapter 4. While the accumulation of pyruvate in the bulk water by this process is unlikely, samples for organic acid analysis were taken at all sampling times and locations in the event that measurable quantities could be detected.

Impact of Amino Acids on Formaldehyde Removal

Figure 6.13 shows the percent removal of formaldehyde versus days since start-up. Analyses indicated that no organic acids were detected as metabolic by-products of the biodegradation of formaldehyde or the added

amino acids. This was expected for the filters where formaldehyde was the sole carbon source because no transformation products were observed in the batch experiments, discussed in Chapter 5.

It is evident from Figure 6.13 that the presence of amino acids had no significant effect on the overall removal of formaldehyde, since the removals were the same for Filters #1 and #2, and for Filters #3 and #4. This was confirmed in an ANOVA at the 1% level, and was true throughout the experiment.

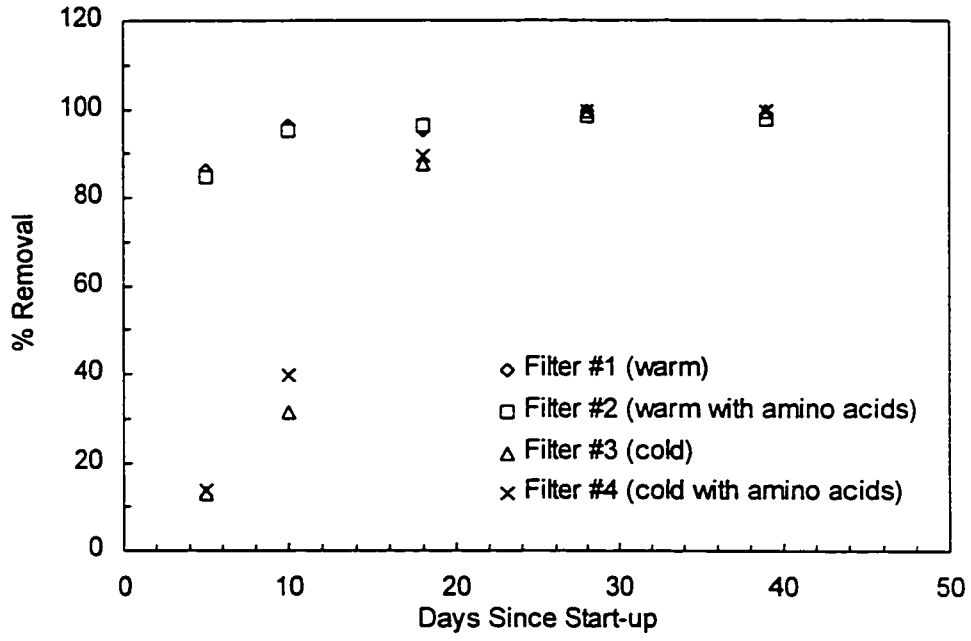

Figure 6.13: Overall percent removal of formaldehyde over the duration of experiment #3.

Impact of Temperature on Formaldehyde Removal

Initially, on days 5 and 10, there was a large difference in the removal of formaldehyde, as a function of temperature, that was found to be highly statistically significant. Almost immediately, very good formaldehyde removals were observed in the warmer filters. Coffey *et al.* (1995) also found that warmer temperatures shortened the time necessary to achieve steady-state removals of aldehydes, especially for anthracite/sand filters.

After the filters had been running for about twenty days, there was no significant difference in the formaldehyde removals in any of the four filters, and this trend continued throughout the remainder of the study. This was mainly due to the fact that all filters exhibited complete removal of formaldehyde.

Figure 6.14 shows the removal of formaldehyde in the filters at one minute of EBCT, which represented a depth of about 12 cm in these filters. This figure was obtained by performing non-linear regressions on the concentration versus EBCT plots for each of the filters. A first order model was found to provide a good fit to the data in all cases. These regressions were used to calculate the formaldehyde concentration at 1 minute of EBCT, from which, the percentage removal was a straightforward calculation. Surprisingly, the removals in the colder filters were slightly better than the warmer filters, on the last two sampling days. These differences were found to be significant at the 5% level. This may have been due to the fact that the cold temperature was essentially the same as the tap water temperature, and hence closer to the native temperature to which the microbial population was acclimated. The influent water for the warm filters was passed through a heater, as explained in Chapter 3, to raise its temperature, and thus was different from the native temperature.

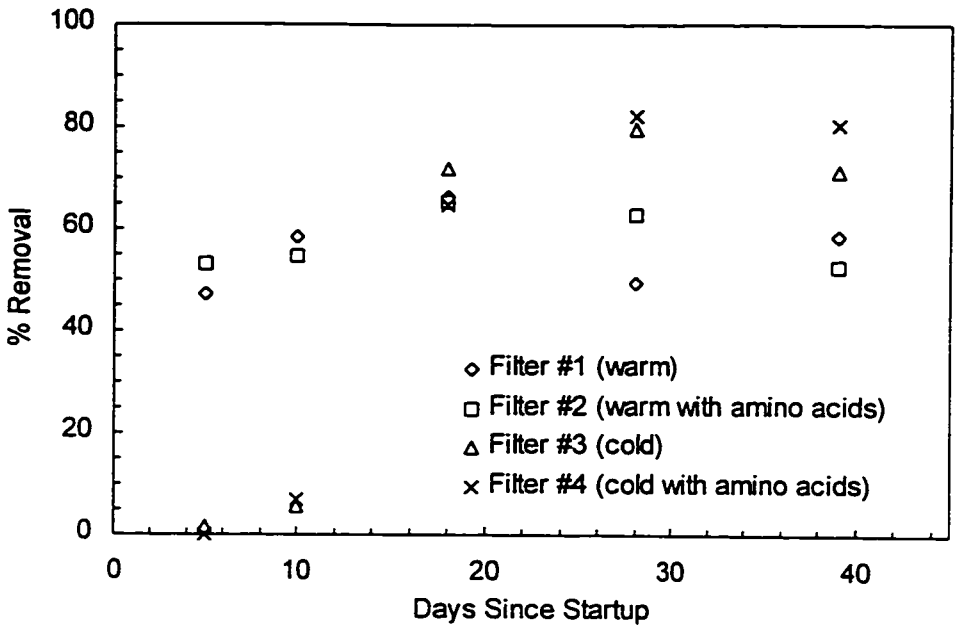

Figure 6.14: Percent removal of formaldehyde at an EBCT of 1 minute, over the duration of experiment #3.

Higher temperatures were expected to increase the rate of BOM utilization, and hence biofilm development, thus increasing the rate at which a steady-state was achieved. At steady-state the growth of cells is balanced by losses, mainly biofilm detachment. Detachment models have been proposed which argue that the detachment rate is a function of the rate of BOM utilization (*e.g.* Peyton and Characklis, 1993), while others argue that it is more strongly dependent on shear stress (*e.g.* Rittmann, 1982). Both of these approaches also show that the detachment rate is dependent on biofilm thickness. If biofilm detachment is not a strong function of temperature (*i.e.* mainly due to shear stress) then a higher BOM removal rate would be expected at higher temperatures, because of the higher growth rate of the biomass. Alternatively, if detachment is temperature dependent (*i.e.* growth related) then the higher rates of growth and detachment would be offsetting. The present research supports the latter hypothesis, because the overall removal of formaldehyde was not temperature dependent at steady-state. Steady-state may be achieved more quickly at higher temperatures, however,

because detachment may be relatively slow during the initial formation of a biomass, when biofilm thicknesses are small.

An alternative explanation of the higher removal rates at the lower temperature is that the endogenous decay rate may have been higher at the warmer temperature. This would have resulted in a lower biomass concentration in the warmer filters. Indeed the biomass concentration was found to be lower in the warmer filters, as discussed below.

The finding that formaldehyde removal rates were not strongly impacted by temperature in this experiment may be due to the relatively narrow range of temperatures tested. Formaldehyde removals may have been slower at lower temperatures than those employed in this research.

Impact of Amino Acids and Temperature on Biomass

Biomass sampling was conducted on days 7, 15, and 42 (Figure 6.15). On days 7 and 15, it was found that the biomass levels, at the top of the filters, were significantly (5% level) and positively impacted by both amino acids and temperature.

By day 42, amino acids positively impacted the amount of biomass at the top of the Filters #2 and #4. This was expected because these filters received about twice as much BOM, on a theoretical oxygen demand basis. However, temperature had the opposite effect, whereby colder temperatures produced significantly more biomass, at the 5% level. This can be seen by comparing the biomass values, given in Figure 6.15, between Filters #1 and #3, and between Filters #2 and #4. The observed higher biomass at colder temperatures corroborates the higher formaldehyde removals in Filters #3 and #4 compared to Filters #1 and #2 at an EBCT of 1 minute, reported above. This may have been due to the fact that the cold temperature was essentially the same as the tap water temperature, and hence closer to the native temperature to which the microbial population was acclimated.

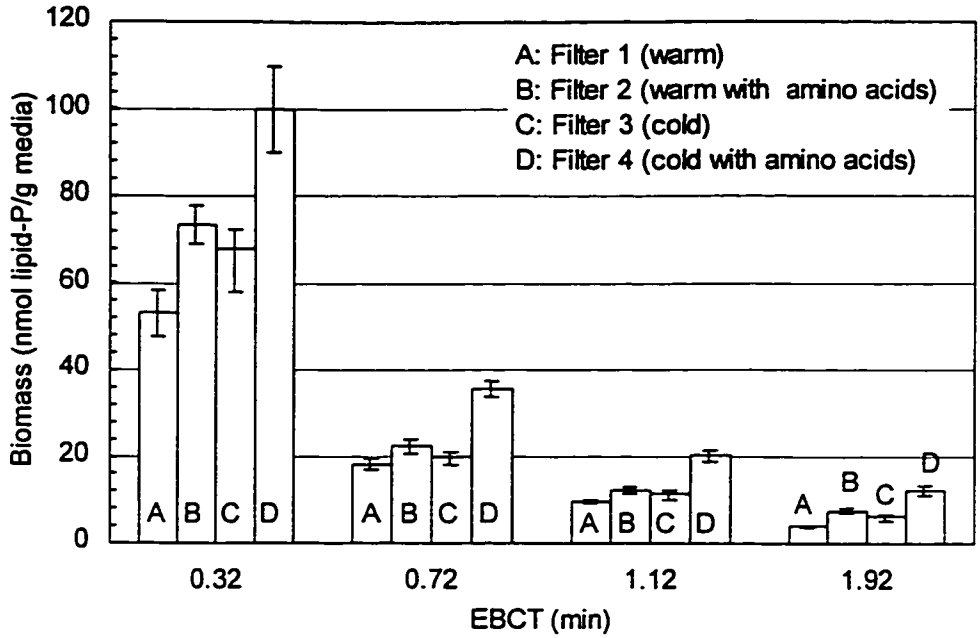

Figure 6.15: Comparison of biomass values at various EBCTs on day 42 (error bars represent ± 1 standard deviation).

Removal of Amino Acids

The overall removal of serine and glycine followed a similar trend as for formaldehyde. It was evident that the warmer filters achieved a steady-state more quickly than the cold filters, as for formaldehyde. After about twenty days all filters exhibited near complete removals. These amino acids appeared to be highly biodegradable, as expected. Gagnon (1997) found that the amino acids aspartate, glutamate, and serine were readily utilized in a model distribution system. That study also found that amino acids increased biofilm development.

Figure 6.16 shows concentration profiles for serine in Filters #2 and #4, on day 39. About 90% removal of serine was observed in less than one minute of EBCT. The removals can be seen to be somewhat faster at the lower temperature, especially by comparing the data points at an EBCT of 0.3 minutes. Similar results were obtained for glycine. These data provide further evidence that more efficient removals were observed at the native water

temperature. This trend was true of formaldehyde, both amino acids, and for the amount of attached biomass on the filter media, in this experiment.

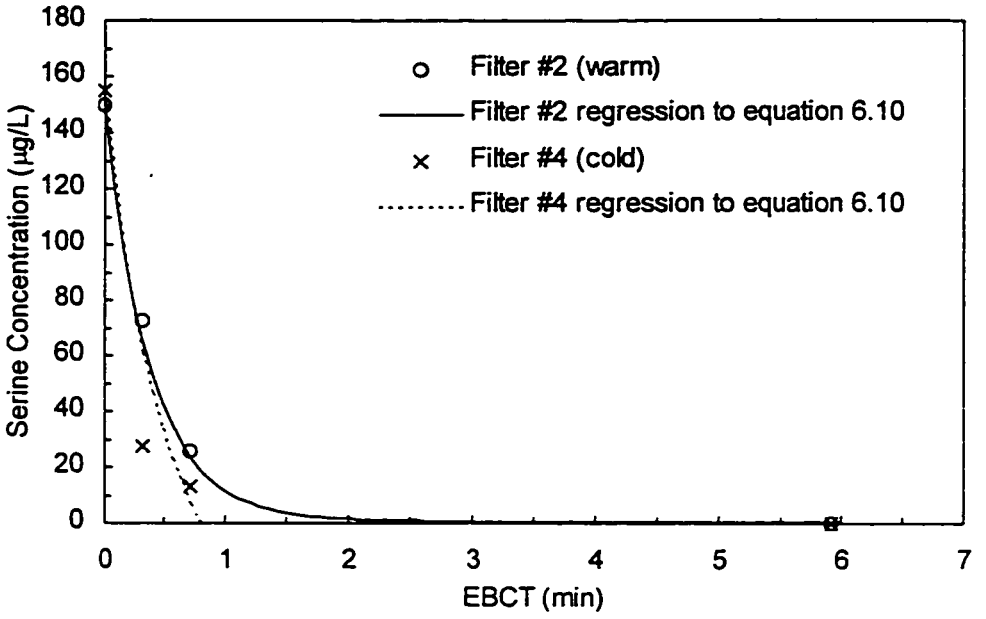

Figure 6.16: Serine concentration profiles on day 39.

Summary

In this experiment neither temperature nor the presence of amino acids had a significant effect on overall formaldehyde removals, at steady-state. However, steady-state was achieved more quickly in the warmer filters. Surprisingly, the colder filters exhibited higher amounts of biomass, and better removals of formaldehyde and amino acids, at very short contact times. This was postulated to have been due to the fact that the colder temperature was essentially the same as the tap water temperature, and hence closer to the native temperature to which the microbial population was acclimated.

CORRELATION OF BIOMASS WITH DISSOLVED OXYGEN

It is expected that an influent water with a higher theoretical oxygen demand (*i.e.* more organics) would result in a higher amount of attached biomass. Theoretical oxygen demand is closely related to the amount of energy which can be obtained from oxidizing a given compound, and hence

the amount of biomass that can be formed from it. However, it has been shown that when biomass is measured by the phospholipid method, it did not strongly correlate with BOM removals (Wang *et al.*, 1995).

Figure 6.17 shows the measured drop in dissolved oxygen across the ten filters for which BOM was fed, in the three filter experiments. In a regression analysis the abscissa values are assumed to contain no error (*i.e.* are perfectly known). In most practical cases the variable with the least error is usually selected for the abscissa. The theoretical oxygen demand was chosen, because it was calculated from the measured BOM component concentrations. It likely contains much less error than the dissolved oxygen drop measurements, which were relatively small in most cases. A strong correlation was observed, indicating that the drop in oxygen was due to the oxidation of the BOM. The oxygen demand exerted by the thiosulphate was also included in these calculations.

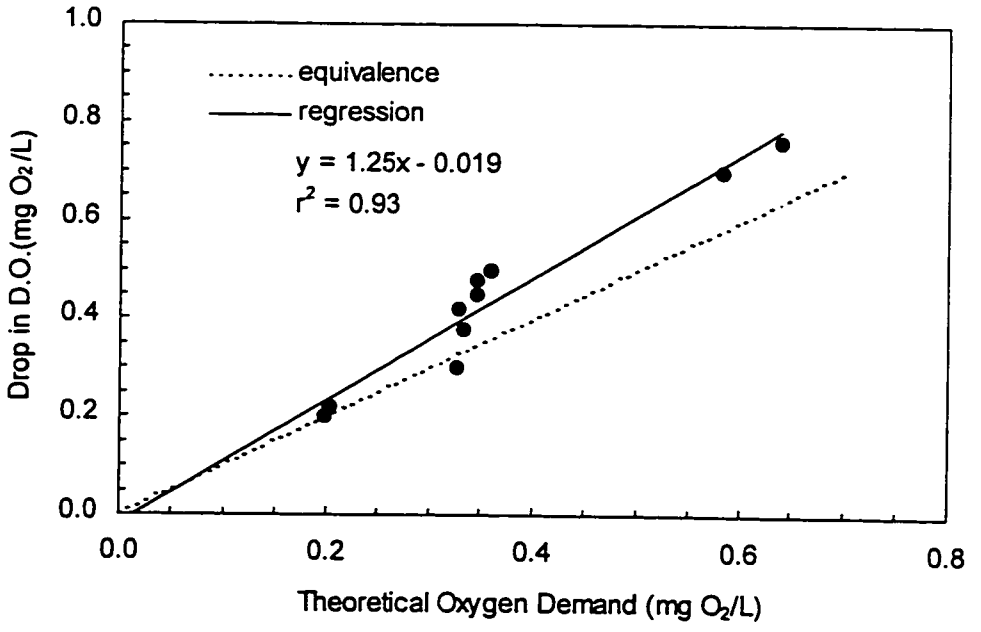

Figure 6.17: Correlation between drop in dissolved oxygen in biofilters and theoretical oxygen demand in the influents.

Figure 6.18 shows the correlation between the biomass measured at the top of each filter, at steady-state, versus the theoretical oxygen demand. The biomass measurement from the top of the filter, usually at a depth of 5 cm, was used because most of the removals took place at the top of the filters, and hence the biomass was greatest there. The regression line was significant at the 5% level (p-value = 0.018), although it is clear that there is scatter in the data. Also, the intercept of the regression line was well above zero, which would not be expected. This figure confirms that although a significant correlation between phospholipid-content and oxygen demand existed, the actual relationship is likely more complex than a simple linear relationship. One possible explanation is that some of the biomass, which is not active with respect to the removal of the measured BOM components, may indeed be living and therefore detected by the phospholipid method. These cells may be respiring endogenously, or may be using soluble microbial products as a source of carbon and energy.

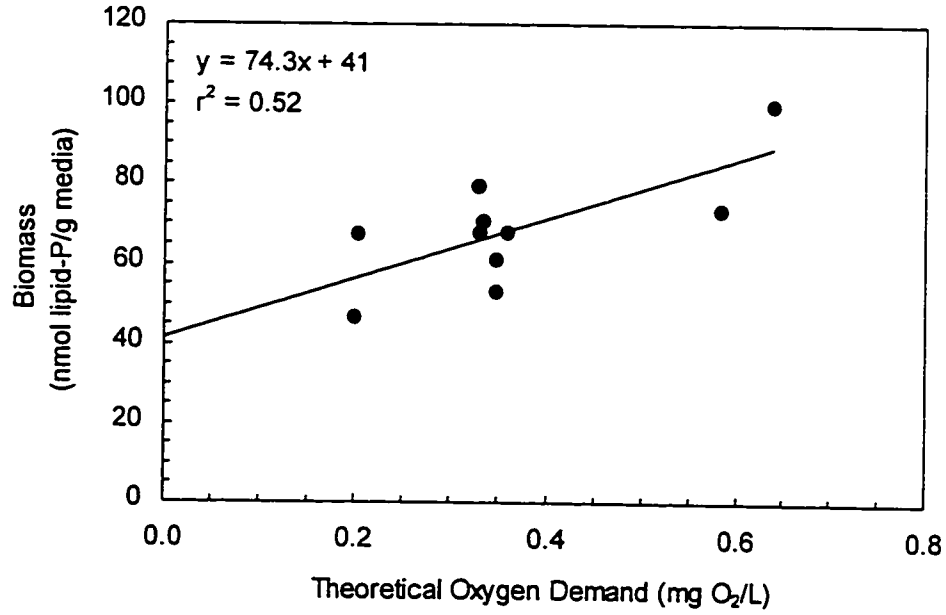

Figure 6.18: Relationship between biomass measured at the top of biofilters to theoretical oxygen demand in the influents.

COMPARISON OF KINETIC PARAMETERS TO BATCH RESULTS

In order to compare the zero-order kinetic parameters calculated in the batch and filter experiments, several assumptions were necessary because of the different methods by which biomass was estimated in the two systems. In the batch experiments HPCs were measured, while in the filter experiments biomass was estimated by the phospholipid method. The mass of cells was estimated from the HPC data by assuming that all cells were culturable on R2A agar, each CFU developed from a single cell, and the cell mass was 10^{-6} μg. Biomass could be calculated from the phospholipid data by assuming a factor of 0.209 mmol lipid-P/g cells, as calculated by Findlay *et al.* (1989), and expressing the mass of dry media on a volume basis by assuming a bed density of 800 g/L. The calculated values appear in Table 6.16. Example calculations of these kinetic parameters for pyruvate follow:

kinetic parameter calculated from pyruvate batch data:

$$\frac{2.29 \times 10^{-8}\ \mu g\ \text{pyruvate}}{\text{CFU hr}} \times \frac{1\ \text{CFU}}{1\ \text{cell}} \times \frac{\text{cell}}{10^{-6}\ \mu g} = 2.29 \times 10^{-2}\ \frac{\mu g\ \text{pyruvate}}{\text{hr}\ \mu g\ \text{cells}} \qquad (6.11)$$

kinetic parameter calculated from pyruvate filter data:

$$\frac{0.393\ \mu g\ \text{pyruvate g dry media}}{\text{L hr nmol lipid - P}} \times \frac{\text{L}}{800\ \text{g dry media}} \times \frac{0.209\ \text{nmol lipid - P}}{\mu g\ \text{cells}} = 1.03 \times 10^{-4}\ \frac{\mu g\ \text{pyruvate}}{\text{hr}\ \mu g\ \text{cells}} \qquad (6.12)$$

Table 6.16: Comparison of Zero-Order Kinetic Parameters

	$k_0 \left(\frac{\mu g \text{ BOM}}{\text{hr } \mu g \text{ cells}} \right)$	
	batch[a]	filters[b]
pyruvate	2.29×10^{-2}	1.03×10^{-4}
methylglyoxal	4.77×10^{-3}	4.39×10^{-5}
formaldehyde	3.68×10^{-3}	7.81×10^{-5}
serine	-	2.86×10^{-5}
glycine	-	3.55×10^{-5}

[a] Calculation of biomass based on HPC data.
[b] Calculation of biomass based on phospholipid data.

In general the batch results were two orders of magnitude greater than those calculated for the filters. This suggests the unexpected finding that biofilms have a lower substrate-degrading capability compared to suspended cells. A portion of the large difference in the values calculated between these two systems may also be due to the assumed conversion factors. For example, the assumed cell mass value may be in error, although a justification for selecting a different value is complicated. A larger cell mass value would have made the batch values closer to the filter values. However, a smaller cell mass value would be required to improve the yield values (*i.e.* reduce some of them below unity), as discussed in Chapter 5. For the sake of consistency the same cell mass value was used in both calculations.

An alternative explanation for the poor agreement between the two systems is the value of the phospholipid lipid-content of the cells. The selected value may not be applicable for the biofilms studied in this research. If the molar phospholipid value of Findlay *et al.* (1989) were an underestimation of the actual phospholipid content of the biofilm cells of this study, the kinetic parameters calculated with the filter data would be underestimated.

Pyruvate appeared to be the most biodegradable compound in both systems. Relatively small differences exist in the zero-order kinetic parameters among the other compounds, within an experimental system.

CONCLUSIONS

The rate of mass transfer was not found to limit the removal rate of the BOM components studied in this chapter (*i.e.* methylglyoxal, formaldehyde, and pyruvate) in biologically active filters. This permitted the omission of mass transfer coefficients from the modeling equations. A zero-order kinetic model adequately described the concentration profiles of these components in biologically active filters. Although, the biomass concentration, measured by the phospholipid method, was found to decrease exponentially with filter depth. All of the components studied were found to be highly amenable to removal in biological filters.

The formation of pyruvate within biologically active filters was observed when methylglyoxal was the sole BOM component in the influent. At higher HLRs both methylglyoxal and pyruvate were measured at lower depths in the filter, as expected. At some higher HLR both methylglyoxal and pyruvate may have appeared in the filter effluent. Also, pyruvate removals were found to be significantly reduced when both methylglyoxal and pyruvate were present in the influent, compared to when pyruvate was the only component in the influent. It was hypothesized that this reduction was due to the formation of pyruvate by the methylglyoxal-using portion of the population.

The performance of the biologically active filters was found to be robust with respect to backwashing and a 48 hour period out of service. BOM removals in the subsequent filter runs were found to be essentially the same prior to, and immediately following these events. However, BOM removal performance was negatively affected by a sudden increase in the influent

methylglyoxal concentration. The filter operating at the higher HLR (10 m/h) had not recovered BOM control after three days at the higher concentration.

During the start-up of the biofilters a monochloramine residual of about 0.25 mg Cl_2/L, continuously present in the influents, severely impaired BOM removals.

Neither temperature nor the presence of amino acids had a significant effect on overall formaldehyde removals, at steady-state. However, steady-state was achieved more quickly in the warmer filters.

REFERENCES

Berne, F.D. (1994). Analyse des Acides Amines dans les Eaux. Developements et Applications: Incidence sur la Consommation en Chlore et la Teneur en Matiere Organique Biodegradable des Eaux Potables, Etude du Mechanisme D'Ozonation des Peptides. Ph.D. thesis, L'Universite de Poitiers, Poitiers, France.

Brock, T.D. and M.T. Madigan (1997). Biology of Microorgansims, 8th Edition. Prentice Hall, Upper Saddle River, New Jersey, USA.

Coffey, B.M., S.W. Krasner, M.J. Sclimenti, P.A. Hacker, and J.T. Gramith (1995). A comparison of biologically active filters for the removal of ozone by-products, turbidity and particles. Proc. AWWA WQTC, New Orleans, Louisiana, USA.

Costerton, J.W., Z. Lewandoski, D. de Beer, D. Caldwell, D. Korber, and G. James (1994). Biofilms, the customized microniche. *J. Bacteriol.*, Vol. 176, pp. 2137-2142.

Findlay, R.H., G.M. King, and L. Watling (1989). Efficacy of phospholipid analysis in determining microbial biomass in sediments. *Appl. Environ. Microbiol.*, Vol. 55, pp. 2888-2893.

Fogler, H.S (1992). Elements of Chemical Reaction Engineering, 2nd Edition. Prentice Hall, Englewood Cliffs, New Jersey, USA.

Gagnon, G.A. (1997). Utilization of Biodegradable Organic Matter by Biofilms in Drinking Water Distribution Systems. Ph.D. thesis, Department of Civil Engineering, University of Waterloo, Waterloo, Ontario, Canada.

Gagnon, G.A., S.D.J. Booth, S. Peldszus, D. Mutti, F. Smith, and P.M. Huck (1997). Formation and removal of carboxylic acids in a full-scale treatment plant. *JOUR. AWWA*, Vol. 89 (8), pp. 88-97.

Jennings, P.A. (1975). A mathematical model for biological activity in expanded bed adsorption columns. Ph.D. thesis, Department of Civil Engineering, University of Illinois, Urbana, Illinois, USA.

Karel, S.F., S.B. Libicki, and C.R. Robertson (1985). The immobilization of whole cells: engineering principles. *Chem. Eng. Sci.*, Vol. 40, pp. 1321-1354.

Krasner, S.W., M.J. Sclimenti, and B.M. Coffey (1993). Testing biologically active filters for removing aldehydes formed during ozonation. *Jour. AWWA*, Vol. 85 (5), pp. 62-71.

Miltner, R.J., R.S. Summers, and J.Z. Wang (1995). Biofiltration performance: part 2, effect of backwashing. *Jour. AWWA*, Vol. 87 (12), pp. 64-70.

Niquette, P., M. Prévost, R. G. Maclean, D. Thibault, J. Collier, R. Desjardins, and P. Lafrance (1998). Backwashing first-stage sand-BAC filters. *Jour. AWWA*, Vol. 90 (15), pp. 86-97.

Perry, R.H., D.W. Green, and J.O. Maloney (Eds.) (1984). Perry's Chemical Engineers' Handbook, 6th Edition. McGraw-Hill, New York, New York, USA.

Peyton, B.M. and W.G. Characklis (1993). A statistical analysis of the effect of substrate utilization and shear stress on the kinetics of biofilm detachment. *Biotechnol. Bioengr.*, Vol. 41, pp. 728-735.

Prévost, M., P. Niquette, R.G. Maclean, D. Thibault, P. Lafrance, R. Desjardins (1995). Removal of various biodegradable organic compounds by first and second stage filtration. Proc. 12th Ozone World Congress, Lille, France, pp. 531-545.

Rittmann, B.E. (1982). The effect of shear stress on biofilm loss rate. *Biotechnol. Bioengr.*, Vol. 24, pp. 501-506.

Rittmann, B.E. and P.L. McCarty (1980a). Evaluation of steady-state-biofilm kinetics. *Biotechnol. Bioengr.*, Vol. 22, pp. 2359-2373.

Rittmann, B.E. and P.L. McCarty (1980b). Model of steady-state-biofilm kinetics. *Biotechnol. Bioengr.*, Vol. 22, pp. 2343-2357.

Servais, P., P. Laurent, G. Billen, and D. Gatel (1992). Studies of BDOC and bacterial dynamics in the drinking water distribution system of the northern Parisian suburbs. *Revue Sci. l'Eau*, Vol. 8, pp. 427-462.

Urfer-Frund, D. (1998). Effects of Oxidants on Drinking Water Biofilters. Ph.D. thesis, Department of Civil Engineering, University of Waterloo, Waterloo, Ontario, Canada.

Wang, J.Z. (1995). Assessment of Biodegradation and Biodegradation Kinetics of Natural Organic Matter in Drinking Water Biofilters. Ph.D. thesis, Department of Civil and Environmental Engineering, University of Cincinnati, Cincinnati, Ohio, USA.

Wang, J.Z., R.S. Summers, R.J. Miltner (1995). Biofiltration performance: part 1, relationship to biomass. *Jour. AWWA*, Vol. 87 (12), pp. 55-63.

Weinberg, H.S., W.H. Glaze, S.W. Krasner, and M.J. Sclimenti (1993). Formation and removal of aldehydes in plants that use ozonation. *Jour. AWWA*, Vol. 85 (5), pp. 72-85.

Weisz, P.B. (1973). Diffusion and chemical transformation. *Science*, Vol. 179, pp. 433-440.

Young, L.C. and B.A. Finlayson (1973). Axial dispersion in non-isothermal packed bed reactors. *Ind. Eng. Chem. Fund.*, Vol. 12 (4), pp. 412-422.

Zhang, S. and P.M. Huck (1996). Removal of AOC in biological water treatment processes: a kinetic modeling approach. *Wat. Res.*, Vol. 30 (5), pp.1195-1207.

CHAPTER 7: CONCLUSIONS AND RECOMMENDATIONS

CONCLUSIONS

1. The conceptual metabolic model, developed in this research, assembled and simplified a number of major metabolic pathways. These metabolic cycles and pathways were expected to be of relevance to the metabolism of the ozonation by-products acetate, formate, pyruvate, oxalate, formaldehyde, and methylglyoxal. This conceptual model was used to demonstrate that the metabolism of acetate, pyruvate, and methylglyoxal were closely linked, and that the metabolism of formate, formaldehyde, and oxalate were similarly linked. Subsequent batch experiments were divided into investigations of these two groups of compounds.

2. A highly statistically significant correlation was determined between the increase in HPC numbers during batch biodegradation and the theoretical oxygen demand initially present in the bioreactors. It was therefore concluded that the HPC measurement was a reasonable surrogate for biomass.

3. In the batch experiments it was also found that the ozonation by-products investigated were readily removed, and in most instances

biodegradation rates were independent of the other organic components present. Also, in most instances transformation products, formed during the biodegradation of these compounds, were not detected. An exception was the transient accumulation of pyruvate during methylglyoxal utilization.

4. Based on calculations using dimensionless moduli neither internal nor external mass transfer rates were found to limit the removal of the ozonation by-products studied in bench-scale biofilters .

5. A zero-order kinetic model appeared to adequately describe the concentration profiles of these ozonation by-products in biofilters. Although the biomass concentration, measured by the phospholipid method, was found to decrease exponentially with filter depth.

6. The biologically mediated formation of pyruvate from methylglyoxal, reported in the batch experiments, was also observed in bench-scale filters. At steady-state the formed pyruvate was observed at intermediate sample ports but not in the effluent of filters operated at 5, 8, and 10 m/h.

7. In filters which had only methylglyoxal in their influents, pyruvate was observed in the effluent, following an increase in the influent methylglyoxal concentration by a factor of four. It was found that the filter operated at the lower HLR (5 m/h) was able to achieve complete pyruvate removal after about 24 hours of operation. The filter operated at the higher HLR (10 m/h) had not achieved complete pyruvate removal after three days of operation at the higher concentration.

8. When pyruvate and methylglyoxal were both present in the influent, the removal rate of pyruvate was significantly reduced, compared to when it was the sole carbon source fed to a biofilter. It was postulated

that the observed reduction in removal rate was due to the formation of pyruvate during methylglyoxal biodegradation.

9. Methylglyoxal and formaldehyde were shown to have similar utilization rates when each was fed as the sole BOM component to biologically active filters. This finding was contrary to much of the literature, which had characterized methylglyoxal as less readily biodegradable than formaldehyde.

10. The removal of methylglyoxal was not found to be impaired by backwashing, nor by a 48 hour filter shut-down. The activity of the existing biomass on the filter media was resilient to these disturbances, and methylglyoxal removal performance was very rapidly re-established.

11. In a factorial experiment it was found that neither the presence of two amino acids (serine and glycine) nor temperature (14 and 25 °C) effected formaldehyde utilization rates. Serine and glycine were shown to be readily biodegradable in biofilters in this experiment, as expected.

12. During the start-up of biofilters a monochloramine residual of about 0.25 mg Cl_2/L, continuously present in the influents, severely impaired BOM removals.

13. Kinetic parameters calculated from the batch data were about two orders of magnitude higher than those calculated from the biofilter data. This was not expected because the BOM degrading ability of the biofilter biomass was not expected to be less than that of the batch system. A number of assumptions were required to convert the HPC and phospholipid results to common biomass units. If the value of 0.209 mmol lipid-P/g cells underestimated the true value for the

biofilm cells under the conditions investigated, than the filter kinetic parameters would have been underestimated.

RECOMMENDATIONS

Recommendations for Design and Operation

1. In assessing the performance of drinking water biologically active filters, it is recommended to measure all BOM components for which methods are available in order to avoid missing transformation products.

2. Spikes in the influent concentration of BOM should be avoided in order to prevent the break-through of BOM in filter effluents. Admittedly, practical means of avoiding such spikes are difficult to provide.

3. The operation of filters at as low an HLR as possible is recommended. In this research a filter operated at 5 m/h was found to have a more robust BOM removal performance, than one operated at 10 m/h, with respect to spikes in the influent BOM concentration. Moreover, most of the BOM removal occurred in the top half of the in the 5 m/h filter, while a greater depth of the 10 m/h filter was required. This implied that the 5 m/h filter could better handle elevated influent BOM levels. A reduction in HLR may require the operation of a greater number of filters to meet the demand for water and therefore, this recommendation may not be practical for some utilities.

4. The presence of oxidants (*e.g.* free or combined chlorine, ozone) in the influents of biologically active filters should be avoided, especially during the start-up phase. A monochloramine residual was found to significantly impede BOM removals during the start-up phase of one of the experiments in this research.

Recommendations for Future Research

1. Other non-steady-state scenarios, involving biofilters with methylglyoxal as the primary organic in the influent could be investigated. For example, the removal of methylglyoxal, and microbially formed pyruvate, could be investigated upon a step increase in the HLR of the biofilters.

2. The potential for pyruvate formation from methylglyoxal should be investigated in biofilters treating ozonated waters. Such studies could determine the importance of the formed pyruvate to biofilter performance, in the presence of other ozonation by-products. Ozonation by-products are formed at different concentrations in different waters thus, a number of water types should be tested.

3. It is recommended that further biological filtration studies include the measurement of biomass profiles with depth. Data from such studies could be used to verify the importance of the biomass distribution in determining the apparent order of BOM utilization kinetics.

4. Additional biomass measurement methods, applicable to drinking water biofilters, should be investigated so that comparisons with the phospholipid method results are possible. A measurement which is more closely linked to BOM utilization would be preferred.

5. Where possible, researchers should avoid altering the temperature of waters from the native temperature in biological filtration studies. This may be of particular concern for groundwaters, which naturally exist within a relatively narrow temperature range. This is recommended because higher removal rates, at an EBCT of 1 minute, were observed at the lower temperature (14 °C) of a two level-factorial experiment, in which the higher temperature was 25 °C. The lower temperature was essentially the same as that of the groundwater-sourced tap water.

6. The factorial experiment in this research, for which temperature was a factor, could be repeated with a greater difference between the target temperatures. The range investigated in this research (14 to 25 °C) was too narrow to observe substantial differences in BOM removal rates, in the biofilters investigated. A low temperature of 5 °C or less is recommended.

7. Because the performance of the biofilters were generally robust with respect to the removal of the BOM components investigated in this research, other performance criteria (*e.g.* particle removal) may dictate optimum operating conditions. It is recommended to investigate biological filtration under conditions under which both BOM and particle removal could be studied.

APPENDIX A: DATA FROM BATCH EXPERIMENTS

APPENDIX A.1: ORGANIC CHEMICAL COMPONENT DATA

Appendix A.1: Organic Chemical Component Data for Acetate, Pyruvate, and Methylglyoxal Experiments

Added Components	Time (hours)	Concentration (µg/L)*		
		acetate	pyruvate	methylglyoxal
acetate	1.5	220.8		
(trial #1)	21.0	37.1		
	75.5	42.5		
	141.0	43.2		
acetate	0.3	216.6		
(trial #2)	6.3	173.7		
	12.3	69.6		
	25.0	24.0		
	76.3	23.9		
pyruvate	1.0		246.8	
(trial #1)	9.5		203.0	
	27.5		3.0	
	53.0		0.0	
	100.0		0.0	
pyruvate	0.3		397.6	
(trial #2)	6.3		301.3	
	12.3		236.9	
	25.0		3.0	
	76.3		0.0	
methylglyoxal	0.5		0.0	229.3
(trial #1)	6.0		0.0	226.2
	10.0		0.0	244.2
	25.5		0.0	251.8
	50.0		0.0	135.4
methylglyoxal	0.5		0.0	242.3
(trial #2)	35.3		35.2	214.1
	55.0		43.1	156.0
	72.0		33.7	111.2
	102.3		3.0	24.4
	132.8		0.0	2.5
acetate and	1.0	246.1	439.4	
pyruvate	9.5	109.9	195.9	
(trial #1)	27.5	5.0	3.0	
	53.0	5.0	0.0	
acetate and	0.3	172.7	389.7	
pyruvate	6.3	123.8	351.0	
(trial #2)	12.3	48.4	176.1	
	25.0	5.0	3.0	
	76.3	39.1	0.0	

* Average values from replicate shake flasks.

Appendix A.1: Organic Chemical Component Data for Acetate, Pyruvate, and Methylglyoxal Experiments (cont'd)

Added Components	Time (hours)	Concentration (µg/L)*		
		acetate	pyruvate	methylglyoxal
methylglyoxal and pyruvate	0.5		308.1	452.1
	6.0		312.9	488.6
	10.0		327.1	442.2
	25.5		82.9	397.7
	48.0		3.0	288.7
	72.0		3.0	261.2
methylglyoxal, pyruvate, and acetate	0.5	420.0	321.1	385.9
	6.0	351.5	331.5	446.1
	10.0	333.5	350.9	398.3
	25.5	**	228.2	398.7
	48.0	**	71.5	292.8
	72.0	**	9.3	202.5

* Average values from replicate shake flasks.

** An unidentified contaminant in the methylglyoxal was found to interfere with acetate quantification.

Appendix A.1: Organic Chemical Component Data for Formaldehyde, Formate, and Oxalate Experiments

Added Components	Time (hours)	Concentration (µg/L)*				
		formaldehyde	formate	oxalate	acetate	pyruvate
formaldehyde	0.5	82.6				
	12.0	76.6				
	20.0	80.0				
	30.0	59.3				
	40.0	58.1				
	55.0	35.2				
formate	1.5		497.2			
(trial #1)	21.0		334.0			
	75.5		2.0			
	141.0		14.7			
formate	0.5		176.9			
(trial #2)	4.8		174.4			
	8.0		162.0			
	12.8		149.3			
	16.5		129.4			
	55.8		2.0			
oxalate	0.5			374.4		
	4.8			338.5		
	8.0			323.5		
	12.8			290.1		
	16.5			276.5		
	55.8			9.0		
formaldehyde and	0.5	86.9	130.2			
formate	12.0	79.5	106.8			
	20.0	69.2	16.8			
	30.0	46.2	3.8			
	40.0	39.5	1.0			
	55.0	14.1	0.0			
formate and	0.5		178.8	344.4		
oxalate	4.8		174.6	327.4		
	8.0		163.5	318.4		
	12.8		140.1	264.2		
	16.5		110.9	248.5		
	55.8		0.0	9.0		

* Average values from replicate shake flasks.

Appendix A.1: Organic Chemical Component Data for Formaldehyde, Formate, and Oxalate Experiments (cont'd)

Added Components	Time (hours)	Concentration (µg/L)*				
		formaldehyde	formate	oxalate	acetate	pyruvate
formaldehyde, formate, and oxalate *(trial #1)*	0.5	86.6	146.6	332.5		
	12.0	83.8	53.1	274.9		
	20.0	70.1	2.3	9.0		
	30.0	49.6	2.0	0.0		
	40.0	36.0	2.0	0.0		
	55.0	14.8	0.0	0.0		
formaldehyde, formate, and oxalate *(trial #2)*	0.5	133.5	179.8	339.5		
	8.0	140.0	147.8	296.7		
	18.0	136.4	81.3	109.5		
	26.0	139.2	45.9	9.0		
	70.0	10.9	0.0	0.0		
formaldehyde, formate, oxalate, acetate, and pyruvate	0.5	136.3	184.2	327.6	222.2	275.0
	8.0	134.7	171.0	273.3	185.2	217.9
	18.0	133.5	51.5	179.2	36.5	146.6
	26.0	129.0	4.4	52.3	5.0	3.0
	70.0	3.7	0.0	0.0	14.9	0.0
	120.0	0.0	0.0	0.0	5.7	0.0

* Average values from replicate shake flasks.

Appendix A.1: Organic Component Data for Sequenced Batch Experiments

Added Components	Time (hours)	Concentration (µg/L)*		
		formaldehyde	methylglyoxal	pyruvate
formaldehyde *(trial #1)*	0.5	137.8		
	49.0	45.6		
	96.3	1.6		
	121.8	150.2		
	145.0	84.9		
	164.3	32.5		
	224.0	0.0		
formaldehyde *(trial #2)*	1.0	137.7		
	19.0	123.8		
	47.5	6.1		
	55.0	3.1		
	74.5	1.6		
	93.0	6.2		
	96.0	143.4		
	120.0	45.3		
	140.0	3.6		
	170.5	0.0		
methylglyoxal *(trial #1)*	0.5		270.0	5.9
	49.0		206.2	106.7
	96.3		2.5	0.0
	121.8		306.0	131.0
	145.0		153.0	136.0
	164.3		2.5	3.0
	224.0		0.0	0.0
methylglyoxal *(trial #2)*	1.0		199.4	**
	19.0		272.8	**
	47.5		83.3	**
	55.0		61.9	**
	74.5		12.5	**
	93.0		2.5	**
	96.0		262.0	**
	120.0		110.5	**
	140.0		2.5	**
	170.5		0.0	**
methylglyoxal in tap water	1.0		252.9	29.8
	20.0		319.6	260.6
	47.5		113.7	115.5
	74.5		3.4	0.0
	95.5		391.6	261.0
	140.0		2.5	92.2
	170.5		0.0	0.0

* Average values from replicate shake flasks.

** Pyruvate concentrations were not measured.

APPENDIX A.2: HPC DATA

Appendix A.2: HPC Data for Batch Experiments

Added Components	Time (hours)	HPCs* (CFU/mL)
acetate	1.5	2.8E+05
(trial #1)	21.0	4.7E+05
	75.5	4.1E+05
acetate	0.3	3.1E+05
(trial #2)	25.0	6.4E+05
	76.3	5.8E+05
pyruvate	1.0	3.3E+05
(trial #1)	27.5	7.9E+05
	53.0	7.5E+05
pyruvate	0.3	3.9E+05
(trial #2)	25.0	9.3E+05
	76.3	9.0E+05
methylglyoxal	0.5	3.2E+05
(trial #1)	25.5	3.3E+05
	72.0	7.7E+05
methylglyoxal	0.5	3.2E+05
(trial #2)	55.0	5.5E+05
	132.8	8.2E+05
acetate and pyruvate	1.0	2.1E+05
(trial #1)	27.5	1.0E+06
	53.0	8.9E+05
acetate and pyruvate	0.3	2.2E+05
(trial #2)	25.0	7.1E+05
	76.3	6.8E+05
methylglyoxal and pyruvate	0.5	1.2E+05
	25.5	6.7E+05
	72.0	1.2E+06
methylglyoxal, pyruvate,	0.5	2.3E+05
and acetate	25.5	6.1E+05
	72.0	1.5E+06

* Average values from replicate shake flasks.

Appendix A.2: HPC Data for Batch Experiments (cont'd)

Added Components	Time (hours)	HPCs* (CFU/mL)
formaldehyde	0.5	3.1E+05
	30.5	3.0E+05
	72.0	5.0E+05
formate *(trial #1)*	1.5	3.0E+05
	21.0	4.2E+05
	75.5	6.8E+05
formate *(trial #2)*	0.5	7.6E+04
	55.8	3.2E+05
oxalate	0.5	2.7E+05
	55.8	3.1E+05
formaldehyde and formate	0.5	2.0E+05
	30.5	3.9E+05
	72.0	5.2E+05
formate and oxalate	0.5	3.6E+05
	55.8	4.7E+05
formaldehyde, formate, and oxalate *(trial #1)*	0.5	2.4E+05
	30.5	4.5E+05
	72.0	5.9E+05
formaldehyde, formate, and oxalate *(trial #2)*	0.5	2.8E+05
	26.0	4.6E+05
	70.0	5.9E+05
formaldehyde, formate, oxalate, acetate, and pyruvate	0.5	2.6E+05
	26.0	9.4E+05
	70.0	1.4E+06
	120.0	1.2E+06

* Average values from replicate shake flasks.

Appendix A.2: HPC Data From Sequenced Batch Experiments

Added Components	Time (hours)	HPCs* (CFU/mL)
formaldehyde	7.5	2.60E+05
(replicate #1)	24.0	3.05E+05
	95.0	4.20E+05
	121.0	5.10E+05
	140.0	6.25E+05
	215.0	6.40E+05
formaldehyde	0.5	3.05E+05
(replicate #2)	24.5	3.50E+05
	74.5	5.30E+05
	96.0	5.35E+05
	141.5	7.00E+05
	170.5	5.50E+05
methylglyoxal	7.5	6.85E+05
(replicate #1)	24.0	7.85E+05
	95.0	1.17E+06
	121.0	1.35E+06
	140.0	1.90E+06
	215.0	1.19E+06
methylglyoxal	0.5	4.95E+05
(replicate #2)	24.5	7.25E+05
	74.5	1.05E+06
	96.0	1.20E+06
	141.5	1.95E+06
	170.5	1.75E+06
methylglyoxal in tap w	19.5	8.16E+05
	47.5	1.28E+06
	74.5	1.62E+06
	95.5	1.45E+06
	141.5	1.79E+06
	170.5	1.04E+06

* Average values from replicate shake flasks.

APPENDIX A.3: BIOLOG RESULTS

Appendix A.3: BIOLOG RESULTS FOR INOCULUM

Sample: Inoculum - January 30, 1997 (duplicate #1)
Microplate: gram negative

	1	2	3	4	5	6	7	8	9	10	11	12
A		+	+		b	+		b		+	+	b
B	b	+		+	b	+	+				+	+
C					+	+	+	+			+	+
D	b	+	+		+	b	+	+	+		+	
E	+	+	b	+		b	b	b	+	+		+
F	b	+		b	+	+	+	+	+	+		b
G	b	+	+	b		+	+		b		b	+
H	+	+	b			+	+		+			

Sample: Inoculum - January 30, 1997 (duplicate #2)
Microplate: gram negative

	1	2	3	4	5	6	7	8	9	10	11	12
A		+	+		b	b				+	+	b
B	b	b		b		+	+			+	+	+
C					+	+	+	+			+	+
D	b	+	+		+	b	+	+	+		+	
E	+	+	b	+		b	b	b	+	+		+
F	b	+		b	+	+	+	+	+	+		b
G	b	+	+	b		+	+		b		b	+
H	+	+	b			b	b		+			

Sample: Inoculum - January 30, 1997 (duplicate #1)
Microplate: gram positive

	1	2	3	4	5	6	7	8	9	10	11	12
A			b	b				b	b	+		
B	+	+			b		+	+		+	+	+
C					+	+						
D						+	+			+		+
E		+			+	b	b	+		+	+	
F		b	+		+	+	b	b	+	+	+	
G	b	+	+	+	+	+	b	+	b	b		
H	b		b		+							

Sample: Inoculum - January 30, 1997 (duplicate #2)
Microplate: gram positive

	1	2	3	4	5	6	7	8	9	10	11	12
A			b	b				b	b	+		
B	+	+		b	+		+	+		+	+	+
C					+	+						
D						+	+			+		+
E		+			+	b	b	+		+	+	
F		+	+		+	+	b	b	+	+	+	
G	b	+	+	+	+	+	+	+	b	+		
H	b		b		+							

NOTE: "+" indicates positive, "b" indicates borderline, and blank cells were negative.

Appendix A.3: BIOLOG RESULTS FOR INOCULUM (cont'd)

Sample: Inoculum - June 20, 1997 (duplicate #1)
Microplate: gram negative

	1	2	3	4	5	6	7	8	9	10	11	12
A		b	b		b	b		b		+	+	b
B	b	+		+	b	+	+			b	+	+
C					+	+	b	+			+	+
D	b	+	+		+	+	+	+	+		+	
E	+	+	b	+		b	b	b	+	+		+
F	b	+		b	+	+	+	+	+	+		b
G	b	b	b	b		+	+		b		b	+
H	+	+	b			b	b		b			

Sample: Inoculum - June 20, 1997 (duplicate #2)
Microplate: gram negative

	1	2	3	4	5	6	7	8	9	10	11	12
A		b	b		b	b				+	+	b
B	b	b		+		+	+			b	+	+
C					+	+	b	+			+	b
D	b	+	+		+	+	+	+	+		+	
E	+	+	b	+		b	b	b	+	+		+
F	b	+		b	+	+	+	+	+	+		b
G	b	b	b	b		+	+		b		b	+
H	+	+	b			b	b		b			

Sample: Inoculum - June 20, 1997 (duplicate #1)
Microplate: gram positive

	1	2	3	4	5	6	7	8	9	10	11	12
A								b	b	b		
B	+	+			b		+	+		+	b	+
C					+	+						
D						+	b			+		b
E		+			+	b	b	+		+	+	
F		b	+		+	+	b	b	+	+	+	
G	b	+	+	+	+	+	b	+	b	b		
H	+		+		+							

Sample: Inoculum - June 20, 1997 (duplicate #2)
Microplate: gram positive

	1	2	3	4	5	6	7	8	9	10	11	12
A			b	b				b	b	b		
B	+	+		b	+		+	+		+	+	+
C					+	+						
D						+	b			+		b
E		+			+	b	b	+		+	+	
F		+	+		+	+	b	b	b	+	+	
G	b	+	+	+	+	+	b	+	b	b		
H	+		+		+							

NOTE: "+" indicates positive, "b" indicates borderline, and blank cells were negative.

Appendix A.3: BIOLOG RESULTS FOR SEQUENCED BATCH EXPERIMENTS

Sample: Sequenced Addition of Methylglyoxal (duplicate #1)
Microplate: gram negative

	1	2	3	4	5	6	7	8	9	10	11	12
A					+	+				+		
B		b		b		b						
C											b	b
D	b									+	+	
E			+			+		+			+	+
F	b					b	b	+	+	+		b
G			b			+	+					+
H	+							b	b			

Sample: Sequenced Addition of Methylglyoxal (duplicate #2)
Microplate: gram negative

	1	2	3	4	5	6	7	8	9	10	11	12
A					+	+				+		
B			b	b								
C											b	b
D	b									+	+	
E			+			+		+			b	b
F						b	b	+	+	+		b
G			b			+	+					b
H	b								b			

Sample: Sequenced Addition of Methylglyoxal (duplicate #1)
Microplate: gram positive

	1	2	3	4	5	6	7	8	9	10	11	12
A		b	b	b				+	+	+		
B		b			b		b			+	+	+
C					b	b						
D						+	+					
E		+						+		+	+	
F			+		+	b	+	b	+	+	+	
G	+	+	+	+	+	+	+	+	+	b		
H	+		+		+							

Sample: Sequenced Addition of Methylglyoxal (duplicate #2)
Microplate: gram positive

	1	2	3	4	5	6	7	8	9	10	11	12
A		b	b	b				+	+	+		
B		b		b	b		b			+	+	b
C					b	b						
D						+	+					
E		+						+		+	+	
F			+		+	+	+	b	+	+	+	
G	+	+	+	+	+	+	+	+	+	b		
H	+		+		+							

NOTE: "+" indicates positive, "b" indicates borderline, and blank cells were negative.

Appendix A.3: BIOLOG RESULTS FOR SEQUENCED EXPERIMENTS (cont'd)

Sample: Sequenced Addition of Formaldehyde (duplicate #1)
Microplate: gram negative

	1	2	3	4	5	6	7	8	9	10	11	12
A					b	b		+	+	+	+	
B	b	b		+		+	+				+	+
C					+	+		+		b	+	+
D		+	+		+	+	+		+		+	
E	+	+		+		b			+	+	b	+
F		+		b	b	b	+	+	+	+		+
G	+	+	b	b		+	+		+		b	+
H	+	+	b			b	b		b			

Sample: Sequenced Addition of Formaldehyde (duplicate #2)
Microplate: gram negative

	1	2	3	4	5	6	7	8	9	10	11	12
A					b	b		+	+	+	+	
B	b	b		+		+	+				+	+
C					+	+		+		b	+	b
D		+	+		+	+	+	+	+		+	
E	+	+		+		+	b		+	+	b	+
F	b	+		b	+	+	+	+	+	+		b
G	+	+	b	b		+	+		+		b	+
H	+	+	b			b	b		b			

Sample: Sequenced Addition of Formaldehyde (duplicate #1)
Microplate: gram positive

	1	2	3	4	5	6	7	8	9	10	11	12
A								b	b	b		
B	+	+			b		+	+		+	+	+
C					+	+						
D						+	+			+		
E		+		b	b	b	b	+		+	+	
F			+		+	b	b	b	b	+	b	
G	b	b	+	+	+	+	b	+	b	b		
H	+		+		+							

Sample: Sequenced Addition of Formaldehyde (duplicate #2)
Microplate: gram positive

	1	2	3	4	5	6	7	8	9	10	11	12
A								b	b	b		
B	+	+			b		+	+		+	+	+
C					+	+						
D						+	+			+		+
E		+		b	b	b	b	+		+	+	
F			+		+	b		b	+	+	+	
G	b	b	+	+	+	+	b	+	b	b		
H	+		+		+							

NOTE: "+" indicates positive, "b" indicates borderline, and blank cells were negative.

APPENDIX A.4: DATA FOR CHEMICAL CONTROLS

Appendix A.4: Chemical Control Data for Acetate, Pyruvate, and Methylglyoxal Experiments

Added Components	Time (hours)	Concentration (μg/L)		
		acetate	pyruvate	methylglyoxal
acetate	1.5	265.1		
(trial #1)	21.0	261.9		
	75.5	299.4		
	141.0	276.7		
acetate	0.3	197.6		
(trial #2)	6.3	179.9		
	12.3	210.3		
	25.0	187.7		
	76.3	219.7		
pyruvate	1.0		258.2	
(trial #1)	9.5		266.6	
	27.5		279.1	
	53.0		280.3	
	100.0		271.3	
pyruvate	0.3		348.8	
(trial #2)	6.3		348.6	
	12.3		352.9	
	25.0		362.1	
	76.3		343.6	
methylglyoxal	0.5			271.3
(trial #1)	6.0			281.8
	10.0			296.9
	25.5			307.5
	50.0			301.6
methylglyoxal	0.5			245.8
(trial #2)	35.3			232.1
	55.0			253.4
	72.0			267.9
	102.3			266.8
	132.8			274.3
acetate and	1.0	267.3	353.5	
pyruvate	9.5	277.7	375.4	
(trial #1)	27.5	239.3	374.3	
	53.0	291.0	374.5	
acetate and	0.3	213.7	417.3	
pyruvate	6.3	223.2	417.8	
(trial #2)	12.3	244.5	415.0	
	25.0	220.9	415.8	
	76.3	240.2	408.6	

Appendix A.4: Chemical Control Data for Acetate, Pyruvate, and Methylglyoxal Experiments (cont'd)

Added Components	Time (hours)	Concentration (µg/L)		
		acetate	pyruvate	methylglyoxal
methylglyoxal and pyruvate	0.5		353.7	392.5
	6.0		351.3	434.4
	10.0		371.9	410.6
	25.5		372.8	446.4
	48.0		368.2	386.2
	72.0		360.4	401.7
methylglyoxal, pyruvate, and acetate	0.5	359.6	363.1	443.9
	6.0	373.8	347.7	479.3
	10.0	368.6	372.0	489.4
	25.5	376.3	367.1	446.5
	48.0	*	350.3	467.1
	72.0	*	361.9	455.6

* An unidentified contaminant in the methylglyoxal was found to interfere with acetate quantification.

Appendix A.4: Chemical Control Data for Formaldehyde, Formate, and Oxalate Experiments

Added Components	Time (hours)	Concentration (μg/L)				
		formaldehyde	formate	oxalate	acetate	pyruvate
formaldehyde	0.5	73.1				
	12.0	70.5				
	20.0	81.5				
	30.0	79.1				
	40.0	74.1				
	55.0	74.1				
formate	1.5		406.7			
(trial #1)	21.0		385.5			
	75.5		385.7			
	141.0		404.3			
formate	0.5		205.6			
(trial #2)	4.8		204.7			
	8.0		204.9			
	12.8		206.9			
	16.5		216.3			
	55.8		208.3			
oxalate	0.5			368.3		
	4.8			351.9		
	8.0			341.0		
	12.8			355.2		
	16.5			369.5		
	55.8			382.6		
formaldehyde and	0.5	83.2	152.0			
formate	12.0	82.1	149.1			
	20.0	94.5	147.5			
	30.0	95.5	146.9			
	40.0	89.0	129.8			
	55.0	95.5	154.2			
formate and	0.5		191.0	365.6		
oxalate	4.8		190.1	365.7		
	8.0		192.7	348.2		
	12.8		194.0	356.7		
	16.5		190.8	351.6		
	55.8		180.6	367.8		

Appendix A.4: Chemical Control Data for Formaldehyde, Formate, and Oxalate Experiments (cont'd)

Added Components	Time (hours)	Concentration (µg/L)				
		formaldehyde	formate	oxalate	acetate	pyruvate
formaldehyde, formate, and oxalate *(trial #1)*	0.5	91.9	152.3	346.0		
	12.0	108.5	155.2	337.0		
	20.0	112.9	144.4	329.4		
	30.0	96.2	149.1	311.2		
	40.0	102.8	138.4	322.8		
	55.0	106.9	151.1	331.1		
formaldehyde, formate, and oxalate *(trial #2)*	0.5	109.0	174.3	335.9		
	8.0	122.3	180.3	327.2		
	18.0	111.3	176.9	346.3		
	26.0	113.1	183.3	329.5		
	70.0	110.4	175.5	347.4		
formaldehyde, formate, oxalate, acetate, and pyruvate	0.5	143.5	195.5	338.9	220.7	327.8
	8.0	149.2	196.9	338.1	223.2	333.7
	18.0	138.2	198.7	335.9	223.8	338.6
	26.0	158.2	195.6	348.6	224.5	333.4
	70.0	157.5	202.7	348.9	235.3	339.7
	120.0	163.4	203.8	340.0	234.3	341.8

Appendix A.4: Chemical Control Data for Sequenced Batch Experiments

Added Components	Time (hours)	Concentration (μg/L) formaldehyde	methylglyoxal	pyruvate
formaldehyde	0.5	137.9		
(trial #1)	49.0	136.1		
	96.3	137.7		
	121.8	135.4		
	145.0	140.3		
	164.3	139.2		
	224.0	137.9		
formaldehyde	1.0	118.7		
(trial #2)	19.0	111.0		
	47.5	131.8		
	55.0	128.7		
	74.5	133.2		
	93.0	137.2		
	96.0	128.2		
	120.0	127.9		
	140.0	127.3		
	170.5	123.4		
methylglyoxal	0.5		292.5	
(trial #1)	49.0		326.6	
	96.3		337.1	
	121.8		344.0	
	145.0		355.2	
	164.3		347.6	
	224.0		353.3	
methylglyoxal	1.0		301.2	
(trial #2)	19.0		317.6	
	47.5		316.6	
	55.0		316.0	
	74.5		334.9	
	93.0		343.2	
	96.0		321.5	
	120.0		303.7	
	140.0		327.0	
	170.5		315.4	
methylglyoxal in tap water	1.0		264.7	
	20.0		264.7	
	47.5		259.4	
	74.5		235.1	
	95.5		249.2	
	140.0		264.5	
	170.5		279.4	

APPENDIX A.5: BIOLOGICAL CONTROL DATA

Appendix A.5: Biological Control Data

Added Components	Time (hours)	HPCs (CFU/mL)
Experiment # 1	0.5	3.0E+04
	72.0	1.5E+05
Experiment # 2	1.0	4.9E+05
	27.5	3.8E+05
	53.0	3.9E+05
Experiment # 3	1.5	5.7E+05
	21.0	5.3E+05
	75.5	5.8E+05
Experiment # 4	1.0	2.2E+05
	27.5	1.8E+05
	53.0	1.7E+05
Experiment # 5	1.5	3.7E+05
	21.0	3.2E+05
	75.5	4.9E+05
Experiment # 6	0.3	2.6E+05
	25.0	3.0E+05
	76.3	4.8E+05
Experiment # 7	0.5	4.7E+05
	25.5	3.2E+05
	72.0	6.7E+05
Experiment # 8	0.5	7.2E+04
	55.8	2.1E+05
Experiment # 9	0.5	1.1E+05
	55.0	2.2E+05
	132.8	3.9E+05
Experiment # 10	0.5	2.4E+05
	30.5	1.1E+05
	72.0	1.8E+05
Experiment # 11	0.5	4.3E+05
	26.0	2.0E+05
	70.0	3.3E+05
	120.0	2.1E+05

Appendix A.5:Biological Control Data (cont'd)

Added Components	Time (hours)	HPCs (CFU/mL)
Experiment # 12	7.5	1.1E+05
	24.0	2.0E+05
	95.0	3.4E+05
	121.0	2.2E+05
	140.0	4.2E+05
	215.0	3.1E+05
Experiment # 13	0.5	4.2E+05
	24.5	3.0E+05
	74.5	5.3E+05
	96.0	4.4E+05
	141.5	5.5E+05
	170.5	6.0E+05
Experiment # 14	19.5	4.5E+05
	47.5	4.1E+05
	74.5	3.9E+05
	95.5	3.8E+05
	141.5	5.2E+05
	170.5	5.3E+05

APPENDIX B: DATA FROM FILTER EXPERIMENTS

APPENDIX B.1: ORGANIC CHEMICAL COMPONENT DATA

Appendix B.1: Organic Chemical Component Data for Filter Experiment #1

	Filter 1
HLR (m/h)	5

Day	Filter	Depth (cm)	EBCT (min)	Concentration (µg/L)* formate	formaldehyde
6	filter 1	0	0.00	9.0	2.6
		9	1.08	6.8	2.8
		39	4.68	3.9	1.6
		74	8.88	2.7	3.4
23	filter 1	0	0.00	4.0	2.3
		9	1.08	2.5	1.6
		39	4.68	7.2	2.1
		74	8.88	2.7	2.4
43	filter 1	0	0.00	4.2	2.2
		4	0.48	2.0	2.9
		9	1.08	11.0	1.6
		24	2.88	7.1	3.1
		74	8.88	20.5	2.5
43	filter 1	0	0.00	26.4	2.2
(after backwash)		74	8.88	6.5	2.7
57	filter 1	0	0.00	13.9	6.0
(start of 24 hr spike)		74	8.88	11.4	10.1
58	filter 1	0	0.00	7.4	3.8
(end of 24hr spike)		74	8.88	14.4	1.6
58	filter 1	0	0.00	5.6	4.4
(4 hr after spike)		74	8.88	4.1	3.1
73	filter 1	0	0.00	8.8	11.9
(day 3 of step increase)		74	8.88	7.0	9.8
83	filter 1	0	0.00	15.9	5.4
(after 48 hr shutdown)		74	8.88	2.0	1.6

* Average of two duplicate samples.

Appendix B.1: Organic Chemical Component Data for Filter Experiment #1 (cont'd)

	Filter 2	Filter 3
HLR (m/h)	5	10

Day	Filter	Depth (cm)	EBCT (min)	Concentration (µg/L)* methylglyoxal	pyruvate
6	filter 2	0	0.00	157.8	0.0
		9	1.08	149.4	0.0
		39	4.68	144.5	0.0
		74	8.88	144.3	0.0
	filter 3	0	0.00	153.4	0.0
		9	0.54	113.9	0.0
		39	2.34	88.8	0.0
		74	4.44	73.4	0.0
23	filter 2	0	0.00	121.3	0.0
		4	0.48	57.4	81.1
		14	1.68	7.1	0.0
		54	6.48	2.5	0.0
		74	8.88	0.0	0.0
	filter 3	0	0.00	129.8	0.0
		4	0.24	116.2	16.9
		14	0.84	86.3	17.0
		54	3.24	11.4	20.0
		74	4.44	2.5	3.0
43	filter 2	0	0.00	151.9	0.0
		4	0.48	47.5	59.4
		9	1.08	16.8	0.0
		24	2.88	2.5	0.0
		74	8.88	0.0	0.0
	filter 3	0	0.00	149.3	0.0
		4	0.24	80.2	19.8
		14	0.84	32.2	16.0
		39	2.34	14.4	3.0
		74	4.44	0.0	0.0
43 (after backwash)	filter 2	0	0.00	141.0	0.0
		14	1.68	22.3	3.0
		74	8.88	2.5	0.0
	filter 3	0	0.00	138.3	0.0
		39	2.34	17.0	3.0
		74	4.44	2.5	0.0

* Average of two duplicate samples.

Appendix B.1: Organic Chemical Component Data for Filter Experiment #1 (cont'd)

Day	Filter	Depth (cm)	EBCT (min)	Concentration (µg/L)* methylglyoxal	pyruvate
57	filter 2	0	0.00	523.2	0.0
(start of 24 hr spike)		4	0.48	389.5	40.0
		9	1.08	289.4	16.6
		74	8.88	203.0	28.6
	filter 3	0	0.00	487.0	0.0
		4	0.24	470.0	41.2
		14	0.84	474.1	29.3
		74	4.44	180.1	109.0
58	filter 2	0	0.00	644.2	0.0
(end of 24hr spike)		4	0.48	510.2	51.0
		9	1.08	276.7	41.3
		74	8.88	12.0	0.0
	filter 3	0	0.00	614.8	0.0
		4	0.24	585.0	62.2
		9	0.54	367.0	132.5
		74	4.44	23.8	5.8
58	filter 2	0	0.00	148.9	0.0
(4 hr after spike)		4	0.48	30.8	25.7
		9	1.08	13.4	0.0
		74	8.88	0.0	0.0
	filter 3	0	0.00	150.0	0.0
		4	0.24	71.4	0.0
		9	0.54	14.8	40.6
		74	4.44	0.0	0.0
73	filter 2	0	0.00	645.6	0.0
(day 3 of step increase)		4	0.48	350.5	58.6
		9	1.08	158.0	50.1
		74	8.88	2.5	0.0
	filter 3	0	0.00	634.0	0.0
		4	0.24	414.5	37.8
		9	0.54	212.5	87.3
		74	4.44	41.5	13.3
83	filter 2	0	0.00	127.9	0.0
(after 48 hr shutdown)		4	0.48	58.8	46.2
		9	1.08	29.6	50.8
		74	8.88	0.0	0.0
	filter 3	0	0.00	122.5	0.0
		4	0.24	97.5	23.2
		9	0.54	46.5	45.8
		14	0.84	17.5	25.4
		74	4.44	2.5	0.0

* Average of two duplicate samples.

Appendix B.1: Organic Chemical Component Data for Filter Experiment #2

HLR (all filters): 8 m/h
Note: Thiosulphate (thio) dosing began on day 37.

Days Since:			Depth	EBCT	Concentration (µg/L)*		
Start-Up	Thio Dosing	Filter	(cm)	(min)	methylglyoxal	pyruvate	formaldehyde
8	-	filter 1	0	0.00	219.0	0.0	
			10	0.75	227.0	0.0	
			25	1.88	226.4	0.0	
			75	5.63	226.3	0.0	
		filter 2	0	0.00		292.8	
			10	0.75		305.8	
			25	1.88		314.7	
			75	5.63		298.0	
		filter 3	0	0.00	105.3	152.6	
			10	0.75	102.3	163.6	
			25	1.88	113.2	161.3	
			75	5.63	106.5	159.9	
		filter 4	0	0.00			234.1
			10	0.75			228.6
			25	1.88			231.6
			75	5.63			220.3
18	-	filter 1	0	0.00	198.4	0.0	
			10	0.75	206.1	0.0	
			25	1.88	206.7	0.0	
			75	5.63	196.4	0.0	
		filter 2	0	0.00		292.5	
			10	0.75		292.9	
			25	1.88		277.3	
			75	5.63		291.0	
		filter 3	0	0.00	119.5	158.3	
			10	0.75	110.4	160.2	
			25	1.88	108.7	158.9	
			75	5.63	106.3	143.6	
		filter 4	0	0.00			254.1
			10	0.75			243.9
			25	1.88			230.9
			75	5.63			225.8

* Average of two duplicate samples.

Appendix B.1: Organic Chemical Component Data for Filter Experiment #2 (cont'd)

Days Since:			Depth	EBCT	Concentration (µg/L)*		
Start-Up	Thio Dosing	filter	(cm)	(min)	methylglyoxal	pyruvate	formaldehyde
45	8	filter 1	0	0.00	200.3	0.0	
			10	0.75	188.2	3.0	
			25	1.88	172.4	3.0	
			75	5.63	165.0	0.0	
		filter 2	0	0.00		289.3	
			10	0.75		246.7	
			25	1.88		209.1	
			75	5.63		103.7	
		filter 3	0	0.00	108.0	150.8	
			10	0.75	100.5	132.9	
			25	1.88	93.2	133.4	
			75	5.63	89.3	130.7	
		filter 4	0	0.00			248.4
			10	0.75			222.0
			25	1.88			216.1
			75	5.63			191.8
59	22	filter 1	0	0.00	198.4	0.0	
			10	0.75	183.2	0.0	
			15	1.13	179.7	3.0	
			40	3.00	148.8	17.1	
			75	5.63	95.2	10.8	
		filter 2	0	0.00		302.3	
			5	0.38		80.2	
			10	0.75		20.3	
			15	1.13		3.0	
			75	5.63		0.0	
		filter 3	0	0.00	96.9	150.6	
			5	0.38	89.2	34.5	
			15	1.13	83.6	3.0	
			40	3.00	52.3	0.0	
			75	5.63	12.4	0.0	
		filter 4	0	0.00			255.2
			10	0.75			86.3
			15	1.13			77.1
			40	3.00			35.5
			75	5.63			29.8

* Average of two duplicate samples.

Appendix B.1: Organic Chemical Component Data for Filter Experiment #2 (cont'd)

Days Since:			Depth	EBCT	Concentration (µg/L)*		
Start-Up	Thio Dosing	filter	(cm)	(min)	methylglyoxal	pyruvate	formaldehyde
64	27	filter 1	0	0.00	203.3	0.0	
			4	0.30	174.8	0.0	
			14	1.05	146.4	23.7	
			39	2.93	115.8	30.2	
			74	5.55	46.6	18.7	
		filter 2	0	0.00		308.7	
			4	0.30		62.6	
			9	0.68		23.1	
			14	1.05		3.0	
			74	5.55		0.0	
		filter 3	0	0.00	96.6	144.5	
			4	0.30	73.1	52.9	
			9	0.68	44.1	22.9	
			14	1.05	26.2	3.0	
			39	2.93	3.2	0.0	
			74	5.55	2.5	0.0	
		filter 4	0	0.00			244.3
			4	0.30			150.6
			9	0.68			85.3
			39	2.93			23.3
			74	5.55			1.6
75	38	filter 1	0	0.00	210.5	0.0	
			4	0.30	129.0	21.5	
			9	0.68	79.3	28.6	
			24	1.80	50.2	7.1	
			74	5.55	0.0	0.0	
		filter 2	0	0.00		293.2	
			4	0.30		55.3	
			9	0.68		23.4	
			14	1.05		3.0	
			74	5.55		0.0	
		filter 3	0	0.00	97.5	148.6	
			4	0.30	59.6	62.0	
			9	0.68	40.4	24.8	
			14	1.05	23.9	3.0	
			74	5.55	0.0	0.0	
		filter 4	0	0.00			255.5
			4	0.30			149.2
			9	0.68			96.3
			24	1.80			48.7
			74	5.55			1.6

* Average of two duplicate samples.

Appendix B.1: Organic Chemical Component Data for Filter Experiment #3

	Filter 1	Filter 2	Filter 3	Filter 4
HLR (m/h)	7.5	7.5	7.5	7.5
temperature (C)	25	25	14	14
amino acid dosing	no	yes	no	yes

Day	Filter	Depth (cm)	EBCT (min)	Concentration (µg/L)* formaldehyde	serine	glycine
5	filter 1	0	0	290.3	< 5.0	< 5.0
		15	1.2	107.7	0.0	0.0
		25	2	95.5	0.0	0.0
		75	6	40.2	0.0	0.0
	filter 2	0	0	270.8	167.4	215.1
		15	1.2	92.4	145.8	189.6
		25	2	70.8		
		75	6	41.4	105.3	156.6
	filter 3	0	0	266.6	< 5.0	< 5.0
		15	1.2	235.8	0.0	0.0
		25	2	236.5	0.0	0.0
		75	6	231.6	0.0	0.0
	filter 4	0	0	295.4	175.2	201.4
		15	1.2	275.5	115.2	125.4
		25	2	265.3		
		75	6	254.7	102.2	110.2
10	filter 1	0	0	294.1		
		5	0.4	197.7		
		15	1.2	105.7		
		75	6	11.4		
	filter 2	0	0	267.5	154.5	181.3
		5	0.4	171.8	95.6	128.6
		15	1.2	109.2	44.2	58.2
		75	6	12.8	5.0	5.0
	filter 3	0	0	290.5		
		15	1.2	300.8		
		25	2	260.6		
		75	6	199.9		
	filter 4	0	0	298.4	172.6	219.0
		15	1.2	295.6	115.4	145.7
		25	2	235.2	100.1	130.2
		75	6	180.1	85.6	105.4

* Average of two duplicate samples.

Appendix B.1: Organic Chemical Component Data for Filter Experiment #3 (cont'd)

Day	Filter	Depth (cm)	EBCT (min)	Concentration (µg/L)* formaldehyde	serine	glycine
18	filter 1	0	0	263.7		
		4	0.32	179.9		
		9	0.72	123.1		
		74	5.92	12.5		
	filter 2	0	0	256.8	133.4	166.7
		4	0.32	150.5	113.6	142.2
		9	0.72	131.6	98.3	118.6
		74	5.92	10.0	5.0	5.0
	filter 3	0	0	297.6		
		9	0.72	101.5		
		24	1.92	52.3		
		74	5.92	37.4		
	filter 4	0	0	290.6	175.0	200.0
		9	0.72	125.3	125.0	135.0
		24	1.92	51.4	89.0	101.4
		74	5.92	30.7	5.0	5.0
28	filter 1	0	0	271.0		
		4	0.32	200.2		
		9	0.72	140.9		
		24	1.92	89.8		
		74	5.92	1.6		
	filter 2	0	0	245.7	148.2	181.6
		5	0.4	137.4	61.4	77.9
		10	0.8	98.9	39.5	45.2
		25	2	60.5		
		75	6	4.0	0.0	0.0
	filter 3	0	0	251.8		
		5	0.4	121.3		
		10	0.8	62.5		
		25	2	50.1		
		75	6	1.6		
	filter 4	0	0	247.3	150.3	175.7
		4	0.32	127.1	28.1	44.6
		9	0.72	73.6	13.3	16.7
		24	1.92	30.0		
		74	5.92	1.6	0.0	0.0

* Average of two duplicate samples.

Appendix B.1: Organic Chemical Component Data for Filter Experiment #3 (cont'd)

Day	Filter	Depth (cm)	EBCT (min)	Concentration (µg/L)* formaldehyde	serine	glycine
39	filter 1	0	0	275.6		
		3	0.24	197.5		
		8	0.64	131.7		
		23	1.84	75.3		
		73	5.84	4.0		
	filter 2	0	0	248.5	150.0	184.3
		4	0.32	185.6	72.5	104.0
		9	0.72	116.9	25.6	35.8
		24	1.92	78.4		
		74	5.92	6.1	0.0	0.0
	filter 3	0	0	281.7		
		4	0.32	167.2		
		9	0.72	106.3		
		24	1.92	50.4		
		74	5.92	1.6		
	filter 4	0	0	297.9	155.0	197.2
		4	0.32	163.3	27.5	55.4
		9	0.72	90.2	12.9	18.2
		24	1.92	40.0		
		74	5.92	1.6	0.0	0.0

* Average of two duplicate samples.

APPENDIX B.2: PHOSPHOLIPID DATA

Appendix B.2: Phospholipid Data for Experiment #1

	Filter 1	Filter 2	Filter 3
HLR (m/h)	5	5	10

Day	Filter	Media	Depth (cm)	EBCT (min)	avg nmol lipid-P* /g	/cm^3 filter
46	filter 1	anth	4	0.48	3.01	2.41
		anth	14	1.68	2.00	2.00
		sand	54	6.48	2.00	2.00
	filter 2	anth	4	0.48	67.46	53.96
		anth	14	1.68	15.13	12.11
		sand	54	6.48	2.00	2.94
	filter 3	anth	4	0.24	46.87	37.49
		anth	14	0.84	29.01	23.20
		sand	54	3.24	4.93	7.40
58	filter 2	anth	4	0.48	91.14	72.91
(end of 24hr spike)		anth	14	1.68	24.76	19.81
		sand	54	6.48	4.23	6.35
	filter 3	anth	4	0.24	68.92	55.14
		anth	14	0.84	45.86	36.68
		sand	54	3.24	7.15	10.73
81	filter 1	anth	4	0.48	4.05	3.24
		anth	14	1.68	2.01	2.00
		sand	54	6.48	2.00	2.00

* Average of two duplicate samples.

Appendix B.2: Phospholipid Data for Exeriment #2

HLR (all filters): 8 m/h

Note: Thiosulphate (thio) dosing began on day 37.

Days Since:				Depth	EBCT	avg nmol lipid-P*	
Start-Up	Thio Dosing	Filter	Media	(cm)	(min)	/g	/cm^3 filter
46	9	filter 1	anth	5	0.38	4.75	3.80
			anth	15	1.13	2.47	1.97
			sand	55	4.13	1.00	1.50
		filter 2	anth	5	0.38	10.27	8.22
			anth	15	1.13	4.28	3.42
			sand	55	4.13	1.00	1.50
		filter 3	anth	5	0.38	3.56	2.85
			anth	15	1.13	1.72	1.38
			sand	55	4.13	1.00	1.50
		filler 4	anth	5	0.38	7.83	6.26
			anth	15	1.13	2.20	1.76
			sand	55	4.13	1.00	1.50
66	29	filter 1	anth	5	0.38	38.28	30.62
			anth	15	1.13	9.76	7.80
			sand	55	4.13	4.10	6.14
		filter 2	anth	5	0.38	64.14	51.31
			anth	15	1.13	17.76	14.21
			sand	55	4.13	4.67	7.01
		filter 3	anth	5	0.38	77.39	61.91
			anth	15	1.13	22.50	18.00
			sand	55	4.13	5.94	8.90
		filler 4	anth	5	0.38	61.06	48.85
			anth	15	1.13	18.56	14.85
			sand	55	4.13	4.85	7.28
76	39	filter 1	anth	4	0.30	61.07	48.86
			anth	9	0.68	15.16	12.12
			anth	14	1.05	8.34	6.67
			sand	54	4.05	3.14	4.71
		filter 2	anth	4	0.30	70.71	56.57
			anth	9	0.68	21.81	17.44
			anth	14	1.05	10.71	8.57
			sand	54	4.05	4.03	6.05
		filter 3	anth	4	0.30	79.53	63.62
			anth	9	0.68	28.20	22.56
			anth	14	1.05	13.06	10.44
			sand	54	4.05	5.31	7.97
		filler 4	anth	4	0.30	67.77	54.22
			anth	9	0.68	22.03	17.62
			anth	14	1.05	12.54	10.03
			sand	54	4.05	4.90	7.34

* Average of two duplicate samples.

Appendix B.2: Phospholipid Data for Exeriment #3

	Filter 1	Filter 2	Filter 3	Filter 4
HLR (m/h)	7.5	7.5	7.5	7.5
temperature (C)	25	25	14	14
amino acid dosing	no	yes	no	yes

Day	Filter	Media	Depth (cm)	EBCT (min)	avg nmol lipid-P* /g	avg nmol lipid-P* /cm^3 filter
7	filter 1	anth	5	0.40	7.93	6.34
		anth	15	1.20	4.10	3.28
		anth	25	2.00	2.01	1.60
		sand	55	4.40	1.00	1.50
	filter 2	anth	5	0.40	10.27	8.22
		anth	15	1.20	3.12	2.50
		anth	25	2.00	1.89	1.51
		sand	55	4.40	1.00	1.50
	filter 3	anth	5	0.40	4.06	3.25
		anth	15	1.20	2.04	1.63
		anth	25	2.00	1.00	0.80
		sand	55	4.40	1.00	1.50
	filter 4	anth	5	0.40	5.08	4.06
		anth	15	1.20	2.00	1.60
		anth	25	2.00	2.04	1.63
		sand	55	4.40	1.00	1.50
15	filter 1	anth	5	0.40	31.03	24.82
		anth	10	0.80	11.10	8.88
		anth	15	1.20	8.19	6.55
		sand	55	4.40	2.04	3.05
	filter 2	anth	5	0.40	39.22	31.38
		anth	10	0.80	15.00	12.00
		anth	15	1.20	11.04	8.83
		sand	55	4.40	1.67	2.51
	filter 3	anth	5	0.40	9.01	7.21
		anth	10	0.80	3.06	2.45
		anth	15	1.20	2.13	1.70
		sand	55	4.40	1.00	1.50
	filter 4	anth	5	0.40	12.05	9.64
		anth	10	0.80	5.27	4.22
		anth	15	1.20	3.73	2.98
		sand	55	4.40	2.24	3.36

* Average of two duplicate samples.

Appenidx B.2: Phospholipid Data for Exeriment #3 (cont'd)

Day	Filter	Media	Depth (cm)	EBCT (min)	avg nmol lipid-P* /g	/cm^3 filter
42	filter 1	anth	4	0.32	53.05	42.44
		anth	9	0.72	18.12	14.50
		anth	14	1.12	9.43	7.54
		anth	24	1.92	3.90	3.12
	filter 2	anth	4	0.32	73.39	58.71
		anth	9	0.72	22.30	17.84
		anth	14	1.12	12.05	9.64
		anth	24	1.92	7.51	6.01
	filter 3	anth	4	0.32	67.73	54.18
		anth	9	0.72	19.77	15.82
		anth	14	1.12	11.26	9.00
		anth	24	1.92	6.31	5.05
	filter 4	anth	4	0.32	99.84	79.87
		anth	9	0.72	35.48	28.38
		anth	14	1.12	20.01	16.01
		anth	24	1.92	12.18	9.74

* Average of two duplicate samples.

APPENDIX B.3: SODIUM THIOSULPHATE DATA

Appendix B.3: Sodium Thiosulphate Data for Exeriment #2

HLR (all filters): 8 m/h

Note: Thiosulphate (thio) dosing began on day 37.

Days Since: Start-Up	Days Since: Thio Dosing	Filter	Depth (cm)	EBCT (min)	Thiosulphate* (mg/L)
45	8	filter 1	0	0.00	0.113
			10	0.75	0.100
			25	1.88	0.102
			75	5.63	0.090
		filter 2	0	0.00	0.102
			10	0.75	0.086
			25	1.88	0.079
			75	5.63	0.066
		filter 3	0	0.00	0.123
			10	0.75	0.127
			25	1.88	0.115
			75	5.63	0.102
		filter 4	0	0.00	0.123
			10	0.75	0.119
			25	1.88	0.094
			75	5.63	0.080
59	22	Filter 1	0	0.00	0.128
			5	0.38	0.103
			15	1.13	0.101
			75	5.63	0.025
		filter 2	0	0.00	0.114
			5	0.38	0.075
			15	1.13	0.044
			75	5.63	0.025
		filter 3	0	0.00	0.130
			5	0.38	0.098
			15	1.13	0.087
			75	5.63	0.025
		filter 4	0	0.00	0.139
			5	0.38	0.098
			15	1.13	0.085
			75	5.63	0.025

* Average of two duplicate samples.

Appendix B.3: Sodium Thiosulphate Data for Exeriment #2 (cont'd)

Days Since: Start-Up	Days Since: Thio Dosing	Filter	Depth (cm)	EBCT (min)	Thiosulphate* (mg/L)
64	27	filter 1	0	0.00	0.135
			4	0.30	0.080
			14	1.05	0.025
			74	5.55	0.000
		filter 2	0	0.00	0.127
			4	0.30	0.064
			9	0.68	0.030
			74	5.55	0.000
		filter 3	0	0.00	0.123
			4	0.30	0.076
			9	0.68	0.029
			74	5.55	0.000
		filter 4	0	0.00	0.117
			4	0.30	0.080
			14	1.05	0.042
			74	5.55	0.000
75	38	Filter 1	0	0.00	0.132
			4	0.30	0.080
			9	0.68	0.048
			74	5.55	0.000
		Filter 2	0	0.00	0.128
			4	0.30	0.063
			9	0.68	0.040
			74	5.55	0.000
		Filter 3	0	0.00	0.121
			4	0.30	0.074
			9	0.68	0.039
			74	5.55	0.000
		Filter 4	0	0.00	0.116
			4	0.30	0.076
			9	0.68	0.037
			74	5.55	0.000

* Average of two duplicate samples.

Appendix B.3: Sodium Thiosulphate Data for Exeriment #3

	Filter 1	Filter 2	Filter 3	Filter 4
HLR (m/h)	7.5	7.5	7.5	7.5
temperature (C)	25	25	14	14
amino acid dosing	no	yes	no	yes

Day	Filter	Depth (cm)	EBCT (min)	Thiosulphate* (mg/L)
5	filter 1	0	0.00	0.120
		15	1.20	0.111
		25	2.00	0.095
		75	6.00	0.064
	filter 2	0	0.00	0.113
		15	1.20	0.097
		25	2.00	0.085
		75	6.00	0.069
	filter 3	0	0.00	0.104
		15	1.20	0.098
		25	2.00	0.096
		75	6.00	0.091
	filter 4	0	0.00	0.124
		15	1.20	0.120
		25	2.00	0.112
		75	6.00	0.105
10	filter 1	0	0.00	0.113
		5	0.40	0.074
		15	1.20	0.048
		75	6.00	0.025
	filter 2	0	0.00	0.120
		5	0.40	0.068
		15	1.20	0.043
		75	6.00	0.025
	filter 3	0	0.00	0.121
		15	1.20	0.114
		25	2.00	0.106
		75	6.00	0.101
	filter 4	0	0.00	0.134
		15	1.20	0.111
		25	2.00	0.102
		75	6.00	0.102

* Average of two duplicate samples.

Appendix B.3: Sodium Thiosulphate Data for Exeriment #3 (cont'd)

Day	Filter	Depth (cm)	EBCT (min)	Thiosulphate* (mg/L)
18	filter 1	0	0.00	0.475
		4	0.32	0.324
		9	0.72	0.221
		74	5.92	0.000
	filter 2	0	0.00	0.462
		4	0.32	0.297
		9	0.72	0.237
		74	5.92	0.000
	filter 3	0	0.00	0.536
		4	0.72	0.273
		9	1.92	0.094
		74	5.92	0.025
	filter 4	0	0.00	0.523
		4	0.72	0.226
		9	1.92	0.092
		74	5.92	0.025
28	filter 1	0	0.00	0.500
		4	0.32	0.369
		9	0.72	0.237
		74	5.92	0.000
	filter 2	0	0.00	0.453
		5	0.40	0.330
		10	0.80	0.182
		75	6.00	0.000
	filter 3	0	0.00	0.464
		5	0.40	0.253
		10	0.80	0.157
		75	6.00	0.000
	filter 4	0	0.00	0.456
		4	0.32	0.234
		9	0.72	0.136
		74	5.92	0.000

* Average of two duplicate samples.

Sodium Thiosulphate Data for Exeriment #3 (cont'd)

Day	Filter	Depth (cm)	EBCT (min)	Thiosulphate* (mg/L)
39	filter 1	0	0.00	0.115
		3	0.24	0.081
		8	0.64	0.051
		73	5.84	0.000
	filter 2	0	0.00	0.125
		4	0.32	0.086
		9	0.72	0.052
		74	5.92	0.000
	filter 3	0	0.00	0.121
		4	0.32	0.073
		9	0.72	0.045
		74	5.92	0.000
	filter 4	0	0.00	0.124
		4	0.32	0.069
		9	0.72	0.040
		74	5.92	0.000

* Average of two duplicate samples.

IMAGE EVALUATION
TEST TARGET (QA-3)

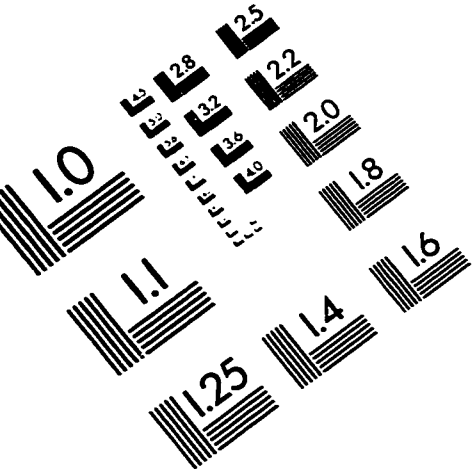

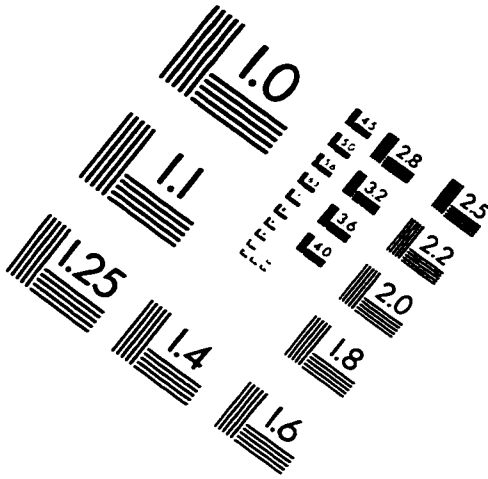

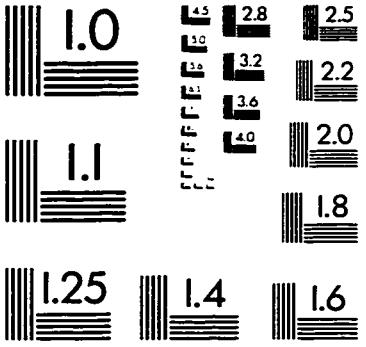

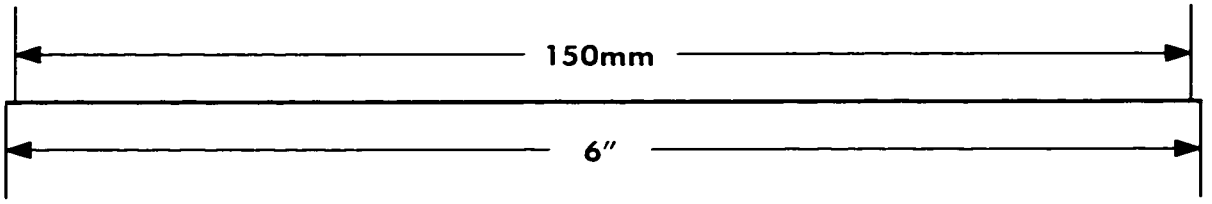

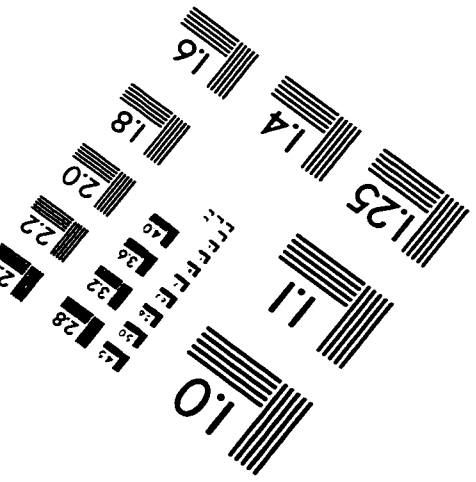

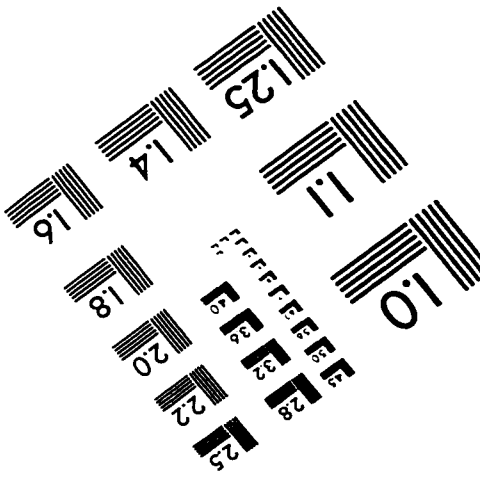

APPLIED IMAGE, Inc
1653 East Main Street
Rochester, NY 14609 USA
Phone: 716/482-0300
Fax: 716/288-5989